Department of Ophthalmology

Saarland University Medical Center Homburg/Saar

Director: Prof. Dr. med. Berthold Seitz ML, FEBO

Visual and tomographic results after accelerated corneal crosslinking for keratoconus and reliability analysis of biomechanical measurements in untreated and crosslinked keratoconus corneas

Dissertation to obtain the Degree of a Doctor of Medicine

of the Faculty of Medicine

of the SAARLAND UNIVERSITY

2024

submitted by

Kassandra Xanthopoulou

born on: 17.12.1992 in Thessaloniki, Macedonia, Greece

Day of presentation: 8th of January 2025

Dekan: Univ.-Prof. Dr. med. dent. Matthias Hannig

1. Berichterstatter: Prof. Dr. med. Berthold Seitz

2. Berichterstatter: Prof. Dr. med. Thomas Tschernig

For my family

The following publications have resulted from this doctoral thesis:

- 1. Xanthopoulou K, Milioti G, Daas L, Munteanu C, Seitz B, Flockerzi E (2022). Accelerated corneal crosslinking causes pseudoprogression in keratoconus within the first 6 weeks without affecting posterior corneal curvature. Eur J Ophthalmol 32:2565-2576. doi: 10-1177/11206721221099257 [332]

- 2. Xanthopoulou K, Seitz B, Belin MW, Flockerzi E (2023). Reliability analysis of successive Corvis ST measurements in keratoconus 2 years after accelerated corneal crosslinking compared to untreated keratoconus corneas. Graefes Arch Clin Exp Ophthalmol 261:1055-1061. doi: 10.1007/s00417-022-05881-6 [333]

- 3. Xanthopoulou K, Milioti G, Daas L, Munteanu C, Seitz B, Flockerzi E (2023). Accelerated corneal crosslinking for the treatment of keratoconus in children and adolescents under 18 years of age. Klin Monbl Augenheilkd 240:1131-1142. doi: 10.1055/a-1933-3084 [334]

Table of contents

1. Glossary

1. $^{1}O_2$: Singlet oxygen
2. 3D: Three-dimensional
3. $^{3}O_2$: Ground stage oxygen
4. A1: First or ingoing applanation at CORVIS ST
5. A2: Second applanation at CORVIS ST
6. ACT: Apical corneal thickness, Pachymetry of the apex of the cornea
7. A-CXL: Accelerated corneal crosslinking
8. AMD: Age-related macular degeneration
9. AL: Applanation length
10. ARC: Anterior radius of curvature
11. ARTh: Ambrósio's relational thickness to the horizontal profile
12. AS-OCT: Anterior segment optical coherence tomography
13. Astia: Astigmatism of the anterior corneal curvature
14. Astip: Astigmatism of the posterior corneal curvature
15. ATP: Activated adenosine tri-phosphatase
16. BAD-D: Belin/Ambrósio-Enhanced-Ectasia-Deviation-Index
17. BCVA: Best corrected visual acuity, here: with spectacles
18. C_3F_8: Perfluorpropan
19. CA: Cronbach's alpha
20. CBI: Corvis Biomechanical Index
21. CBiF: Corvis Biomechanical Factor, the linearized term of the Corvis Biomechanical Index
22. CCT: Central corneal thickness
23. CL: Contact lens(es)
24. CLEK study: Collaborative Longitudinal Evaluation of Keratoconus study
25. CORVIS ST (CST): Corneal Visualization Scheimpflug Technology
26. CRCS: Central serous chorioretinopathy
27. CT1: Intraoperative corneal pachymetry before corneal debridement
28. CT2: Intraoperative corneal pachymetry after corneal debridement

29. CT3: Intraoperative corneal pachymetry before irradiation
30. CT4: Intraoperative corneal pachymetry after irradiation
31. CVel: Corneal velocity
32. CXL: Corneal collagen crosslinking
33. CXLG: Group including crosslinked corneas
34. D: Diopter(s)
35. DA ratio 2 mm: Deformation amplitude ratio 2 mm
36. DALK: Deep anterior lamellar keratoplasty
37. DCR: Dynamic Corneal Response
38. Df: Degrees of freedom
39. DMEK: Descemet membrane endothelial keratoplasty
40. EDTA: Ethylenediaminetetraacetic acid
41. eg.: exempli gratia (for example)
42. EI-CXL: Enhanced iontophoresis corneal collagen crosslinking
43. Epi-off: Epithelium-off
44. Epi-on: Epithelium-on
45. etc.: et cetera (and other similar things)
46. Excimer-PTK: Excimer laser assisted phototherapeutic keratectomy
47. FDA: Food and Drug Administration
48. GAGs: Glycosaminoglycanes
49. H_2O: Water
50. HH: Hornhaut (cornea)
51. HKC: Homburg Keratoconus Center
52. HpD: Hematoporphyrin derivative
53. HR: High resolution
54. ICL: Implantable collamer lens
55. ICRS: Intracorneal ring segments
56. I-CXL: Iontophoresis corneal crosslinking
57. IL: Interleukin
58. INTACS-SK: Type of intracorneal ring segments
59. IVCM: In vivo confocal microscopy

60. J/cm^2: Joule/cm^2
61. K^+: Potassium
62. K1: Steep keratometry
63. K1a: Anterior steep keratometry
64. K1p: Posterior steep keratometry
65. K2: Flat keratometry
66. K2a: Anterior flat keratometry
67. K2p: Posterior flat keratometry
68. KC: Keratoconus (English)
69. KK: Keratokonus (german)
70. Km: Mean keratometry
71. Kma: Mean anterior keratometry
72. Kmax: Maximal anterior keratometry
73. Kmp: Mean posterior keratometry
74. LogMAR: logarithm of the minimum angle of resolution
75. mw/cm^2: Milliwatt/centimeter^2
76. mm: Millimeter(s)
77. MMP: Matrix metalloproteinase
78. mRNA: Messenger ribonucleic acid
79. Na^+: Sodium
80. nm: Nanometer(s)
81. O_2: Oxygen
82. O_2^-: Superoxide anion
83. OCT: Optical coherence tomography
84. ORA: Ocular Response Analyzer
85. p: p-value
86. PACK-CXL: Photoactivated Chromophore for Keratitis – corneal collagen crosslinking
87. PDT: Photodynamic therapy
88. P-CXL: Pulsed corneal crosslinking
89. PCV: Polypoidal choroidal vasculopathy

90. PG: Proteoglycan
91. PKP: Penetrating keratoplasty
92. PMD: Pellucid marginal degeneration (keratotorus)
93. PMMA: Polymethylmethacrylate
94. Post-CXL: After corneal crosslinking procedure
95. PRC: Posterior radius of curvature
96. Pre-CXL: Before corneal crosslinking procedure
97. PRK: Photorefractive keratectomy
98. PTK: Phototherapeutic keratectomy
99. RF: Riboflavin
100. RMS: Root mean square
101. ROS: Reactive oxygen species
102. S_0: Ground singlet state
103. S_1: Excited singlet state
104. S-CXL: Standard corneal crosslinking
105. SF_6: Sulfur hexafluoride
106. SP-A1: Stiffness parameter A1
107. T_1: Excited triple state
108. T4: Thyroxine
109. TBI: Tomographic Biomechanical Index
110. TE-CXL: Transepithelial corneal crosslinking
111. TKC: Topographic Keratoconus Classification
112. TNF-α: Tumor necrosis factor α
113. UKS: Universitätsklinikum des Saarlandes (Saarland University Medical Center)
114. UVA: Ultraviolet-A
115. vPDT: Verteporfin PDT
116. µm: Micrometer(s)

2. Summary

2.1 Summary

Introduction:

Corneal crosslinking (CXL) represents a minimally invasive surgical method to stabilize the progression of keratoconus (KC) corneal disease, and can provide good visual results and prevent/postpone the need for a penetrating keratoplasty. The purpose of this study was: 1. to evaluate the effectiveness of epithelium-off accelerated CXL with a fluence of 9 mW/cm^2 for 10 minutes (A-CXL, 9 mW/cm^2, 10 minutes) in patients < 18 years and ≥ 18 years of age, and 2. to assess the reliability of successive measurements of corneal biomechanics using the Corneal Visualization Scheimpflug Technology (Corvis® ST, CST, Oculus, Wetzlar, Germany) in KC ≥ 2 years after A-CXL (9 mW/cm^2, 10 minutes), compared to untreated KC corneas.

Patients and methods:

For the evaluation of the effectiveness of this A-CXL, 151 KC corneas of 124 adult patients and 41 KC corneas of 30 underaged patients were included. The parameters analyzed were the best corrected visual acuity (BCVA) with spectacles (in LogMAR) and the tomographic readings measured with Pentacam® High Resolution (Pentacam® HR, Oculus, Wetzlar, Germany), including the anterior and posterior steep, flat and mean keratometry, as well as astigmatism, the maximal keratometry, thinnest and apex corneal pachymetry at 24 months, 12 and 6 months preoperatively, prior to surgery and 6 weeks, 6 months, 1, 2 and > 2 years postoperatively. The demarcation line was assessed by anterior segment optical coherence tomography (SS-1000 and CASIA 2, Tomey, Nagoya, Japan). Regarding the reliability analysis of CST measurements, two groups were formed, the first (CXLG) consisting of 20 KC corneas of 16 patients ≥ 2 years after A-CXL, and the second control group consisting of 20 non-operated KC corneas of 20 patients, matched according to the ABC parameters of Belin's ABCD KC grading system. The maximal keratometry, the Belin/Ambrósio-Enhanced-Deviation-Index (BAD-D), the biomechanical parameters A1 velocity, deformation amplitude (DA) ratio 2 mm, Ambrósio's relational thickness

to the horizontal profile (ARTh), integrated radius, stiffness parameter A1 (SP-A1) and the Corvis Biomechanical Factor (CBiF, the linearized term of the Corvis Biomechanical Index) were evaluated, presenting the mean values, standard deviations and Cronbach's alpha (CA).

Results:

In the adult group, comparing pre- to postoperative findings after 6 weeks with paired t-test, there was a statistically significant increase of the anterior steep (46.8 ± 4.0|47.1 ± 4.1 diopters, D), flat (50.2 ± 4.3|50.6 ± 4.6 D) and maximal keratometry (57.6 ± 6.8|58.3 ± 6.8 D, p-value < 0.05), while the thinnest pachymetry decreased significantly (459 ± 39|444 ± 42 μm, p-value < 0.05), followed by a statistically significant decrease for the anterior flat (1, 2 and > 2 years, p < 0.0001), mean (1 year, p-value = 0.01 and 2 years, p-value = 0.03) and maximal keratometry (1, 2 and > 2 years, p-value < 0.0001). Similarly for the underaged group, a statistically significant increase preceded at 6 weeks postoperatively, regarding the anterior steep (47.2 ± 5.1|48.5 ± 5.2 D), flat (52.7 ± 5.4|43.8 ± 5.8 D) and mean keratometry values (47.1 ± 2.9|49.8 ± 5.0 D, p-value < 0.05) with parallel significant decrease of the thinnest pachymetry (460 ± 37|439 ± 36 μm, p-value < 0.05), followed by statistically significant decrease for the steep and mean keratometry until 2 years postoperatively. The maximal keratometry increased without statistical significance 6 weeks postoperatively (61.5 ± 8.5|62.6 ± 8.0 D) and decreased significantly even > 2 years after A-CXL. The posterior keratometry values did not change significantly for both groups after A-CXL. The BCVA showed in both adult and underaged groups a statistically significant decrease at 6 weeks postoperatively (0.35 ± 0.02|0.39 ± 0.02, 0.44 ± 0.04|0.48 ± 0.05 respectively, p-value < 0.05), followed by gradual improvement until > 2 years postoperatively. The demarcation line reached on average a similar corneal depth of 53.6 % and 52.1 % for both groups respectively. Concerning the reliability analysis of the Corvis® ST biomechanical measurements, both established control and CXLG groups were tomographically comparable in terms of BAD-D and maximal keratometry (p-value > 0.05, paired t-test). Comparable values with excellent reliability measurements were found for A1 velocity, DA ratio 2

mm, integrated radius and CBiF in both groups ($p > 0.005$, CA ≥ 0.960). The values of ARTh were found to be higher in the control group compared to CXLG (1771 ± 59|155.21 ± 65, p-value = 0.0062, CA: 0.993|0.993), while SP-A1 values were higher at CXLG (52.2 ± 16|59.2| 13, p-value = 0.0018, CA: 0.912|0.912).

Conclusions:

Epithelium-off A-CXL (9 mW/cm^2, 10 minutes) can successfully provide stabilization of KC and reach a deep demarcation line. Features of progression, within the first 6 weeks postoperatively, which we called “pseudoprogression” are not indicative of the long-term effect. The reliability analysis of the biomechanical measurements shows in summary excellent reliability in both control and crosslinked KC corneas, whereas the values of ARTh and SP-A1 showed a statistically significant difference between the groups, indicating that CXL affects the biomechanical measurements over more than 2 years.

2.2 Zusammenfassung

Einleitung:

Die Hornhautvernetzung, das so gennante Crosslinking (CXL), ist eine minimalinvasive operative Methode zur Stabilisierung der fortschreitenden Keratokonus-Hornhauterkrankung (KK) und kann gute visuelle Ergebnisse liefern sowie die Notwendigkeit einer perforierenden Keratoplastik verhindern bzw. verzögern. Ziel dieser Studie war es, 1. die Wirksamkeit der beschleunigten Epithel-Off-CXL-Behandlung mit einer Fluence von 9 mW/cm^2 für 10 Minuten (A-CXL, 9 mW/cm^2, 10 Minuten) bei Patienten im Alter <18 und von ≥ 18 Jahren zu untersuchen, und 2. die Zuverlässigkeit aufeinanderfolgender Messungen der Biomechanik der Hornhaut mit der Corneal Visualization Scheimpflug Technology (Corvis® ST, CST, Oculus, Wetzlar, Deutschland) bei KK ≥ 2 Jahre nach A-CXL 9 mW/cm^2, 10 Minuten, im Vergleich zu unbehandelten KK-Hornhäuten zu bewerten.

Patienten und Methoden:

Für die Bewertung der Wirksamkeit von dies A-CXL, wurden 151 KK-Hornhäute von 124 erwachsenen Patienten und 41 KK-Hornhäute von 30 Patienten < 18 Jahren einbezogen. Die analysierten Parameter waren die bestkorrigierte Sehschärfe (BCVA) mit Brille (LogMAR) und die mit der Pentacam® High Resolution (Pentacam® HR, Oculus, Wetzlar, Deutschland) gemessenen tomographischen Werte, einschließlich der vorderen und hinteren steilen, flachen und mittleren Keratometrie sowie des Astigmatismus, der maximalen Keratometrie, der dünnsten und der Apex-Hornhautpachymetrie 24 Monate, 12 und 6 Monate präoperativ, vor der Operation und 6 Wochen, 6 Monaten, 1, 2 und > 2 Jahren postoperativ. Die Demarkationslinie wurde mittels optischer Kohärenztomographie des vorderen Augenabschnitts (SS-1000 und CASIA 2, Tomey, Nagoya, Japan) beurteilt. Für die Zuverlässigkeitsanalyse der Corvis® ST-Messungen wurden zwei Gruppen gebildet, die erste (CXLG), bestehend aus 20 KK-Hornhäuten von 16 Patienten ≥ 2 Jahre nach A-CXL, und die zweite Kontrollgruppe, bestehend aus 20 nicht operierten KK-Hornhäuten von 20 Patienten, die nach den ABC-Parametern des ABCD-KK-Gradingsystems von Belin gematcht wurden. Die maximale Keratometrie, der Belin/Ambrósio-Enhanced-

Deviation-Index (BAD-D), die biomechanischen Parameter A1 Velocity, Deformation Amplitude (DA) Ratio 2 mm, Ambrósio‘s relational Thickness to the horizontal Profile (ARTh), integrated Radius, Stiffness Parameter A1 (SP-A1) und Corvis Biomechanic Factor (CBiF, der linearisierte Term des Corvis Biomechanic Index) wurden unter Angabe der Mittelwerte, Standardabweichungen und Cronbach‘s Alpha (CA) ausgewertet.

Ergebnisse:

In der Erwachsenengruppe zeigte sich im Vergleich der prä- und postoperativen Befunde nach 6 Wochen mit dem gepaarten t-test eine statistisch signifikante Zunahme der vorderen steilen (46,8 ± 4,0|47,1 ± 4,1 Dioptrien, D), flachen (50,2 ± 4,3|50,6 ± 4,6 D) und der maximalen Keratometrie (57,6 ± 6,8|58,3 ± 6,8 D, p-Wert < 0,05), während die dünnste Pachymetrie signifikant abnahm (459 ± 39|444 ± 42 µm, p-Wert < 0,05), gefolgt von einer statistisch signifikante Abnahme der vorderen flachen (1, 2 und > 2 Jahre, p-Wert < 0,0001), mittleren (1 Jahr, p-Wert = 0,01 und 2 Jahre. p-Wert = 0,03) und maximalen Keratometrie (1, 2 und > 2 Jahre, p-Wert < 0,0001). Auch in der Gruppe der Minderjährigen war ein statistisch signifikanter Anstieg der vorderen steilen (47,2 ± 5,1|48,5 ± 5,2 D), flachen (52,7 ± 5,4|43,8 ± 5,8 D) und mittleren Keratometriewerte (47,1 ± 2,9|49,8 ± 5,0 D, p-Wert < 0,05) bei gleichzeitiger signifikanter Abnahme der dünnsten Pachymetrie (460 ± 37|439 ± 36 µm, p-Wert < 0,05) zu verzeichnen, gefolgt von einer statistisch signifikanten Abnahme der steilen und mittleren Keratometrie bis 2 Jahre postoperativ. Die maximale Keratometrie stieg ohne statistische Signifikanz 6 Wochen postoperativ an (61,5 ± 8,5|62,6 ± 8,0 D), nahm im Verlauf aber bis > 2 Jahre nach A-CXL signifikant ab. Die Werte der posterioren Keratometrie änderten sich nach der A-CXL in beiden Gruppen nicht signifikant. Die bestkorrigierte Sehschärfe zeigte sowohl in der Erwachsenen- als auch in der Minderjährigen-Gruppe eine statistisch signifikante Abnahme nach 6 Wochen postoperativ (0,35 ± 0,02|0,39 ± 0,02, 0,44 ± 0,04|0,48 ± 0,05, p-Wert < 0,05), gefolgt von einer allmählichen Verbesserung bis > 2 Jahre postoperativ. Die Demarkationslinie erreichte im Durchschnitt eine ähnliche Hornhauttiefe von 53,6 % bzw. 52,1 % für beide Gruppen. Was die

Zuverlässigkeitsanalyse der biomechanischen CST Messungen betrifft, so waren die beiden etablierten Kontroll- und CXLG-Gruppen tomographisch vergleichbar in Bezug auf BAD-D und maximale Keratometrie (p-Wert > 0.05, gepaarter t-Test). Vergleichbare Werte mit ausgezeichneter Zuverlässigkeit wurden für A1-Velocity, DA Ratio 2 mm, integrated Radius und den CBiF in beiden Gruppen ermittelt (p > 0,005, CA ≥ 0,960). Die Werte von ARTh waren in der Kontrollgruppe höher als in der CXLG-Gruppe (177 ± 59|155,21 ± 65,00, p-Wert = 0,0062, CA: 0,993|0,993), während die SP-A1-Werte in der CXLG-Gruppe höher waren (52,2 ± 16,0|59,2 ± 13,0, p-Wert = 0,0018, CA: 0,912|0,912).

Schlussfolgerungen:

Epithel-off A-CXL (9 mW/cm^2, 10 Minuten) kann erfolgreich zur Stabilisierung des KK beitragen und eine tiefe Demarkationslinie erreichen. Progressionserscheinungen innerhalb der ersten 6 Wochen postoperativ, die wir als "Pseudoprogression" bezeichnet haben, sind kein Indikator für den langfristigen Effekt. Die Zuverlässigkeitsanalyse der biomechanischen Messungen zeigt insgesamt eine ausgezeichnete Zuverlässigkeit sowohl bei den Kontroll- als auch bei den vernetzten KK-Hornhäuten, während die Werte von ARTh und SP-A1 statistisch signifikante Unterschiede zwischen den Gruppen aufwiesen, was darauf hindeutet, dass CXL die biomechanischen Messungen über mehr als 2 Jahre beeinflusst.

3. Introduction

3.1 Anatomy and physiology of the human cornea

The cornea consists of a complex structure with utmost importance for the function of the eye. It is transparent and avascular and acts as a structural and barrier for infections of the eye. The cornea is convex and its refractive power, meaning the degree at which the cornea converges or diverges light, has a significant contribution of about 75 % of the dioptric system of the eye, aiming at focusing the light to the retina [158,190]. Thus, the loss of corneal transparency and refractive errors can lead to significant visual impairment [251].

The cornea of an adult has an averaged horizontal diameter of 11.5 to 12 mm, which is about 1 mm larger than its vertical diameter. The thickness of the cornea is about 0.5 mm, increasing from the center to its periphery until a thickness of about 0.7 mm, which creates flattening peripherally and steepening centrally, leading to asphericity, and facilitates peripheral vision [61,158]. Its structure consists of five layers: the corneal epithelium, the Bowman's lamella, the corneal stroma, the Descemet membrane and the endothelium [61,98], all of which play an essential role in maintaining the transparency and the functionality of the cornea [251]. The corneal layers are pictured in **Figure 1**. The functions of the corneal layers, the tight packing of the stratified squamous corneal epithelial cells and the high metabolic activity, which takes place in each one of the corneal layers, along with the lack of vascularization, ensure the corneal transparency [30,297]. Dua et al. presented in 2013 a sixth layer between the corneal stroma and the Descemet's membrane, which was called Dua's layer [70,71], the existence of which was refuted by a multicenter study based on transmission electromicroscopy [263].

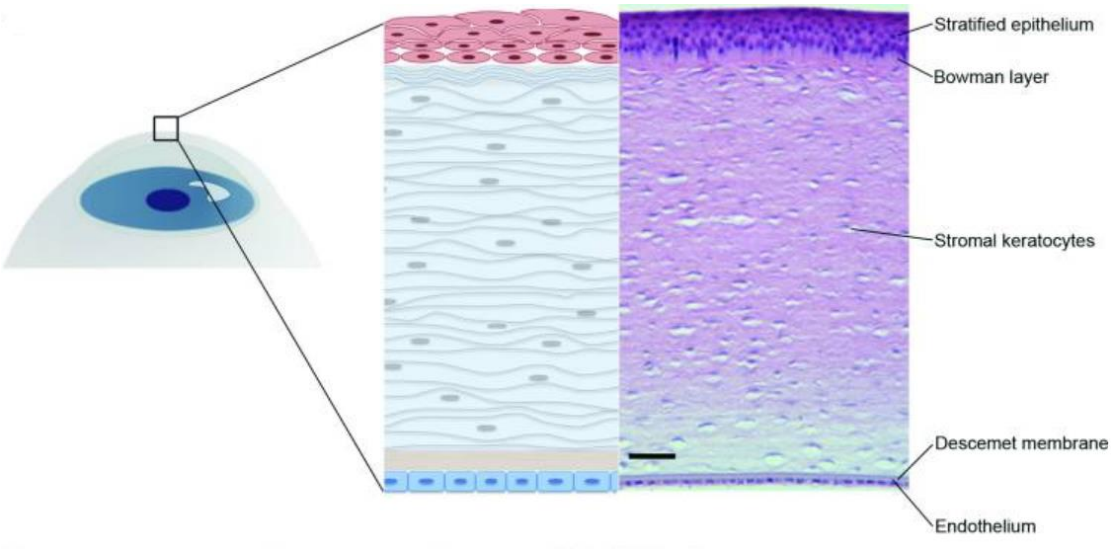

Figure 1: *Corneal layer structure and histological analysis. Source: Ghezzi CE, Rnjak-Kovacina J, Kaplan DL (2015). Corneal tissue engineering: Recent advances and future perspectives. Tissue Eng Part B Rev 21:278-287. doi: 10.1089/ten.teb.2014.0397* [98].

Corneal epithelium

The development of the human eye starts at the 17th day of gestation, while the cornea derives from the ocular surface ectoderm which already forms at the 6th gestation week, along with the lens and conjunctival epithelium, the lacrimal glands and the epidermis of the eyelid [50,331]. At that time the lens vesicle has detached from the overlying ectoderm which is the speculated corneal epithelium and first consists of two layers of cells. The basal lamina of the basal epithelial cells is well-structured, the number of mitochondria is larger, the Golgi complex is better developed and the nucleolus of the nuclei is more prominent. At the 7th gestation week the corneal epithelium includes flattened peridermal cells and basal cells [331].

The adult corneal epithelium consists of 4-6 layers nonkeratinized, stratified, squamous epithelial cells (~ 50 μm) with a basal columnar layer which is attached via hemidesmosomes to the basal lamina [61]. The epithelial cells lack large numbers of organelles, which, in combination with the tight positioning of the cells and the lack of vascularization, reduces the scattering of incoming light and reinforces the corneal

transparency [30]. Over the basal cell layer, there are two to three layers of polygonal “wing cells”, whereas the superficial epithelial cells are very thin and are connected to each other by occluding to the zonular fibers. The superficial cells have microvilli which make the apical surface of the cells irregular and wider, permitting better adherence to the mucinal tear film, which smoothens the corneal surface [61,85]. The lifespan of the corneal epithelial cells is estimated about 7-10 days, then involution, apoptosis and desquamation take place. Hence, every week the renewal of a corneal epithelial layer happens, with replacement of the superficial desquamating cells from the deeper layers [61,123].

The epithelial cell regeneration is regulated by stem cells located at the limbus, which is the anatomical and functional margin between the cornea and the conjunctival epithelium [251]. Davanger and Evensen first described in 1971 that the corneal epithelium is renewed through migration of the epithelial cells which are located at the corneal limbus [55], while the existence of stem-like and progenitor cells at the peripheral corneal endothelium and stem cells in the human corneal stroma has been observed [69,93,251], which contribute to the corneal homeostasis. The deeper epithelial cells show a continuous movement towards the tear film where they are suspended in the end [85].

Between the epithelial cells, different cell populations can be found, mainly histiocytes, macrophages, lymphocytes and pigmented melanocytes, mostly in the peripheral cornea. Furthermore, antigen-presenting Langerhans cells move from the periphery towards the center of the cornea in cases of inflammation and physiologically with increasing age [214,217].

Bowman’s lamella

The Bowman’s lamella or Bowman’s layer, consists of irregularly placed, tough collagen fibrils in a thin compartment of approximately 8-12 μm thickness, positioned between the basal lamina of the corneal epithelium and the corneal stroma. These fibrils are thinner as those met in the corneal stroma and are mainly collagen types I, III, V and VII, with the latter anchoring to the corneal epithelium. The existence of the

Bowman's layer contributes to maintaining the corneal shape. In case of disruption there is no ability of regeneration and instead scarring can occur [61].

Corneal stroma

The corneal stroma occurs at the 7th gestation week, at the second wave of neural crest migration, where mesenchymal cells, deriving from the neural crest, move centrally between the corneal epithelial and endothelial cells [56,57,61]. It comprises the 80-85 % of the corneal thickness [61] and consists of collagen-producing keratocytes, proteoglycans (PGs) and glycoproteins [206] as well as collagen lamellae. The latter are packed in parallel arrangement and form fibrils [61]. The fibrils, depending on the arrangement of the lamella can be recognized microscopically either as parallel aligned linear structures or as hexagonal arranged circular structures [216]. The arrangement of the corneal fibrils and the hydration of the stroma are essential for the maintenance of the corneal transparency [216]. In 1957, Maurice first investigated the corneal transparency and proposed the lattice theory, according to which the collagen fibrils have equal diameter and are equally spaced from each other, thus providing transparency and reducing light scattering [30,190]. These get obliquus orientation in the anterior third of the stroma and parallel orientation in the posterior two thirds and cover the entire diameter of the cornea up to the corneal limbus [214,222,223]. The stroma is thicker peripherally than centrally and the orientation of the collagen fibrils is more cyclical near the limbus [204]. The number of layers of collagen lamellae is estimated ~ 300 at the center of the cornea and ~ 500 at the periphery near the limbus [242]. Furthermore, the packing of the lamellae was found to be more dense at the central cornea compared to the periphery [206], whereas the collagen lamellae are narrower and set more obliquely at the anterior third of the stroma compared to the posterior two thirds [190,242].

The PGs are essential for the arrangement of the collagen fibrils in the stroma and are complex macromolecules, comprising of linear chains of sulphated glycosaminoglycans, set by repeating disaccharides, which are connected with covalent bonds to a central core protein [267,268]. Morphometry of cupromeronic blue-stained proteoglycan molecules in animal corneas, versus that of purified proteoglycans

stained in vitro, implies that tertiary structures contribute to the corneal ultrastructure [267]. In the corneal stroma three types of GAG side chains can be found, the chondroitin/dermatan sulfate, keratan sulfate and heparan sulfate. In cases of corneal opacification, a reduction of the keratan sulfate was observed, implicating the role of these glycosaminoglycans (GAGs) for the maintenance of corneal transparency [128].

In a swollen cornea with edema and lost transparency, the distance between the fibrils is increased [207]. The collagen included in the corneal stroma is mainly of type I, III, V and VI, although type VII forms can be found anchoring to the epithelium [158,216]. At a hydration level of < ~3.5 mg H_2O/mg dry tissue, the corneal stroma remains transparent. The stromal hydration is maintained by the corneal endothelium through active transport mechanisms [30].

The keratocytes existing in the corneal stroma produce collagen, GAGs and other extracellular substances [30,49,214]. They have high metabolic activity through embryogenesis but remain mostly quiet under physiological conditions throughout life [128,214] but are activated in cases of corneal injury and/or inflammation [30,49]. They comprise of a compact cell body and many cytoplasmic lamellapodia, thus acquiring a dendritic-like morphology which enables them to connect to each other in a three dimensional (3D) network [119,128]. The anatomy of the keratocytes enables them to diminish the light scattering and permit cell communication [128].

The corneal stroma includes a small number of corneal stromal stem cells, cited in the anterior peripheral stroma near the limbus and the epithelial stem cells [49], which generate keratocytes [238].

Descemet membrane

The Descemet membrane starts to form at the beginning of the 8th week of gestation from deposits of the endothelial cells, at first as spots of lamellar material until completion of a complete layer in the 16th week of gestation, while collagen deposition continues until the 8th month of gestation, leading to a 3 μm thick layer [303]. The Descemet membrane is found to be unidentifiable from the corneal endothelium at 8 weeks of gestation, and at 3 months prepartum it is thin and vague in structure.

Maturation continues involving increase of thickness and during the 7th month of gestation and it is mainly completed before eye opening, leading to formation of an anterior banded layer and a posterior non-banded layer The first appears to develop until birth, while the latter continues to increase in thickness during the adult life as a result of endothelial cell activity [59]. The Descemet membrane represents also the basal lamina of the corneal endothelium with slow, gradual thickening with increasing age [284] and serves as its supporter [206].

Corneal endothelium

The cornea is a highly hydrated structure, consisting by 78 % of water. During embryogenesis, at the 5th week of gestation until the 7th week of gestation, mesenchymal cells, which derive from the neural crest, separate from the neural plate and migrate from the periphery towards the center of the ectoderm and lens in order to form a double-layered primary endothelium [57,303,331]. At the 8th gestation week the endothelium becomes single-layered [56,57], at the 5th-7th month of gestation the density of Na^+/K^+- activated adenosine tri-phosphatase (ATPase) pumps of the endothelial cells reaches the levels of adult cells and the cornea is dehydrated and gains transparency [56,57]. The junctions between the endothelial cells start to form after the monolayer is complete, first the gap junctions and then the apical band, until completion of the adult formation at 20th week of gestation [30].

At birth the corneal endothelium reaches 500.000 cells and a maximal density of 7.500 cells/mm^2 (mean cell density ~ 3000 cells/mm^2) but both number and cell density decrease through life [56,57,284,303]. The endothelial cells of the human cornea cannot regenerate but they tend to enlarge after corneal injury [303]. The corneal endothelium is a single layer of mainly hexagonal cells, about 4 μm thick [30]. The corneal endothelium is responsible for maintaining stromal hydration and nutrition of the corneal cells and securing the transparency of the cornea [30]. In fact, all the nutrient substances deriving from the aqueous humor, including glucose, pass into the cornea through the corneal endothelium, apart from oxygen [168]. They present high metabolic activity, containing mitochondria in abundance and scatter little amount of light. The gap junctions and tight junctions at the apical membrane of the endothelial

cells act as a barrier of the posterior cornea limiting this way the influx of water and solutes into the hydrophilic stroma [56,57,207], but are still passively permeable to nutrients, water and metabolites into the cornea [207]. This permits the maintenance of corneal thickness and transparency, given that the volume of fluid inserting into the corneal stroma is equal to the amount removed by the activity of the corneal endothelium [31,207]. Of utmost importance is the function of the corneal endothelium to maintain the corneal transparency by regulating the corneal hydration [83,283,303]. The routes contributing to this regulation are until today under investigation. It is mainly achieved by the presence of Na^+-K^+-ATPases [295], of HCO_3 and chloride anions, by the carbonic anhydrase activity [30], the existence of voltage-gated ion channels, sodium, potassium, chloride, and calcium channels [30,207]. Furthermore, the presence of a local recirculating electric current is proposed at the intracellular junctions, which permits the dragging of water paracellularly, and was named electro-osmosis [86]. In case of dysfunction of the corneal endothelium (eg. trauma, corneal dystrophies, inflammation etc.), the corneal dehydration is disrupted and corneal edema occurs, which can lead to corneal opacification [30].

Corneal nerve plexus

The cornea is densely innervated. In 1831, Schlemm was the first to announce the discovery of innervation at the limbal region of the cornea [129,261,262]. The majority of the nerve fibers are sensory, originating from the trigeminal nerve and are stimulated through mechanical, thermal and chemical stimuli. Furthermore, small populations of sympathetic fibers from the superior cervical ganglion have been described [215]. In 1982 Schimmelpfennig described four main structures for innervation of the corneal epithelium, including: stromal nerves penetrating the Bowman's lamella mostly dichotomously; the basal epithelial nerve plexus which mainly contain long fibers originating from the stromal nerves; the dendritic cells which disperse among the basal plexus and may connect with nerve fibers; nerve ends which derive from the basal nerve plexus and divide in a dichotomous way in the superficial nerve plexus [261]. The nerves found in the corneal stroma derive from the sclera and ciliary body. The scleral nerves are dense in the region of the corneal limbus

and disperse into horizontal branches towards the stroma in a radial way, where they form smaller branches, most of which penetrate into the epithelium to generate the peripheral epithelial nerve network [129]. The central epithelial nerve density was found to decrease with increasing age and irregular lesions could be observed at the peripheral region of the superficial stroma under the basement membrane [129]. The corneal nerve distribution is depicted in **Figure 2**.

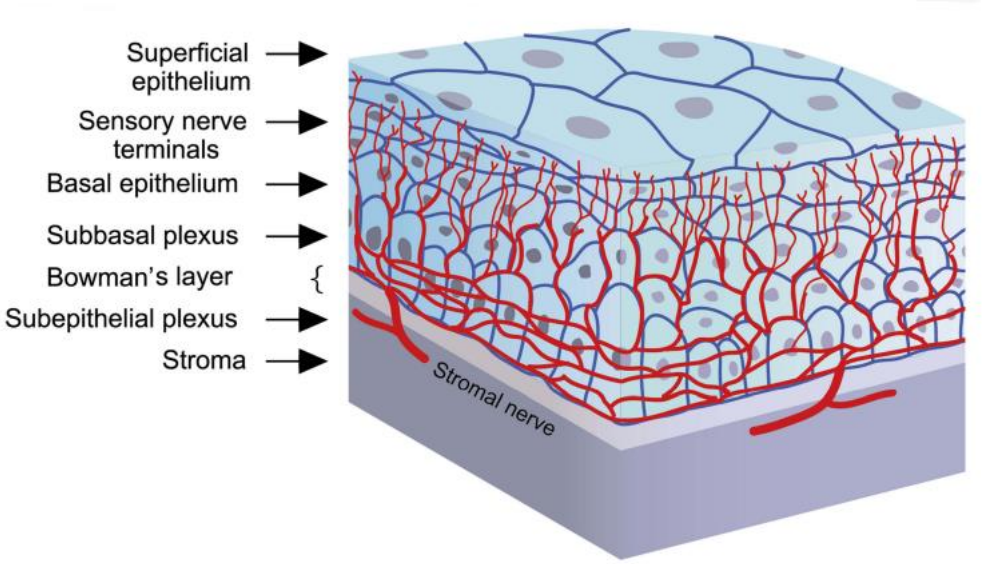

Figure 2: *Distribution of corneal nerves. Source: Sheha H, Tighe S, Hashem O, Hayashida Y. Update on Cenegermin eye drops in the treatment of neurotrophic keratitis (2019). Clin Ophthalmol 13:1973-1980. doi: 10.2147/OPTH.S185184* [98].

Dua's layer

In 2013, Dua and colleagues proposed that the most posterior region of the stroma, consists of a separate 6th corneal layer of ~ 10 µm thickness, (range 6-16 µm), almost completely deprived of keratocytes and containing mainly type I and less type VI collagen as well as elastin in a concentration higher than in other layers of the cornea. It was described to extend peripherally further than the Descemet membrane, reaching the trabecular meshwork [70,71]. In 2015, Schlötzer-Schrehardt et al. investigated the

consistency of the posterior stroma and did not confirm the existence of a separate acellular region pre-descemetally [263]. Its existence is until today controversial.

3.2 Study of the corneal surface: Keratometry, corneal topography and corneal tomography

As mentioned above, the cornea is flatter peripherally and steeper centrally (prolate) and thus is characterized by asphericity. It has a leading role regarding the refractive power of the eye, thus it is an object of study since more than three centuries [64,157,178]. The analysis of the corneal properties is essential for refractive surgery not only for the screening of candidate patients but also for examining the postoperative outcome. Furthermore it is crucial for the recognition, diagnosis and observation of the course of corneal diseases such as corneal scarring, corneal dystrophies and corneal ectasias [143]. The evaluation of the refractive corneal properties continues to develop at a galloping pace, permitting the thorough investigation of the corneal entities and the evolution of the corneorefractive surgical techniques [250].

In 1670 Isaac Barrow and Isaac Newton studied the astigmatism produced from oblique rays on a spherical lens. The corneal astigmatism was discovered at two different time points, in 1800 by Thomas Young and in 1825 by G.B. Airy [178]. The first attempts to measure the corneal curvature were performed by Scheiner in the 17th century, who invented spheres made of glass, with diameters comparable to the anterior corneal curvature, and studied their reflections [290]. He relied on the hypothesis that, when the size of an object and the distance between it and the cornea is known, the curvature of the anterior surface of the cornea can be calculated by measuring the size of the reflection of an object from the anterior part of the cornea [102,259]. The device produced to measure the corneal surface was called keratometer.

3.2.1 Keratometer

The first term for the device used to study the anterior corneal curvature was “ophthalmometer”, and given by Francois-Pourfour du Petit in 1728 who created a

device for studying cadaver eyes. The term “keratometer” was introduced many years and studies later, in the 1800s, by Swan M. Burnett. The keratometer (or ophthalmometer) is a device used for the calculation of the anterior corneal curvature and astigmatism. Jesse Ramsden and Everard Home constructed a preceding form of keratometer in 1796 using the ‘principle of visual doubling’, practically meaning the congruence of the image of the object through two mirrors, enabling the reduction of artefacts because of motion. The first keratometer was invented by Hermann von Helmholtz in the 19th century, aiming at studying the changes of the shape of the cornea *in vivo* [102]. The principle of keratometry is that the anterior surface of the cornea acts like a mirror with different sizes according to the corneal curvature. Thus, the radius of the corneal curvature could be estimated depending on the image size from the anterior corneal surface [102,157] . Helmholtz described his ophthalmometer in 1855 as a form of telescope, comprising two movable glass plates placed close to one another in front of an objective. The position of the plates is parallel in such way that one half of the image could be seen through one plate and the second half of the image through the other plate. By rotating the plates in opposite directions, the image would split into two parts and the distance of the formed images was related to the degree of rotation of the two plates. A box containing adjustable glass plates was attached to one end of the telescope. It was of great importance that the calculation of the anterior corneal curvature was independent of the distance of the object. Other than that, the device could tolerate small eye movements because the images would move to the same direction, maintaining their relative positions [157].

Several studies and modifications of the Helmholtz keratometer followed since then [102,110,178]. Another important historical modification took place in 1881, when Javal and Schiötz evolved the Helmholtz keratometer by replacing the parallel glass plates with a birefringent quartz prism and using two small screens with anterior illuminations instead of transillumination. Other than that, the device became more compact, smaller and easier to use [12] and offered the ability to determine the direction of the steepest and flattest meridians of the cornea by rotating 90° [102,157]. The keratometer enables the localization of the steepest meridian and power of the

meridian in a distance of 90°. Because the device assumes the cornea as a spherocylindrical surface, it provides no information of the topography central or peripheral to the points of measurement, whereas mild irregularities of the corneal surface may lead to significant mire distortion [322]. The assumption of spherocylindrical surface centrally correlates to a normal corneal surface, and this makes the keratometer a useful tool for contact lens fitting [322]. The keratometry device calculates the anterior curvature at 2.5-4.0 mm and the normal values range between 40-47 D (mean 43 D) [157]. However, only small distortions of the corneal topography can lead to visual impairment [157]. One of the most important corneal entities that causes irregular astigmatism, corneal thinning with alteration of the corneal curvature and structure is keratoconus (KC).

3.2.2 From the keratoscope to the evolution of corneal topography and tomography

The keratometry principles were essential for the development of the keratoscope and the further examination of corneal irregularities. In 1827 David Brewster studied the distortion of the image of the flame reflected on the corneal surface [178]. The keratoscope was first constructed by Henry Goode in 1847 [250]. António Plácido da Costa, an ophthalmologist and microbiologist of Portuguese origin, further advanced this invention in 1880 creating a hand-held keratoscope (or Placido disc) comprising of a flat disk with alternating white and black circular bands like rings. A circular aperture is located at the center of the disc, through which the examiner can look at the eye of the examined person in order to observe the form of the rings reflected upon the anterior corneal surface [143,178]. In case of existence of astigmatism or aberration, the rings will not appear circular but like an ellipsoid instead [157]. The steeper the cornea, the less the diameter of mires produced at the image created from the keratoscope, which, in case of irregularity is distorted. The calculation of the radius of curvature from a specific point of the corneal surface can be performed by observing the separation of the mires at that point [322]. The addition of a camera behind the keratoscope creates the photo-keratoscope, which permits the observation of progression of a corneal entity and the potential healing effect of a therapy [156,157].

The photokeratoscope surpasses the keratometer in that it provides information from a larger region of the corneal surface [322]. In 1896 Gullstrand et al. presented the use of the Placido disc in order to create a corneal map in both the horizontal and vertical meridian by measuring the cornea at central and eccentrical fixation. Using a camera and photography of the mires of the keratoscopy, measurements were performed and power profiles of each cornea were achieved in both meridians [111,157]. In 1981 Rowsey et al. introduced the corneascope, a refinement of the Placido disc permitting the calculation of the midperipheral and peripheral corneal radius and curvature values [250]. Cohen et al. made equations to assess the abnormalities of the corneal shape from photographs taken by the keratoscope [47], while Doss et al. reported indices calculated from statistical analysis of digitized photographs taken with the keratoscope, which could be useful in diagnosis of corneal diseases and contact lens fitting [66]. Stephen D. Klyce extended the algorithm of Doss and developed a computer-assisted system with high resolution, which could record up to 8000 points per photokeratograph. This enabled the reduction of movement errors, represented the shape of a cornea through 3D graphs and presented improved data formats which facilitated clinical assessment [156]. The addition of color-coded topographic maps at the era of computerized corneal topography improved the comprehension of the corneal configuration and power as well as the clinical interpretation [185].

3.2.3 Applications of the corneal topography

The computer-assisted corneal topography has been used first and foremost for the interpretation of the normal cornea [64,143]. It is also essential for screening patients who are candidates for refractive surgery and helps to improve surgical procedures such as laser in situ keratomileusis (LASIK) and photorefractive keratectomy (PRK). Its application is critical for the detection of corneal irregularities and disease entities such as KC or pellucid marginal degeneration (PMD) even before the presentation of clinical signs [9], as well as for the observation of the clinical course, including corneal scarring, limbal dermoid and pterygium [143]. Whereas the corneal topography permits the study of the corneal surface, it must be differentiated from corneal

tomography which offers a 3D corneal analysis and is widely preferred for the analysis of KC [143].

3.2.4 Corneal tomography

The word ‘topography’ derives from the ancient Greek words *τόπος* (‘*topos*’ = “place”) and *γράφω (‘grafo*’ < ‘grafein’ = “write”) and it means “to describe a place” [292]. It is practically used to describe the study of the surface and features of the Earth. Corneal topography is a term describing the imaging of a map of the surface curvature of the cornea. The word ‘tomography’ derives from the ancient Greek words *τομή* (‘*tomi*’) meaning “slice” and *γράφω (‘grafo*’) which means “write” [292]. Corneal tomography is a term used to describe the acquirement of multiple slit images of the cornea, thus providing data from both anterior and posterior cornea [9].

Hence, the main differentiation between the corneal topography and tomography is that the former enables the study of the curvature of the anterior cornea without the ability to present information of the posterior cornea, while the latter provides a 3D presentation and analysis of both anterior and posterior corneal segment as well as pachymetry mapping [80]. The use of slit-imaging technologies was an important step in regards to corneal imaging as it permitted the measurement not only of the anterior but also the posterior corneal surface, as well as the spatial relationship between these surfaces, thus creating a corneal thickness map [9]. Horizontal slit scanning, rotational Scheimpflug imaging, arc scanning with very high-frequency ultrasound and optical coherence tomography are advanced technologies used worldwide for tomography measurements [9]. Current corneal tomography devices that are widely used, are: 1) Scanning slit devices such as Orbscan IIz (Bausch & Lomb, Rochester, New York, USA, 2) Scheimpflug cameras such as the Pentacam® (Oculus Optikgeräte GmbH, Wetzlar, Germany), Galilei (Ziemer Ophthalmic Systems AG, Port, Switzerland) and Sirius (Costruzione Strumenti Oftalmici, Florence, Italy), which, along with Galilei include a large cone shaped Placido disc as well and 3) Optical coherence tomography (OCT)-based devices, such as the Anterion (Heidelberg Engineering, Heidelberg, Germany, Visante (Carl Zeiss Meditec AG, Jena Germany) [143]. The Scheimpflug principle was first introduced by Theodor Scheimpflug, an Austrian cartographer

[9,10]. Some examples of corneal topography and tomography devices are listed in **Table 1**. The most common and widely used tomography device is the Pentacam®, which we will further analyze.

Table 1: Corneal topography and tomography devices

Corneal topography		
Technology		Devices
Placido disc - Large cone topography		Antares, Sirius and MS-39 (Costruzione Strumenti Oftalmici, CSO, Florence, Italy), Keratograph® 5M (Oculus, Optikgeräte, Wetzlar, Germany), Topcon KR-1W (Topcon, Tokyo, Japan), Zeiss Atlas (Carl Zeiss AG, Jena, Germany), Galilei† (Ziemer Ophthalmic Systems AG, Switzerland)
Placido disc - Small cone topography		Medmont E300 (Medmont International Pty Ltd.)
Color light-emmitting diode		i-Optics Cassini and i-Optics Cassini Ambient (Cassini, The Netherlands)
Corneal tomography		
Technology		Devices
Scanning slit - white flash light	Horizontal slit scan (with * including Placido disc)	Orbscan® II* (Bausch & Lomb, Rochester, New York)
Scheimpflug imaging - blue-light emitting diode (470-475 nm)	Rotating Scheimpflug (with * including Placido disc)	Galilei* (Ziemer, Port, Switzerland), Pentacam® (Oculus Optikgeräte, GmbH, Wetzlar, Germany), Oculyzer® (Wavelight AG< Erlangen, Germany), Preciso (iVIS Technologies, Toronto, Italy), Scansys (Mediworks, Shangai, China), Sirius*† (Costruzione Strumenti Oftalmici, CSO, Florence, Italy), TMS-5* (Tomey Corp, Nagoya, Japan)
Optical coherence tomography (OCT) - superluminescent diode laser (830-845 nm)	Spectral domain	CSO MS-39 (Costruzione Strumenti Oftalmici, CSO, Florence, Italy), Optopol Revo, CIRRUS™ HD-OCT 5000 with FastTrac™ (Carl Zeiss AG, Jena, Germany), Spectralis diagnostic imaging platform (Heidelberg Engineering Inc), iVUE spectral domain OCT (Optovue, Incorporated), 3D OCT-1 Maestro System (Topcon Medical Laser Systems)

OCT - rapidly tuned laser with longer wavelength (1310 nm)	Swept source	Anterion® (Heidelberg Engineering, GmbH, Heidelberg, Germany), Casia SS-1000/ Casia 2 (Tomey, Nagoya, Japan), Zeiss Visante® omni† (Carl Zeiss AG, Jena, Germany)
Arc scanning with very high-frequency ultrasound		Artemis (ArcScan, Momson, Colorado)

Table 1: *Examples of corneal topography and tomography devices. With * marked Scheimpflug systems including Placido disc, with † marked devices which produce both topography and tomography analysis. Based on: Ambrósio R, Belin MW (2010) Imaging of the cornea: T Topography vs tomography. J Refract Surg 26:847–849* [9], *Kanclerz P, Khoramnia R, Wang X (2021) Current developments in corneal topography and tomography. Diagnostics (Basel) 11:1466* [143], *Koh, S. (2022). Topography and tomography of keratoconus. In: Das, S. (eds) Keratoconus. Springer, Singapore* [161].

3.2.5 Corneal tomography – Pentacam High Resolution (HR)

The Pentacam® system is widely used in daily clinical practice for evaluation of cataract and the power of intraocular lenses, detection of glaucoma, examination of corneal transplants and perioperative guidance, observation of corneorefractive operations such as LASIK and PRK and corneal irregularities such as KC [212]. The device uses a monochromatic blue light-emitting diode (LED) at 475 nanometers (nm) and includes a rotating Scheimpflug camera to analyze the anterior segment. It captures 25 to 50 images within 2 seconds, and each slit image is created from about 25.000 points, including 500 true corneal elevation points and forms a 3D corneal map [278]. The Pentacam® High Resolution (HR) device generates the 3D image from 138.000 elevation points using high-resolution, 1.45 mega-pixel camera [8,10,212]. There are several options of scanning available, including a 25-picture (1 second) scan, a 50-picture (2 seconds) scan and a cornea fine (50 pictures in 1 second) scan. Any eye movement is detected by a second included camera and corrected [202]. The device provides topo-/tomography data, pachymetry mapping, chamber angle, volume and height, densitometry of the lens and a number of corneal indices. The function of the rotating Scheimpflug camera creates three imaginary perpendicular planes, the lens, image and object and not only two as it happens with the traditional camera. This permits an extension of depth of focus, hence resulting in a sharp image resolution

[8,10,212]. Pentacam® HR provides repeatable and reproducible results, offering precise pachymetry maps, corneal maps, anterior chamber depth maps, corneal volume, topometric Q values and indices (**Figure 3**) [202]. Furthermore, the software of Pentacam® HR enables a fast screening report, the Topographical Keratoconus Classification (TKC), a Tomographical Keratoconus Classification, including the Belin ABCD Keratoconus Staging (**Figure 4**) and Progression Display, and comparative displays for follow-up [342]. Important is the Belin-Ambrósio enhanced ectasia display total deviation value (BAD-D), a multivariate index derived from a combination of data of anterior and posterior corneal elevation, as well as pachymetric values of the cornea, thus enabling recognition of ectasia and an effective screening for refractive surgery (**Figure 5**) [65].

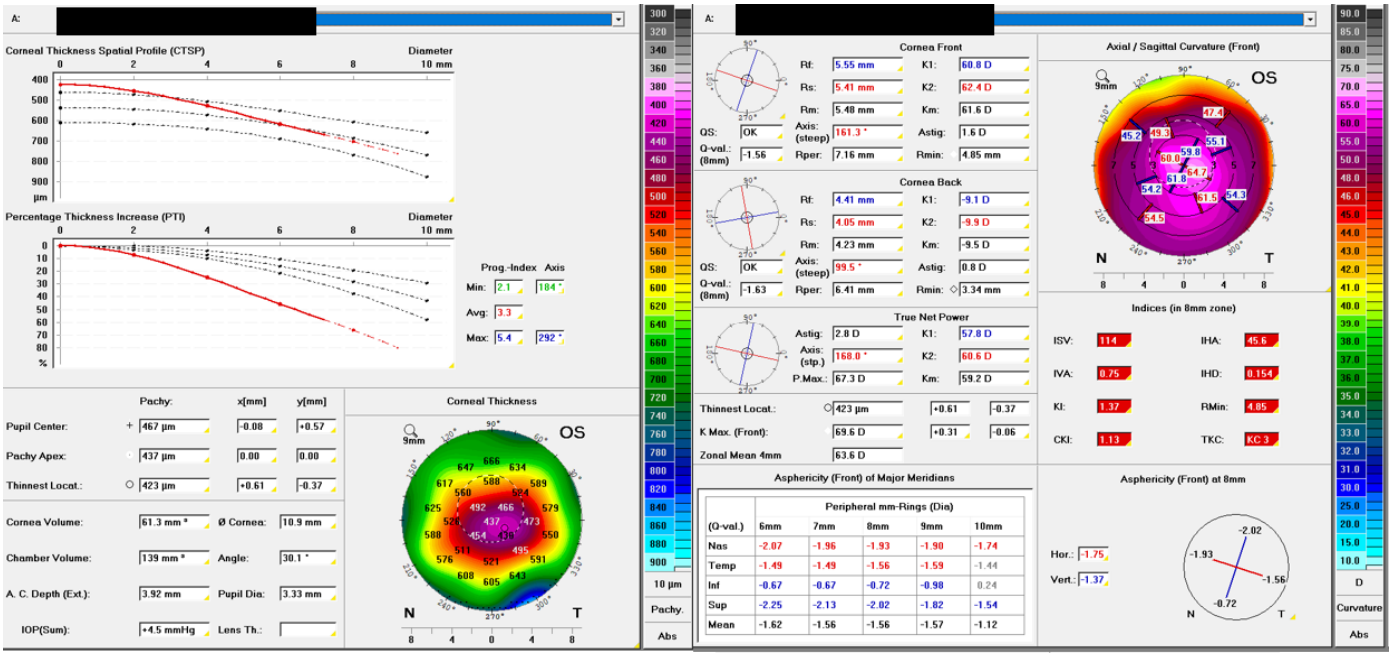

Figure 3: *Pentacam® HR analysis of a keratoconic cornea. Analysis of anterior and posterior curvature, pachymetry, anterior chamber depth, and corneal indices. Image from archive of the Department of Ophthalmology, Saarland University Medical Center, UKS.*

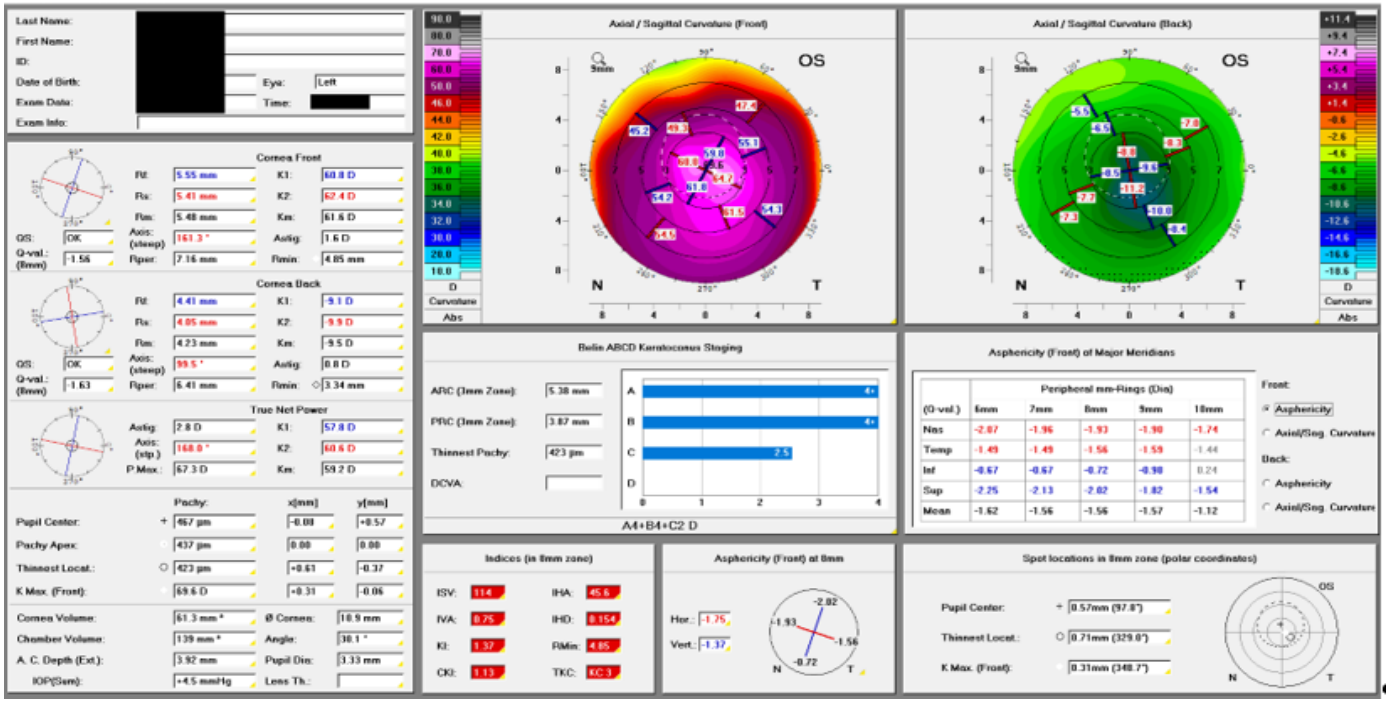

Figure 4: *Pentacam® HR analysis of a keratoconic cornea. Display of ABC(D) Grading according to Belin's ABCD keratoconus grading system. Image from archive of the Department of Ophthalmology, Saarland University Medical Center, UKS.*

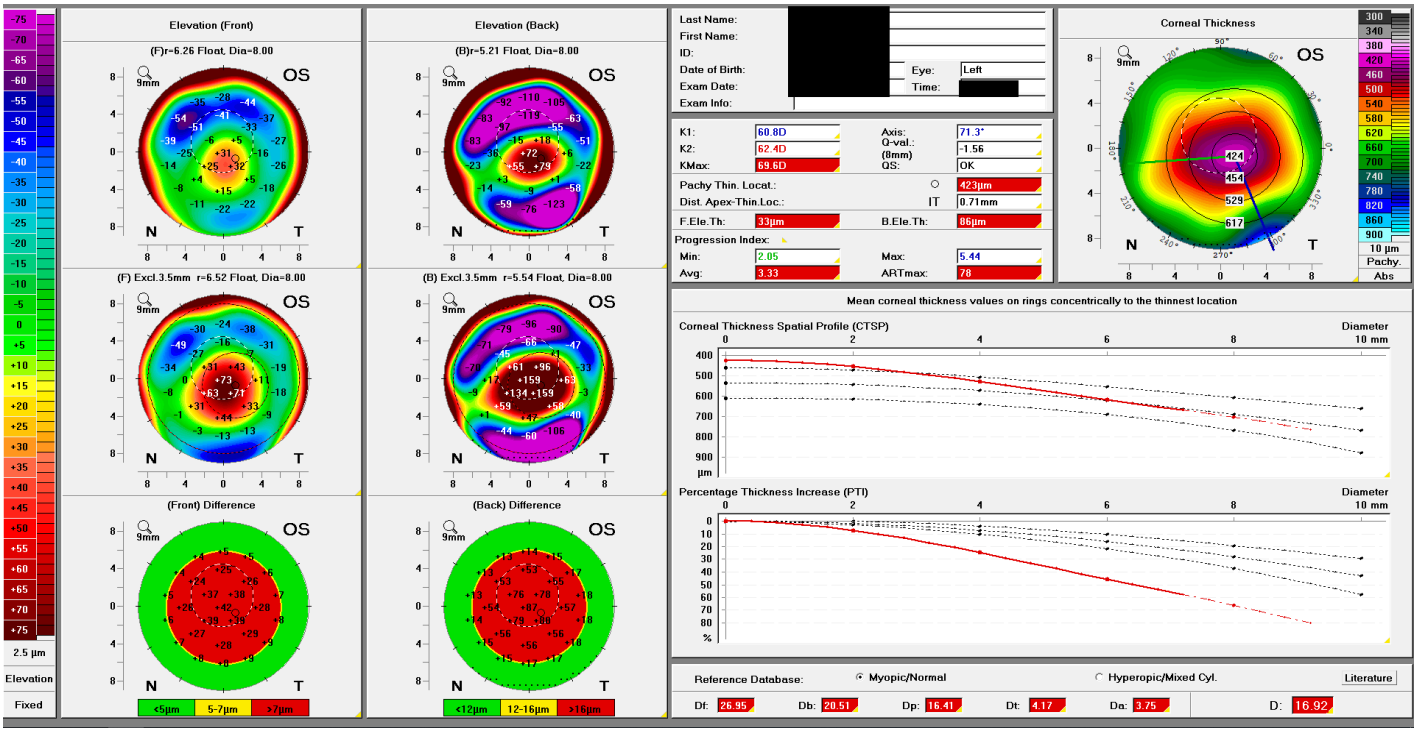

Figure 5: *Pentacam® HR analysis of a keratoconic cornea. Display of anterior and posterior elevation and calculation of the Belin-Ambrósio enhanced ectasia display total deviation value (BAD-D). Image from archive of the Department of Ophthalmology, Saarland University Medical Center, UKS.*

Among several tomographic devices, the Pentacam® HR shows excellent reliability and repeatability of measurements regarding corneal power and pachymetry values in several studies [134,278,318]. Although Wang et al., who compared the repeatability of eight several devices, spoke of comparable results [318], Crawford et al., who examined the repeatability of Orbscan® II, Pentacam® and Galilei [53], as well as Shetty et al. and Anayol et al., who investigated the repeatability and realiability of Pentacam®, Sirius® and Galilei, concluded that the measurements of these tomography devices are independent and thus the devices should not be considered as interchangeable [13,53,278]. A similar conclusion was obtained from De la Parra-Colín et al., who compared measurements from Pentacam® with Sirius [58] and lateron from Doctor et al. [65]. Pentacam® HR showed also superiority in the differentiation of

KC and subclinical KC from normal eyes, based on the sensitivity of corneal indices, compared to those of Galilei and Sirius® device [282].

3.3 Corneal biomechanics

Biomechanics are an essential characteristic of the cornea and severely affect its shape and power. They are thoroughly investigated through the last decade as they seem to play a significant role in the diagnosis, follow-up and treatment of several corneal conditions including glaucoma, refractive challenges and a variety of corneal diseases [77]. Especially the emersion of refractive surgery since the 1990s made the need of the comprehension of the biomechanical properties of the cornea imperative, while, the advance of corneal crosslinking as minimal invasive treatment for stabilization of corneal ectasias is supported on the principle of increasing the rigidity and stiffness of the cornea [320], as will be discussed below.

In order to better understand the concept of corneal biomechanics, there are two basic concepts of mechanical engineering to be presented [22]:

The first is the elastic modulus or Young's modulus: this describes how much a load can deform a material under certain conditions [120]. This deformation (strain), results in an internal response within the material. The slope of the stress-strain diagram depicts the Young's modulus. The greater the slope, the higher the modulus and the stiffer the material, thus a greater force is necessary to deform a material of higher rigidity.

The second is the viscoelasticity: it characterizes every living tissue and means that the behavior of a material depends on the strain rate (time) and differs during phases of loading and unloading, in contrast to the pure elastic material which shows a symmetric loading and unloading behavior. The difference between the loading-unloading behavior is called hysteresis and it represents the amount of energy released during this process, mostly as thermal energy [99].

Recalling the complex structure of the human cornea, it comprises different layers and its pachymetry is not uniform, getting thinner from the periphery towards the center. The most important layer of the cornea concerning its strength and biomechanical behavior is the stroma, which represents over 90 % of the corneal thickness [320]. More specifically, the anterior stroma, which consists of a well-organized and structured network of collagen fibers oriented along the superior-inferior and the nasal-temporal meridians that anchor to the Bowman's lamella, is the toughest part of the cornea [1,320,321]. Due to increased interconnections, it is 50 % stiffer than the middle and posterior stroma [46,320]. The organized structure of the anterior stroma prevents swelling and assures the preservation of the corneal curvature. Approaching the corneal periphery, the collagen fibers present a more circumferential structure, creating an annulus at the limbus, which is significant for absorbing changes of intraocular pressure and maintaining stability of the curvature of the central cornea [46,320]. Furthermore, the "collagen crimp", meaning, the natural waviness of collagen fibers under physiological tension, plays an important role in corneal biomechanics [320]. The corneal epithelium, Descemet's membrane and corneal endothelium seem to have a small part in corneal biomechanics [77], while the role of the Bowman's lamella remains controversial. On the one hand, a study of Seiler et al. showed no significant relevance of Bowman's lamella to the mechanical stability within the cornea [271]. On the other hand, a disrupted Bowman's lamella appears in corneal ectasias [184].

Apart from its strength, rigidity and stiffness, the cornea exhibits viscoelastic properties as well, which enables it to absorb conditions of stress and retain its form [77]. It is characterized mainly as an anisotropic composite with nonlinear viscoelastic properties rather than a linear elastic structure [22].

Corneal biomechanics have been long investigated *in vitro* [132] using virtual mathematical corneal finite element models. The first device to assess the rigidity of the cornea *in vivo* was the Ocular Response Analyzer (ORA, Reichert Ophthalmic instruments Inc., Depew, New York, USA), a non-contact tonometer. Other described technologies are the radial shearing speckle pattern interferometry, the Brillouin optical

microscopy, the optical coherence elastography (optical coherence tomography (OCT) with elastography), and most recently, the Corneal Visualization System (Corvis® ST, CST, Oculus Optikgeräte GmbH, Wetzlar, Germany) [8,321].

The ORA device is a noninvasive device which includes a high-speed air puff and produces a transient corneal deformation, and thus permits the measurement of corneal hysteresis [60,150]. The device offers an accurate measurement of intraocular pressure (IOP) by generating two separate IOP output parameters, the Goldmann-correlated IOL (IOPg) and the corneal-compensated IOP (IOPcc). The fully automated alignment system permits a precise measurement at the apex of the cornea. The transient corneal deformation is recorded by an electro-optical infrared detection system [150].

In 2010, the CST was introduced. This device is a non-contact tonometer generating an air puff and equipped with an ultra-high-speed Scheimpflug camera that records the deformation of the cornea at over 4300 frames/second along an 8 mm horizontal corneal cross-section during corneal deformation [237]. The Scheimpflug camera has blue light LED (455 nm, UV free) and covers 8.5 mm of a single slit horizontally. The air puff is constant from measurement to measurement [60,237]. A video of 140 images, each having 576 measuring points, taken within 31 millisecond (ms) after the start of the air pulse, gives a precise assessment of the corneal biomechanics [8,314]. It dynamically pictures the corneal deformation during the non-contact tonometry; the recording starts with the cornea at its natural convex shape, then, due to the air puff the cornea is forced inwards (ingoing phase, through first or ingoing applanation A1), until reaching the highest concavity, followed by an oscillation period before reaching the outgoing (or returning) phase. Then, a second applanation (A2) is conducted before the cornea returns to its natural convex shape, with a possible oscillation [8]. The device has an ergonomic design, enabling the patient to comfortably sit and properly place the forehead and chin for the measurement, and the air puff is automatically released when alignment with the first Purkinje reflex of the cornea is achieved, while a manual setting is also available [8]. The device detects the timing and pressure at first and second applanation and at the moment of highest concavity. A biomechanically corrected IOP (bIOP) is calculated, based on the timing of the first applanation and it

depends on the corneal resistance. At the time of highest concavity, the highest corneal displacement (deformation amplitude, DA), is detected. The radius of curvature at highest concavity is also calculated, while CST records applanation lengths (AL) and corneal velocities (CVel) during the ingoing and outgoing phases. The corneal thickness is also calculated and the lowest value is displayed. The main Dynamic Corneal Response (DCR) display pictures various biomechanical corneal properties. It enables a detailed analysis of the Scheimpflug images being taken during corneal deformation as well as the Corvis Biomechanical Index (CBI) and Tomographic Biomechanical Index (TBI, **Figure 6**) [8,11,314]. The CBI, comprises an essential score that describes the risk of ectasia and is useful in differentiating KC from a normal cornea. It results from the analysis of 5 CST biomechanical parameters, the deformation amplitude ratio 2 mm (DA Ratio 2 mm), the speed of corneal apex at first applanation - applanation 1 velocity (A1 velocity), the sum of the inverse radii of the concave state between the first and second applanation (integrated radius), Ambrósio's Relational Thickness to the horizontal profile (ARTh) and stiffness parameter (SP-A1, **Figure 6**) [11,255,311]. With regards to the information obtained, the CST allows the early detection of ectatic diseases such as KC, the biomechanical changes after corneal crosslinking (CXL) and can be useful for the follow-up of glaucoma [11,314].

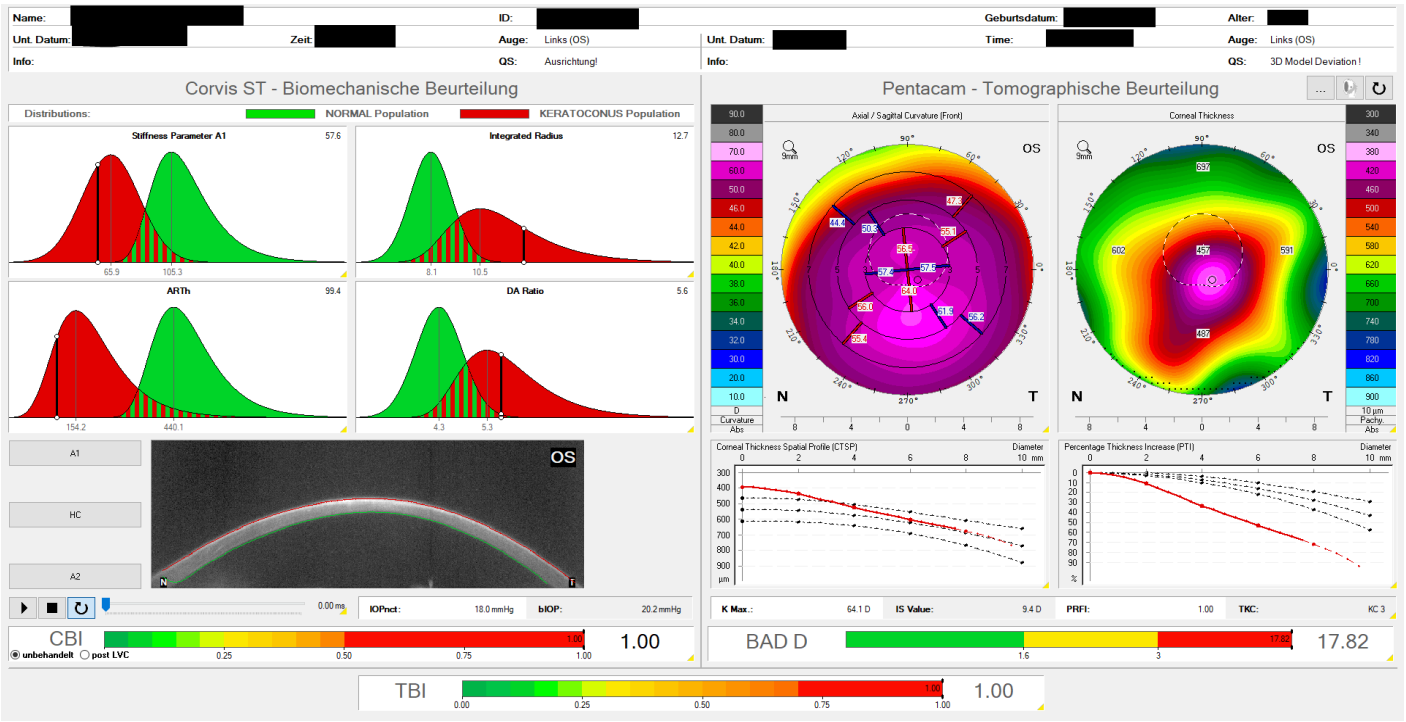

Figure 6: *Biomechanical analysis of keratoconic cornea by means of Corneal Visualization Scheimpflug Technology (Corvis® ST) combined with the Pentacam® tomographic analysis. Image from archive of the Department of Ophthalmology, Saarland University Medical Center, UKS.*

3.4 Keratoconus and other corneal ectasias

3.4.1 Definition of keratoconus

The word keratoconus (KC) derives from the Greek words “keras” meaning cornea and “konus” meaning cone, because of the conical shape that the cornea can gradually acquire because of its protrusion [106]. KC is a progressive, mostly bilateral, often asymmetrical corneal disease [258], characterized by corneal thinning, leading to protrusion, scarring, high astigmatism and myopia [164,165,241,258]. The first official reference to this corneal entity, dates back to 1854 to John Nottingham, who described KC, its epidemiology, clinical manifestation, causality and treatment options [103,153]. He then described keratoconic corneas as “conical corneas”, weakened and associated with polyopia and not sufficient visual correction with the use of spectacles [153]. Other corneal ectasias include keratoglobus, PMD (or keratotorus), posterior

keratoconus and postoperative corneal ectasia following corneal refractive surgery [164,273].

Hereby we will further analyze KC as corneal disease entity and we only included patients with diagnosed progressive KC.

3.4.2 Epidemiology of keratoconus

Its incidence reaches 1:2,000 and it can cause severe visual impairment with decreasing quality of life [241]. This corneal entity typically starts at puberty and progresses until the fourth decade of life, when the rate of progression decreases significantly but not consistently for all patients, until the fifth decade of life [153,164,165,241]. Known as a mostly bilateral and asymmetrical disease, there are studies to present a unilateral entity [92]. However, because of the evolution of corneal topography and tomography devices, as well as of the biomechanical assessment, the incidence of KC has increased and very early cases of KC can be now detected [105,164,165,240,241,302]. Characteristically, one of the relatively more recent epidemiology studies for KC showed 5x to 10x higher values of estimated incidence prevalence in comparison to earlier reports [101]. The prevalence of keratoconus varies, reaching as high as 5 % of the population in the Middle East [105]. A recent review by Santodomingo-Rubido et al. based on several epidemiological studies presented prevalence rates between 0.2 and 4,790 per 100,000 persons and an incidence between 1.5 and 25 per 100,000 persons/year, with the highest prevalence in 20 to 30-year old persons [258]. The high range of the prevalence and incidence is due to the differences in geographic location and ethnicity, but also to the diagnostic criteria, study design, age and cohort of examined populations set at each study [258]. A study of Georgiou et al. that examined Asian and Caucasian KC patients, revealed that the Asian patients presented with KC were younger compared to Caucasians, whereas the incidence of atopic disease was found to be significantly higher among Caucasians. As the majority of Asian patients with KC were of northern Pakistani origin who are traditionally consanguineous, conducting first-cousin marriages, it is suggested that the etiology of KC between these two populations can differ [96].

3.4.3 Pathogenesis of keratoconus

Although it is characterized in older literature as a non-inflammatory disorder [164,241], it seems that, on the contrary, inflammation plays a key role to the formation and progression of this corneal entity [142,176]. The overexpression of inflammatory factors such as cytokines and interleukin (IL)-6 (IL-6) in tears of patients with different stages of KC has been described [142,175,176]. Elevated IL-6, tumor necrosis factor α (TNF-α) and matrix metalloproteinase (MMP)-9 in the tear film of patients with KC has been detected, whereas another study observed increased binding of IL-1 and corneal fibroblasts at KC eyes with onset or progression [79,142,175,176]. A main characteristic of corneal ectasias is the presence of a weaker cornea with distortion of the corneal curvature [248]. In case of KC, several studies throughout the years revealed keratocyte apoptosis, abnormal regulation of important regulation of corneal regeneration and metabolism such as collagenases, proteases, tissue inhibitors of MMP-1 and MMP-3, which lead to abnormalities of the organization of the stromal collagen fibers and a defective connection to Bowman's lamella, as well as stromal thinning [154,189,205,210,248]. Imaging of second-harmonic signals combined with 3D reconstruction of keratoconic eyes revealed less lamellar interweaving and reduction of anchoring to Bowman's lamella [210].

Kenney et al. conducted a survey in order to study the alterations of corneal structure in cases of KC. In areas of non-scarred cornea, decreased staining of the epithelial basement membrane for entactin/nidogen, fibronectin, alpha 3-alpha 5 chains of type IV collagen and chains of laminin-1 were found, whereas areas of corneal scars had increased staining of the epithelial basement membrane for the components above, as well as for laminin-5, perlecan and type VII collagen. In areas of gaps of the Bowman's lamella, fibrotic areas between direct contact of corneal epithelium with stroma were found, containing type VIII collagen, fibrillin-1, tenascin-C, alpha 1-alpha 2 type IV collagen and normal stromal extracellular matrix and epithelial basement membrane components [152].

The analysis of KC corneas by means of *in vivo* confocal microscopy (IVCM) revealed an increased mean diameter of the wing cell nuclei as well as of the average basal cell

diameter of the epithelium, compared to normal corneas [133]. The superficial epithelial cells were found to be elongated and spindle-shaped [73]. The Bowman's lamella is disrupted in the region of the cone, with epithelial cells and stromal keratocytes [73]. The analysis of the corneal stroma showed various degrees of haze in cases of present scarring. High levels of corneal haze were associated with reduction of the keratocyte density, and a keratoconic haze grading scale was formed, which, however did not show a relationship with KC severity in association with corneal curvature. Interestingly, the anterior keratocyte density was found to be strongly related to the presence of corneal staining, history of atopy and eye rubbing [133]. Furthermore, alterations within the subbasal corneal nerve plexus can be visible using IVCM, including a reduced length of the corneal nerve fibers and a winding course of the plexus [87].

Analysis of the corneal epithelium of KC corneas by Kanellopoulos et al. using AS-OCT revealed that the epithelium is thinner at the center of KC eyes and inferiorly, while thicker elsewhere, compared to normal controls, and, between the different severity stages of KC. According to corneal tomography, the epithelium seems to be thinner with increasing KC stage [146].

Corneal ectasia develops through chronic biomechanical weakness/decompensation, which leads to thinning of the corneal stroma and protrusion, steepening, increase of astigmatism and myopia [11].

3.4.4 Causality of keratoconus

KC comprises a multifactorial disease, as eye rubbing, contact lens (over-)wear, trauma, Down's syndrome, atopic disease, diseases of the vascular and connective tissue such as Ehlers Danlos syndrome, Leber's congenital amaurosis, mitral valve prolapse, pigmentary retinopathy, Marfan's syndrome, floppy eyelid syndrome and, in some cases, heredity are included [104,151,164,241]. More specifically, the relevance with Down's syndrome is strong, with a prevalence of 0.5-15 %, according to several studies. This can be attributed to the genetic disorder of trisomy 21, but can be also related to frequent eye rubbing, mechanical damage and blepharitis [54,72,241]. Similarly the association to the Leber's congenital amaurosis is mainly because of the

excessive eye rubbing taking place in the context of the oculo-digital response [72]. An interesting study showed also that corneal biomechanics and topography are negatively affected during pregnancy and the hormonal changes during this period could be thyroid-related [293]. Dysthyroidism may affect the corneal biomechanics and could be related to KC progression [293]. The role of sex hormones and thyroid hormones in the pathogenesis of KC has been examined and it has been found that thyroxine (T4) levels as well as estrogen mRNA levels have been found to be increased in the tear film of patients with KC, while progression of KC can occur during pregnancy, puberty and after infertility treatment [15,104]. The Collaborative Longitudinal Evaluation of Keratoconus (CLEK) study, which is an eight-year, multi-center, natural history study of 1,209 patients with KC, examined annually for eight years, revealed that a history of eye rubbing was positive in 50 % of the KC patients [317]. As far as the heredity of the disease is concerned, this is not fully cleared and there may be other coexistent factors that can attribute to the occurrence of KC such as environmental conditions, atopy and eye rubbing or use of contact lenses [72,151,164,165]. Principally KC is considered as a sporadic disorder [72,151]. Since 1974 Hammerstein suggested an irregular dominant inheritance with an approximate 20 % gene penetrance which increases with age, whereas they did not exclude autosomal or sex-linked inheritance [121]. Nowak et al. underlined that KC is a multifactorial disease which shows genetic heterogeneity which mainly gives the disease a sporadic form [94]. However, he presented other studies that show a high prevalence of undiagnosed KC in family members of patients with KC and in the case of familial KC, 90 % of pedigrees showed an autosomal dominant inheritance with low penetrance [72,94,149], while in other studies an autosomal recessive inheritance was found in families after consanguineous marriage [72,94]. In fact, the association of KC with several diseases as referred above and the variance of the prevalence of KC between the different ethnicities suggests that the genetic basis of KC is far more complex [72]. The CLEK study revealed only 14 % of the patients with positive family history of KC [317]. As far as the eye rubbing is concerned, it has been found that the cells of the tarsal conjunctiva are affected, inflammatory cytokines are released which lead to damage of

the corneal epithelial cells and thinning of the keratocytes. The degree and time period of eye rubbing affects significantly the excess of possible damage [72,219,253].

3.4.5 Clinical manifestations of keratoconus

The clinical manifestations of KC are various, depending on the severity of this corneal entity. In early stages it can be that there are no symptoms and no clinical manifestations, while at advanced stages it can be responsible for significant visual impairment. The use of retinoscope with retroillumination after pupil dilation can reveal a characteristic scissoring reflex as well as the "Charleux" oil droplet sign, caused by the corneal steepening and the alteration of the retinal reflex [165,241]. During slit-lamp examination several entities can be detected (**Figure 7**): corneal (stromal) thinning; prominent corneal nerves; mostly paracentrally-inferiorly or inferotemporally; corneal protrusion; iron deposits partially or completely around the conus area called Fleischer's ring; well defined vertical – seldom horizontal – lines in the deep corneal stroma, mostly centrally which disappear after applying pressure on the cornea, called Vogt's lines or striae; corneal scarring subepithelially or/and stromally, even epithelial nummuli-like opacities and subepithelial fibrillary lines [164,241]. Furthermore, in advanced stages, a V-shaped deformation of the lower lid can be observed at downgaze because of displacement of the lid by the coned-shaped cornea, called Munson's sign. Another specific for KC observation is the sharply focused light beam near the nasal limbus when the cornea is laterally illuminated in advanced stages of KC, called Rizzuti's sign [241]. In advanced KC stages a disruption of Descemet's membrane can occur with invasion of aqueous within the corneal stroma, which is accompanied of pain and is called "corneal hydrops". The corneal edema can gradually resolve within weeks/months with reduction of the superficial inflammation and the pain and lead to severe corneal scarring [241].

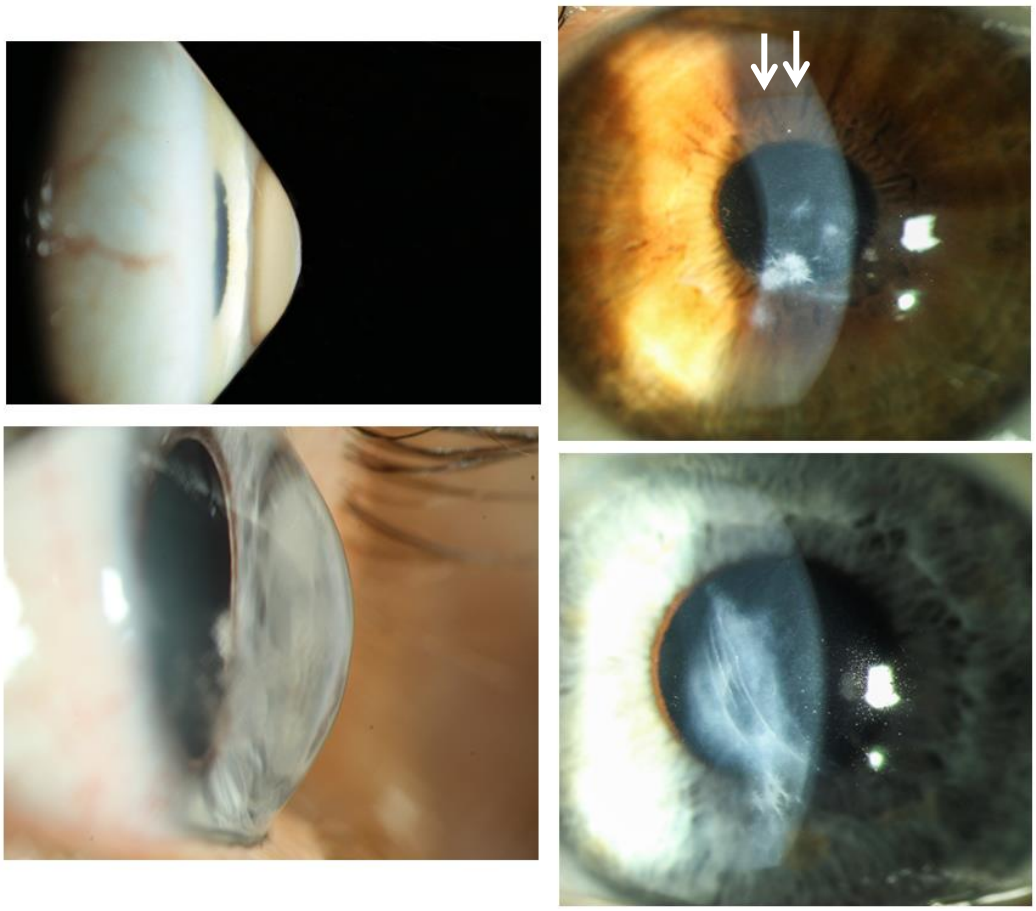

Figure 7: *Clinical manifestations of keratoconus: conical formation of the cornea in advanced stages, Fleischer ring (white arrows), corneal thinning Vogt lines and corneal scarring. Figures from archive of the Department of Ophthalmology of Saarland University Medical Center, UKS.*

3.4.5 Diagnosing keratoconus and classification of keratoconus

KC is a disease with several clinical manifestations or can be also clinically absent at early stages and only be suspected by decreased visual acuity [241]. Although KC can be easily detected based on its clinical manifestations at advanced stage, diagnosis at very early, even preclinical stage is challenging [188,240]. The term form fruste KC is a term that was firstly introduced in 1938 by Amsler, in order to describe a light, nonprogressive and abortive corneal ectasia with asymmetrical astigmatism, found in the fellow eye of a patient with a described unilateral KC or at relatives of patients with KC [12]. For the examination he used the handheld keratoscope – placido disks

and defined a limit of ≤ 4 degrees of downward deflection of the horizontal axis as abnormality, and 4-8 degrees as a mild KC [12]. Since then there were other attempts to identify early KC such as the examination of corneal pachymetry difference between the thinnest and near points [186] and the topographic corneoscope of Rowsey et al. in 1981 [250], while the study of genetics of KC and the findings of IVCM were also included in the diagnostic tools. The continuously emerging technology and evolution of computerized corneal assessment, including computerized videokeratoscopes, rotating Scheimpflug optical cross-sectional analysis, IVCM, OCT, very high-frequency ultrasound and biomechanical analysis, gave space for a new terminology for characterizing KC and for its grading and classification [27,153,240].

A “simplified nomenclature” with minimal terminology based on the high technology available for the diagnosis and follow-up has been proposed [153]. Thus, KC can be characterized as symptomatic or asymptomatic based on visual impairment, even despite use of spectacles, and progressive or nonprogressive changes on corneal wavefront analysis, pachymetry or values of the anterior and posterior corneal surfaces [153]. A KC suspect is a term used for these patients where none of the former findings are present other than strong family history or/and biomechanical measurements outside the normal range values or/and clinical corneal characteristics that do not fully correspond to the KC entity [153].

The term “subclinical keratoconus” is used to define an incipient stage of KC where no clinical signs are present and is practically misdiagnosed in everyday practice. The term is used for patients who do not demonstrate full extend of disease but exhibit either a strong family history of ectatic corneal disorder or one and more of the following known relevant parameters: corneal thickness, anterior and posterior corneal elevation, biomechanical change, which are out of normal values but do not meet the criteria of clinical disease [131,153].

Grading KC has been a challenge until today and several grading systems have been published.

Morphological (Buxton) classification: based on the cone shape and position and classifies KC as oval, affecting one or two corneal quadrants, mostly the inferior one, nipple and globe, (nipple, with diameter ≤ 5 mm located centrally or paracentrally and globe, when the cone affects > 75 % of the anterior cornea) [235,258].

Keratometric classification: KC is classified into four grades according to the central corneal power values as mild (< 45 Diopters, D), moderate (46-52 D), advanced (53-59 D), and severe (> 59 D) [258,307].

Hom's classification: this system is based on clinical signs and sets KC as preclinical, when no signs are detected; mild, when little corneal thinning and scissors reflex are present; moderate, when visual impairment and corneal thinning without scarring are present; severe, when scarring, excessive corneal thinning and unstable refraction are present [241,258].

Amsler-Krumeich classification: This classification system is one of the oldest and until recently the most widely used in everyday practice [28,167,258]. It presents four grades and takes into consideration the existence of corneal scarring, spherical equivalent refraction values, mean central corneal power and corneal thickness: Grade I includes eccentric corneal steepening, induced myopia and/or astigmatism > -5 D, mean central corneal power < 48 D; Grade II includes no presence of scarring, corneal thickness > 400 μm, induced myopia and/or astigmatism > -8 D, mean central corneal power < 53 D; Grade III includes no presence of corneal scarring, corneal thickness > 300 μm, induced myopia and/or astigmatism > -10 D, mean central corneal power < 55 D; Grade IV includes central corneal scarring, corneal thickness > 200 μm, non-measurable refraction and mean central corneal power > 55 D [167,258]. However, this grading system presents practical weaknesses, as overlaps between the different criteria from each grade are much probable and this sets a clear categorization impossible [28,29,104].

Fourier-Domain OCT classification (Sandali Classification system): It is based on findings of Fourier-domain OCT system and proposes 5 stages according to structural corneal alterations: Stage 1 for thinning of otherwise normal epithelium and stroma in

conus area; Stage 2 for hyperreflective abnormalities at the Bowman's lamella and thickening of the epithelium in conus area; Stage 3 for displacement of the hyperreflective abnormalities at the Bowman's lamella backwards, with more thickening of the epithelium and thinning of the corneal stroma; Stage 4 for stromal scarring; Stage 5 for corneal hydrops, with 5a acute onset (break at Descemet's membrane, big intrastromal cysts and disorganization of corneal stroma) and 5b healing stage (corneal scarring) [257].

Alio-Shabayek keratoconus grading system: is based on the Amsler-Krumeich classification but includes anterior corneal aberrations (RMS coma at 6 mm) instead of the refraction: Grade I – no scarring, coma-like RMS 1.50-2.50 μm, mean central corneal power < 48 D; Grade II – no scarring, corneal thickness > 400 μm, coma-like RMS > 2.50 μm, ≤ 3.50 μm, mean central corneal power < 53 D; Grade III – no scarring, corneal thickness > 300 μm, coma-like RMS > 3.50 μm, ≤ 4.50 μm, mean central corneal power < 55 D; Grade IV – central corneal scarring, corneal thickness > 200 μm, coma-like RMS > 4.50 μm and mean central corneal power > 55 D [234]. Again, this grading system is complex and overlaps between the different parameters of each grade are possible, which leads to difficulty in classifying KC [104].

Keratoconus severity score (KSS): grades KC as normal (regular axial topography pattern, normal clinical findings, spectacle corrected acuity optimal); atypically normal (abnormal axial topography explained by clinical findings or medical history such as contact lens warpage, corneal scarring atypical for KC, history of refractive surgery and normal or reduced visual acuity); KC suspect (suspicious topography with corneal steepening > 48 D, normal clinical finding, optimal visual acuity); mild KC (topography findings analogous for KC, flat keratometry value < 51 D, clinical findings consistent with KC without scarring, reduced visual acuity); moderate KC (pathological topography, flat keratometry values between 51.25 and 56.00 D or astigmatism ≥ 8 D, clinical findings including scarring, reduced visual acuity); severe KC (pathological topography, flat keratometry value > 56.01 D, clinical findings including scarring and reduced visual acuity) [203,258].

RETICS classification: this system evaluates KC based on clinical signs, optical and visual function variables and corneal hysteresis parameters [6,258].

The Belin ABCD Keratoconus classification system: In 2016, Belin et al. published a new KC classification/staging system that uses basic tomographic parameters for the evaluation of KC [28]. It includes the anterior and posterior curvature, thinnest pachymetry, best corrected visual acuity with spectacles and the presence or absence of corneal scarring, The fact that it is based on measurements at the thinnest point and not the apex, enables it to better reflect the anatomical changes of KC. Each letter of the A/B/C/D classification system corresponds to one of the evaluated parameters and is separately graded from 0 to 4: **A** to the **A**nterior radius of curvature (ARC) at 3 mm zone, **B** to the posterior radius of curvature (PRC) at 3 mm – **B**ack surface, **C** to **C**orneal pachymetry at thinnest point (thinnest corneal thickness, TCT), **D** to **D**istance best corrected visual acuity (with spectacles) and a sign is added: (-) for absence of corneal scarring, (+) presence of corneal scarring without obscuring iris details and (++) for corneal scarring which obscures iris details [26,28]. **Table 2** shows the ABCD classification system and the range values for each stage [28]. The ABC(D) grading system is incorporated in Pentacam® software and at each measurement, the device can provide an exact evaluation according to this grading system. In 2021 Flockerzi et al. published a retrospective study of 1000 patients of the Homburger Keratoconus Center (HKC) of the Department of Ophthalmology at Saarland University Medical Center in Homburg/Saar (UKS), where the distribution of the stage of KC based on Belin's ABCD grading system according to different age groups was analyzed. It was found that there was a similar distribution of stages in all different age groups. An early KC stage was depicted mainly by the PRC (B) and interestingly higher grades of PRC grading where found at early as well as at advanced KC stages, facts which show the necessity of classifying and assessing the PRC when studying KC [88].

Table 2: ABCD Keratoconus Grading System

ABCD Criteria	A	B	C	D	Corneal scarring
	ARC (3 mm zone)	PRC (3 mm zone)	Thinnnest pachymetry (μm)	Best corrected spectacle visual acuity	
Stage 0	> 7.25 mm (< 46.5 D)	> 5.90 mm	> 490 μm	= 20/20 (= 1.0)	-
Stage I	> 7.05 mm (< 48.0 D)	> 5.70 mm	> 450 μm	< 20/20 (< 1.0)	-, +, ++
Stage II	> 6.35 mm (< 53.0 D)	> 5.15 mm	> 400 μm	< 20/40 (< 0.5)	-, +, ++
Stage III	> 6.15 mm (< 55.0 D)	> 4.95 mm	> 300 μm	< 20/100 (< 0.2)	-, +, ++
Stage IV	≤ 6.15 mm (≥ 55.0 D)	≤ 4.95 mm	≤ 300 μm	< 20/400 (0.05)	-, +, ++

Table 2: *The ABCD Keratoconus Grading System by Belin MW et al. Based on Belin MW, Kundu G, Shetty N, Gupta K, Mullik R Thakur P (2020). ABCD: A new classification for keratoconus. Indian J Ophthalmol 68:2831-2834. doi: 10.4103/ijo.IJO207820* [26].

Flockerzi et al. extended the ABCD KC staging system by adding an additional biomechanical parameter "E" [89], reflecting the modified linear term of the CBI of CST device, CBiF, which was developed at the Department of Ophthalmology at the UKS. It is again graded from 0 to 4, and enables a biomechanical assessment of KC corneas and possible ectasia detection before the existence of tomographic abnormalities [89]. This parameter was found to be highly correlated to PRC and TCT, and thus with KC severity [90].

The ABCDE KC classification system is the one used in the Department of Ophthalmology at the UKS and also included in our studies presented in this doctoral thesis.

3.5 Therapeutic options for keratoconus

As it already seems, KC is a disease entity with various manifestations, and, in combination with the severity of the possible resulting visual impairment. The evolution of diagnostic tools for KC which has enabled the earlier detection of this corneal entity has supported the reinforcement of the available therapeutic tools [104]. The aim of the treatment is halt of progression of the disease and improvement of

vision [104]. According to the stage of KC, different treatment options are available [273].

Essential in the non-surgical treatment of KC patients is a thorough explanation of the disease, and the importance of avoiding eye rubbing. If necessary, topical hydration and use of topical or/and systemic antiallergic and antiinflammatory medication in order to help the patients to this cause, can be prescribed. In early stages, and with aim to ameliorate the visual acuity with conservative measures, the use of glasses and soft contact lenses can contribute to the correction of the myopia and of the regular part of the astigmatism but are practically of limited help for KC [104,273]. The use of rigid, gas-permeable contact lenses (CL), hybrid lenses which are softer peripherally and rigid centrally, toric, piggy-back, corneoscleral and scleral – or/and miniscleral CL can contribute to better visual outcomes [273]. Unfortunately, the use of CL might be difficult or non-tolerable for the KC patients, taking into consideration the ground of atopy and inflammation. Thus a surgical treatment for visual rehabilitation comes often as the only solution [104].

In case of subepithelial nodules and superficial scarring, an excimer laser-phototherapeutic keratectomy (Excimer-PTK) may be of help for the clearance of the optical zone, and the facilitation of tolerance of CL [273].

The intracorneal ring segments (ICRS) were firstly used in 1978 by Burris T. for the management of myopia [33] but first approved from the United States Food and Drug Administration (FDA) in 1999 [20]. They were first proposed as a surgical option for treatment of KC in the midperiphery by Colin et al. [48] in 2000. They are small polymethylmethacrylate (PMMA) corpuscles that can be implanted deep intrastromally and act as creator of space between the collagen lamellae, thus shortening the central arc length (arc shortening effect), leading to a corneal reshaping (**Figure 8**). The implantation results in flattening of the central cornea, reduction of myopia and astigmatism and improvement of visual acuity [20,48,75,236,254]. Possible candidates for the procedure are patients with best corrected visual acuity of $\geq$ 0.2 decimal, corneal thickness > 400 μm, clear central cornea without scarring or CL intolerance [20,48]. The procedure was first conducted with use of a diamond knife, vacuum-

centering guide and semi-circular dissection tools [48]. It can now be aided by means of femto-second (photodisruptive laser, infrared Neodymium:Glass laser beam with a wavelength of 1053 nm) laser which reduces possible postoperative complications as it is more precise and prevents a possible perforation or epithelial ingrowth [236]. The results after the procedure show an improvement of visual acuity and astigmatism, as well as a reduction of the keratometry values and improvement of the corneal geometry thanks to the postoperative flattening permits the fitting of CL, even glasses [48]. The ICRS implantation can be also helpful in cases of PMD and post-LASIK ectasia [75,236].

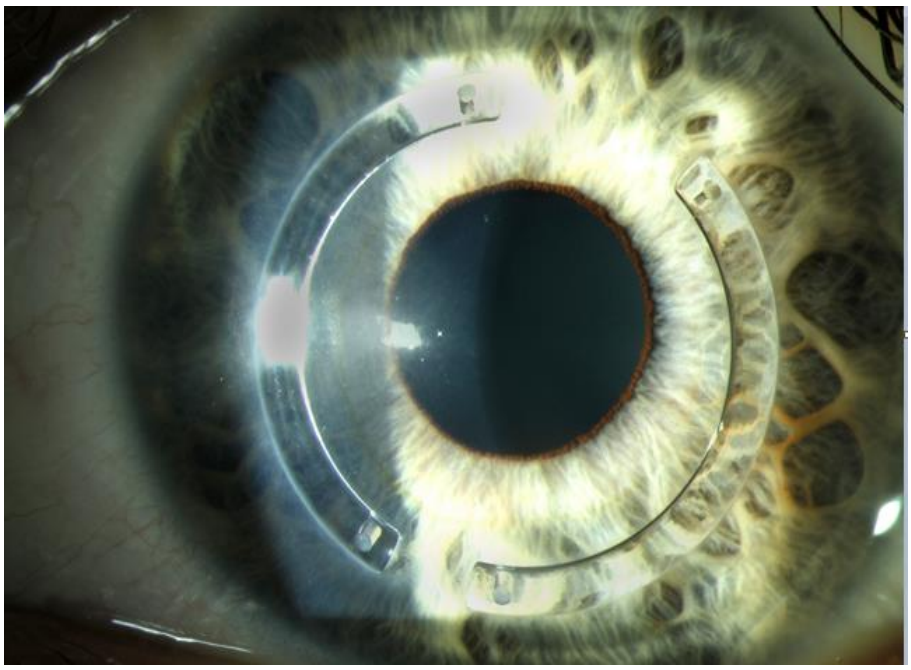

Figure 8: *Intracorneal ring segments (INTACS-SK). Image from archive from the Department of Ophthalmology, Saarland University Medical Center, UKS.*

In case of excessive corneal thinning, corneal scarring, and contact lens intolerance, the corneal transplantation, either as deep anterior lamellar keratoplasty (DALK) or as penetrating keratoplasty (PKP) remains the only solution (**Figure 9**) [104,273]. The latter technique is the only method available after the disruption of Descemet's membrane and deep scarring that remains after a corneal hydrops [229].

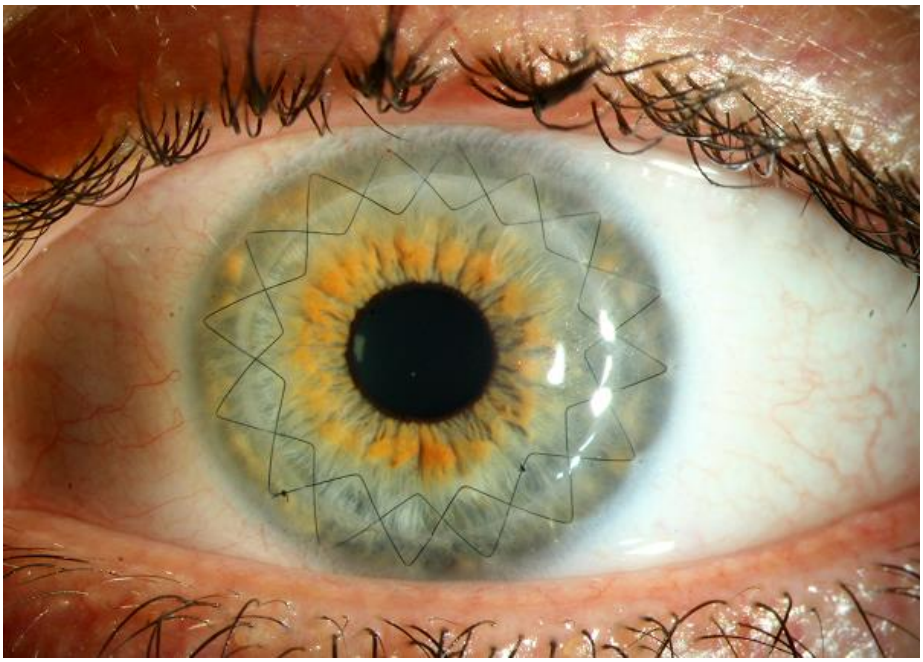

Figure 9: *Postoperative result after penetrating keratoplasty with double running suture in a case of advanced keratoconus. Image from archive of the Department of Ophthalmology, Saarland University Medical Center, UKS.*

When a corneal hydrops occurs, a conservative treatment path may be followed, which includes the use of hypertonic ophthalmic eyedrops, topical steroids and cycloplegia until resolution of the corneal edema [229]. However, when the edema persists, the risk of infections, neovascularization, intense stromal scarring, corneal perforation and persistent inflammation, which can affect the course of an imminent corneal transplantation, is higher, thus it is essential to achieve a quicker reduction of the edema [229,260]. Shaw et al. conducted corneal cauterization and thermokeratoplasty for acceleration of edema resolution [277]. A very successful technique is the placement of predescemetal corneal sutures (Muraine sutures [335] vertically at the Descemet disruption under a filled anterior chamber with non-expandable gas (eg. 14 % Perfluorpropan, C_3F_8 or 20 % sulfur hexafluoride, SF_6) [23,231]. In a comparative study of Zhao et al, the technique of thermokeratoplasty was found to be inferior in terms of visual and clinical outcomes compared to the intracameral air injection [339].

Händel et al proposed a mini-Descemet Membrane Endothelial Keratoplasty (mini-DMEK) in the area of the Descemet's membrane disruption for the reduction of the corneal edema, with promising results, compared to the Muraine suture technique [122]. A PKP is the only option for treating the remaining deep stromal scarring after the resolution of edema and inflammation [276].

In all the above therapeutic options, the main aim is the improvement of vision of the KC patients. The only method in existence so far, that permits the halt of the progression of disease, is the corneal collagen crosslinking (CXL), that was first introduced in 1998 by Seiler et al. [288] and remains until nowadays a key option that can relieve the patients' anxiety and visual impairment and postpone more invasive and complicated operative measures [273]. The CXL procedure will be further thoroughly described and explained in this study.

3.6 Background of corneal crosslinking – photodynamic therapy

In order to better understand CXL, the principles of its prodromal procedure, photodynamic therapy (PDT), will be firstly explained. The PDT involves the injection or topical application of a photosensitizing substance that accumulates in a target cell area, which is excited by irradiation with light of a certain wavelength and then reacts with the molecular oxygen (O_2) to create reactive oxygen species, leading to cell death [52].

The roots of this therapeutic entity can be traced back to antiquity, when Herodotus from Greece, also known as the father of heliotherapy, underlined the importance of sun exposition of the whole body for health restoration. Niels Finsen in 1903 received the Nobel prize in physiology of medicine for his work on treatment lupus vulgaris, using sunlight or light from a carbon arc lamp with heat filter [2,52,208]. An important milestone was the work of von Tappeiner and his student Raab in 1900, who first described, that cell death can result from interaction of light and chemicals, by studying the effect of combination of light and acridine red on protozoa, as a result of fluorescence which occurred from the energy transferred from the light to the

substance. Seven years later, Tappeiner and one of his colleagues, who studied the treatment of skin tumors with topical eosin and white light, found the importance of oxygen in the photosensitization reaction, and described the process as “photodynamic action” [2,52,208]. In the next years the PDT therapy was further studied and applied, guided by the principle of the three essential components, light, photosensitizer, oxygen [2,52,208]. Important for the evolution of PDT were the experiments studying porphyrins and mainly hematoporphyrin that showed their fluorescent ability and their contribution to localizing tumors [2]. Landmark for the further evolution of PDT were the studies of Schwartz et al. in 1955, where it was explained that the hematoporphyrin is a mixture of various porphyrins, which may have different properties and the purified hematoporphyrin itself was poorly identified in tumors, whereas the remain of the substances had high affinity for the tumor tissue [2,182]. He produced derivative substance by mixing hematoporphyrin with acetic and sulfuric acids, filtering and neutralizing with sodium acetates, which are known as hematoporphyrin derivative (HpD) [7,182]. Another important landmark in the history of PDT is the work of Dougherty and colleagues who reported the first successfully completed tumor cure in animal experiments, using HpD and activation with red light [67]. These interventions opened the way for a wide use of PDT therapy, targeting at selective cell death and/ or damage of specific tissue vasculature [7,67,130].

PDT therapy includes laser treatment that does not have neither thermal nor mechanical damage, but photochemical damaging effect, by the induction of oxidative mechanisms [264]. The photosensitizer is inserted, mainly intravenously and then light irradiation at a certain wavelength follows, according to the photosensitizer used [130,264]. The photosensitizer absorbs light energy and is thus transformed from its ground singlet state (S_0) to an excited singlet state (S_1). From this situation, molecular changes on electron level lead to an excited triple state (T_1) which is magnetically different from the previous two ones. Via intersystem crossing, fluorescence is produced mainly from S_1 state, whereas phosphorescence is produced mostly from the T_1 state, or, the T_1 state can activate photochemical reactions from reactive cytotoxic free radicals (Type I reaction), or by energy transfer to ground state oxygen ($^3O_2$),

leading to photo-oxidative disruption of biological targets (Type II reaction – mediated by singlet oxygen) [226,264]. In type I reaction, the transfer of an electron or hydrogen atom results in the production of superoxide anions (O_2^-), whereas, in type II reaction, which is found to be the main mechanism of damage produced by PDT, energy transfer to molecular oxygen leads to creation of singlet oxygen ($^1O_2$) [264]. PDT, through these mechanisms, can lead either to direct cellular destruction, or to triggering of disruption of vascular permeability and subsequently cause of ischemia, or to activation of immunological response that lead to tissue destruction [7,226,264,294,316].

PDT now is used in detecting tumors and treating malignancies including recurrent gynecological tumors, brain tumors, hematological malignancies, lesions of head and neck, rectal area and urinary tract, intraocular lesions as well as a variety of dermatological diseases [2,52,208]. PDT has also been established as official treatment of ophthalmological retinal conditions, including neovascular age-related macular degeneration (AMD), polypoidal choroidal vasculopathy (PCV), choroidal vascularization not in the context of AMD, central serous chorioretinopathy (CRCS) and choroidal hemangioma [24,25]. As far as the use of PDT in the ophthalmological field is concerned, the main photosensitizing substance used is verteporfin (Visudyne^{TM}, Novartis Ophthalmics, Basel, Switzerland) which is injected intravenously and lasts for about 10 minutes [24]. After approximately 5 minutes, time to permit the substance to be accumulated in the diseased tissue, a treatment with PDT laser follows, by use of light of wavelength 689 nm (verteporfin PDT therapy, vPDT) [221,246]. vPDT targets vascular endothelial cells and results in selective vascular occlusion, increase of platelet concentration in the area and activation of the clot creation, thus being useful in the treatment of CNV, as explained above [221,246,264]. The first application of PDT therapy in the eye was developed in the decade of 1990s for the treatment of AMD, and the standard proposed protocol was the use of verteporfin 6 mg/m^2, with laser fluence 50 Joules/cm^2 (J/cm^2) [221]. Since its first applications, several protocols of verteporfin dosage and fluence and duration of laser

treatment, as well as treatment intervals have been proposed for the amelioration of treatment results [24,25].

3.7 Corneal crosslinking and its use for keratoconus treatment

3.7.1 Background and basic principles

Corneal collagen crosslinking (CXL) is the only surgical procedure known to halt progression of KC. In the Global Consensus for Keratoconus, it is stated that it is an essential procedure for the treatment of KC, performed by the majority of the ophthalmological society and there should not be an age limit to conduct it when progression of KC is present [104]. It can be a life-saving solution for the course of the disease and prevent the need for corneal transplantation [227,320].

The technique was first published in 1998 by Spoerl et al. who conducted corneal crosslinking experimentally in porcine eyes aiming at improvement of elasticity and corneal stiffness [288]. The first application in human eyes for the treatment of KC was published in 2003 by Gregor Wollensak, Eberhard Spoerl and Theo Seiler, changing in a groundbreaking way the treatment of KC entity [323]. The surgical technique included: corneal debridement under topical anesthesia (epithelium-off, epi-off CXL procedure); instillation of a photosensitizer, riboflavin (vitamin B_2) 0,1 % (RF, 20 mg riboflavin-5-phosphate in a 10 ml dextrane T500 20 % solution), applied for at least 20 minutes before irradiation and every 5 minutes during irradiation, which consisted of ultraviolet A light (UVA, 370 nm) for 30 minutes, at an irradiance of 3 mW/cm^2 at 1 cm distance from the treated cornea, corresponding to a dose (fluence) of 5.4 J/cm^2; postoperative instillation of antibiotic eye drops until epithelialization (**Figure 10**) [323]. The first protocol was named standard or Dresden CXL protocol (S-CXL) because it was first developed at the Technical University of Dresden, Germany [323].

Figure 10: *Intraoperative image of irradiation with ultraviolet A light during corneal crosslinking procedure. Image from archive of the Department of Ophthalmology, Saarland University Medical Center, UKS.*

The very first postoperative outcomes of the inventors until 47 months showed an improvement of keratometric readings and visual acuity [323]. RF is a non-toxic photosensitizer that is also water-soluble and can easily penetrate the corneal stroma after epithelium removal, and thus it enables a deeper effect of the UV-radiation and induction of crosslinks in the corneal stroma. The use of RF with sequential use of irradiation, as already similarly explained at the mechanisms of PDT therapy, causes a photoreaction and active species of oxygen (free radicals) which allow the induction of crosslinks and improvement of biomechanical strength of the cornea [288]. An early aerobic phase is studied, where the RF molecule is excited in its triplet state and reacts with ground-state oxygen, producing reactive oxygen species (ROS, type 2 reaction). ROS are responsible for the formation of crosslinks by reacting with proteins of the collagen and stroma, leading to increase of corneal stiffness. This phase is followed by an anaerobic reaction (type 1 reaction) which starts after the oxygen is consumed at the first 15 seconds of the procedure, where the RF at its triplet state reacts with stromal

proteins, leading to the production of ROS. The oxygen reduces quickly with halt of the UVA radiation [14]. The combination of UV-radiation and RF shows higher achievement of crosslinks compared to UV-radiation alone, as the latter fails to penetrate deeper in the corneal stroma and to induce mechanical changes, whereas longer wavelengths that can achieve deeper penetration, fail to achieve crosslinks [288]. Concerning the role of instillation frequency of RF during the UV exposure, a too high frequency has been associated with reduced CXL efficacy, however, the complete absence of intermittent RF instillation throughout the radiation phase has been associated with lower efficacy of the procedure [180]. UV-radiation is toxic as it causes keratocyte apoptosis and potentially damage of endothelial cells [325]. RF has been found not to have a cytotoxic effect contrary to the UVA light, and the capability of RF to absorb UVA light prevents deeper penetration of damage of deeper structures such as the corneal endothelium, lens and retina [288,324]. Exposal of corneas to CXL using different irradiation levels has shown a cytotoxic effect at $\geq$ 0.35 mW/cm^2 (corresponding to an irradiation dose of 0.63 J/cm^2), thus a limit of 400 μm corneal thickness is set for treatment of KC progression, according to the Lambert-Beer equation [324]. Analysis of porcine eyes treated with CXL showed an increase of corneal transparency, while a histological analysis showed that three different zones could be recognized: an anterior stromal part with light discoloration and no swelling, an intermediate stromal zone with light edema and a deeper posterior stromal zone, moderately edematous. This analysis indicates that CXL acts more anteriorly, where biomechanical changes are also mainly detected, having stronger effect at the anterior stroma and a moderate effect more intermediately, leaving a posterior zone untreated, and that it holds a dehydrating effect [162,327]. What is more, increased resistance of corneal tissue to enzymatic degradation has been found postoperatively, which is related to the intensity of UVA light, as well as increased resistance to MMPs' (MMP-1, 2, 9 and 13) mediated collagen and leucine-rice proteoglycans' degradation, a process which, as explained above, is crucial at the pathogenesis of KC [227,289,337]. A postoperative increase of the diameter of the collagen lamellae in rabbit corneas is reported as well [326].

An important postoperative feature of CXL is the demarcation line which can be detected at the slit lamp as early as two weeks after the procedure and represents a limit of the crosslinked and the non-crosslinked cornea at about a 60 % depth centrally (**Figure 11**) [272]. The demarcation line is strongly affected by the CXL-induced oxygen reactions in the corneal stroma, the RF concentration, the duration and distribution of the irradiation within the corneal stroma, the availability and oxygen diffusion and ROS production [198]. Anterior segment optical coherence tomography (AS-OCT) is an important tool to illustrate the demarcation line horizontally and allows a precise measurement of its depth at several parts of the cornea [286]. Analysis by means of IVCM shows a distinct vertical and lateral transition zone at the limit area of the CXL-treated cornea. The anterior-treated zone, that increases from the first month postoperatively until six months postoperatively, shows edema, few keratocytes and poor reflectivity, compared to the posterior non-treated area which shows a normal keratocyte population and reflectivity [36]. The existence of this boundary line in the cornea is related to changes of the refraction index, tissue density and light scattering [198]. It surely represents an indicator of the safety of the CXL procedure [198]. It has been debated whether the depth of the demarcation line is an indicator of the effectiveness of the CXL procedure [286]. However, there is no standardized calculating method for examining the corneal stromal demarcation line and there is a big variation of the depth of demarcation line that can be recorded according to the CXL method applied [95,173]. The depth of the demarcation line increases with increased depletion of RF in the corneal stroma, augmented irradiation dose and duration of irradiation, as well as due to the induction of type II reaction in the corneal stroma [180].

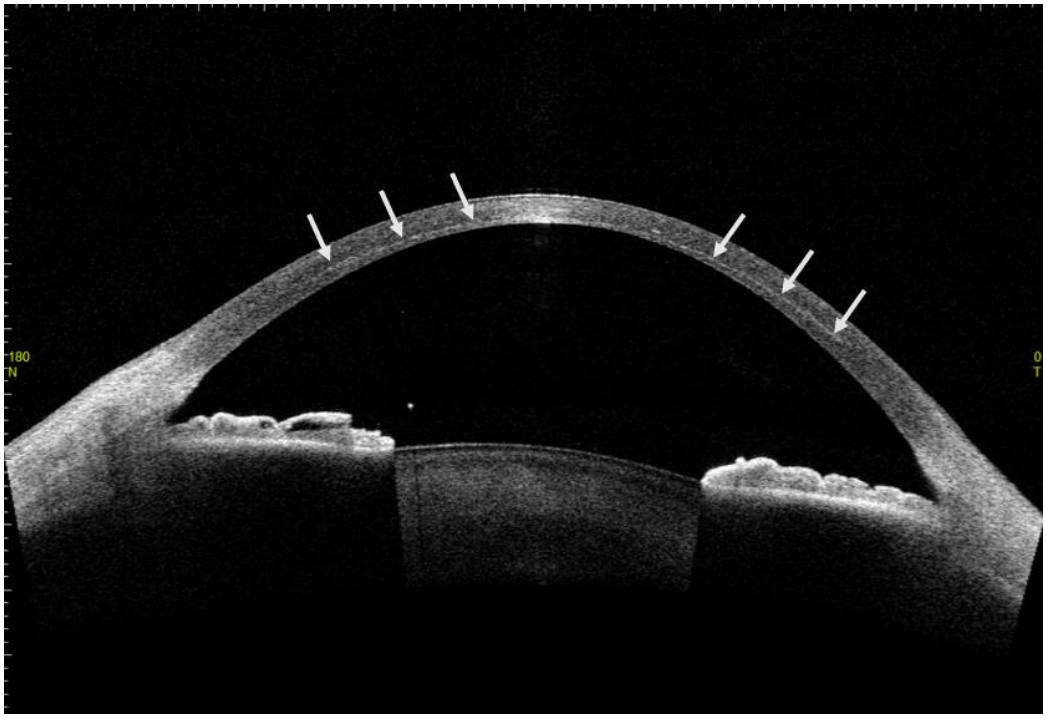

Figure 11: *Demarcation line (white arrows), pictured by means of anterior segment optical coherence tomography device. Image from archive of the Department of Ophthalmology, Saarland University Medical Center, UKS.*

3.7.2 CXL protocols

S-CXL has been proved to achieve significant long term results in large studies, achieving stabilization of KC even after 13 years with improvement and stabilization of KC keratometric values and low progression rates of approximately 7.2 %, leaving the corneal endothelium intact [76,244,296,313].

The most important features for conducting a procedure are its safety and efficiency, in case of CXL, to protect the endothelium and achieve an increase of corneal stiffness and generation of more crosslinks in the corneal stroma [266]. The concentration of RF is essential in order to achieve deeper penetration of the irradiation in the cornea, however, it was found that a higher concentration ≥ 0.15 %, could lead to the opposite result, meaning a superficial penetration of the irradiation and thus a fail to achieve crosslinks deep in the stroma [266]. Although CXL is shown to be a minimally invasive procedure including the removal of the corneal epithelium (epi-off CXL), the

treatment time based on the Dresden protocol is 1 hour, including the 30 minutes of the instillation of RF and the 30 minutes for the UVA radiation. The need of reducing patients' discomfort and allowing surgeons to utilize the surgical time for more patients, a time-shortening of the CXL procedure has been sought. Essential was here the Bunsen and Roscoe rule of reciprocity which states that the photochemical reaction mechanism is characterized by the total absorbed energy and does not depend neither on the intensity or the exposure time [32,187]. Based on that law, it can be assumed that by increasing the intensity of the irradiation with maintaining the total energy of 5.4 J/cm^2, the time of irradiation can be reduced. However, it was shown that for higher intensities from 50 mW/cm^2 up to 90 mW/cm^2 no statistically significant stiffness improvement is observed, thus the limit of highest intensity of irradiation applied in CXL was set up to 40-45 mW/cm^2, in order to conduct CXL with safety and efficiency [319]. Several treatment protocols that occur, called accelerated CXL protocols (A-CXL) due to the reduced treatment time, based on the Dresden protocol (3 mW/cm^2, 30 minutes, 5.4 J/cm^2), can be produced. Some (applicable) examples are: 6 mW/cm^2, 15 minutes, 5.4 J/cm^2| 9 mW/cm^2, 10 minutes, 5.4 J/cm^2| 18 mW/cm^2, 5 minutes, 5.4 J/cm^2| 20 mW/cm^2, 4.5 minutes, 5.4 J/cm^2| 34 mW/cm^2, 2.65 minutes, 5.4 J/cm^2| 45 mW/cm^2, 2 minutes, 5.4 J/cm^2 [319]. Nevertheless, the more the time-shortening of the procedure, the less oxygen remains available and thus the less induction of free radicals occurs, that are essential for the effectivity of the procedure [247]. Indeed, the comparison of two different A-CXL protocols, (18 mW/cm^2, 5 minutes, versus 9 mW/cm^2, 10 minutes), showed better visual and topographic results with the latter protocol being efficient independently of the severity of KC [155]. Nicula et al. compared the conventional S-CXL with A-CXL after treating eyes with progressive KC (irradiance 9 mW/cm^2, 10minutes) and could find similar visual and topographical results [225], similarly to the study of Vounotrypidis et al. [315], whereas the A-CXL of 18 mW/cm^2, 5 minutes reached less corneal flattening compared to the standard method [125]. Another comparative study between different A-CXL protocols showed superiority of A-CXL of 9 mW/cm^2, 10 minutes compared to 18 mW/cm^2, 5 minutes and 30 mW/cm^2, 3 minutes protocols [155,281].

3.7.3 Other CXL modifications

Epithelium-on (Epi-on) CXL

In order to avoid the postoperative discomfort and possible complications such as infections caused by the removal of the corneal epithelium, transepithelial CXL (TE-CXL) or epithelium-on (epi-on) CXL was proposed [34]. Main disadvantage of the procedure is the preservance of a big obstacle for the penetration of the water-soluble RF through the lipophilic cornea and the tight junctions of the epithelium. Several techniques are proposed for the increase of RF penetration such as use of several substances such as benzalconium chloride, ethylenediaminetetraacetic acid (EDTA) polyethylene glycol, lysine or epithelial flap/pocket or partial debridement [14,51,113,126]. However epi-on CXL [14,310] shows inferiority according to the postoperative visual acuity, halt of progression, topometric results, depth of demarcation line and recurrence rates [14,220].

Transepithelial Iontophoresis CXL

Iontophoresis is a noninvasive procedure which includes a small electric current that is used to facilitate the penetration of an ionized substance into a tissue. In ophthalmology, it has been used since the 1940s for the administration of antibiotics for the treatment of bacterial keratitis and endophthalmitis [41]. As RF has negative charge and low molecular weight, iontophoresis-CXL (I-CXL) has been proposed as an epi-on CXL method and relies on repulsive electromotive forces which are created by a small electrical current delivered to an iontophoretic chamber in order to deliver RF into the stroma of the treated cornea [14,41]. The technique showed comparable results to S-CXL [310]. However, in a study of Jian et al., limited concentration and depth of penetrance of RF was observed in the corneal stroma after I-CXL, compared to the S-CXL method [141]. In 2021, an enhanced iontophoresis CXL protocol was proposed (EI-CXL), including two circles of iontophoresis. The clinical findings, the findings of corneal topography and IVCM were comparable to S-CXL procedure but with slightly higher recurrence rates at 5 years follow-up [330].

Pulsed CXL

The technique includes the administration of UVA radiation with pulses which restarts the photodynamic type 2 reaction and allows oxygen to replenish the corneal stroma, thus leading to more $^1O_2$ release and induction of crosslinking [14]. Pulsed CXL (P-CXL) seemed to achieve inferior tomographic outcomes compared to S-CXL [147], it showed however a deeper demarcation line which agrees with the increased oxygen spread in the corneal stroma [199].

CXL plus

The term CXL plus has been proposed for describing the CXL procedure combined with refractive procedures for the treatment of ectatic corneal disorders. It includes methods aiming at stabilizing the corneal ectasia and offering better visual outcomes as well [171].

Kanellopoulos et al. proposed the simultaneous treatment with PRK followed by immediate S-CXL, which was named “Athens Protocol”, and presented better visual and tomographic outcomes compared to PRK with sequential CXL after 6 months, as well as stability even after 30 months postoperatively [144,166]. The same author introduced also the “enhanced Athens protocol”, which includes the application of partial topography-guided PRK and topographically customized, higher fluence and variable pattern CXL [144].

Similarly, Kymionis et al. proposed the “Cretan Protocol” consisting of transepithelial PTK for the removal of the epithelium in CXL, aiming at epithelial removal and regularization of the anterior cornea surface at the apex of the cone area [109,172].

Other presented combined procedures include the INTACS implantation followed by CXL and CXL followed by implantation of phakic intraocular lenses, with promising results [16,42].

CXL for thin corneas

Epi-on CXL and the modifications of I-CXL and P-CXL to enhance its effectivity have served the aim to treat KC corneas that exceed the limit of 400 μm corneal thickness by preserving the corneal epithelium and thus preventing the thinning of cornea during treatment [113,115].

Another technique to increase the preoperative corneal thickness is the use of hypo-osmolar RF solution that induces swelling of the cornea and increase of its thickness [113]. However, a limit of 330 μm corneal thickness is proposed in order to achieve stabilization postoperatively, as it was found that, at thinner corneas, no sufficient biomechanical stability could be reached in order to stop progression [115]. The appearance of Descemet folds and endothelial damage because of the corneal edema may be a possible consequence [45].

Moreover, a customized epithelial debridement technique was described, which involved removal of the epithelium sparing the area over the apex of the cone, according to corneal topography [170]. The technique provides protection of the thinner cone area and allows better penetration of RF into the paracentral area of the cone at the border of the epithelial debridement, and, as a result, an increased corneal stiffening postoperatively [170]. However, another study showed that the effect of the procedure is shown at a depth of 150 μm compared to a depth of 250 μm at the deepithelized cornea, presuming a lower effect of CXL at the cone area [201].

Jacob et al. proposed the use of a contact lens onto the surface of the cornea after epithelial debridement and before instillation of RF solution in order to treat thin corneas, as a safe and effective solution [139]. Although the method appears to be a more non-invasive solution for CXL treatment without causing corneal edema, the irradiance of the corneal stroma is significantly reduced by 40-50 % and the oxygen diffusion is also restricted, which reduces the effect of CXL procedure [45]. A similar but more invasive and controversial technique that has been published is the removal of stromal lenticule from patients who have undergone small incision lenticule

extraction (SMILE) for correction of myopia, and application of this tissue onto corneas treated with CXL [62].

The “sub400” individualized fluence CXL protocol enables the treatment of corneas as thin as 214 μm of corneal stroma and is based on an algorithm that is used for individualization of the irradiation settings according to the thinnest pachymetry after the soaking of cornea with RF [117].

Mazzotta et al. proposed the “M Nomogram” for the A-CXL treatment of corneas of several pachymetries ranged between 250-400 μm (with epithelium), based on the preoperative corneal thinnest point and the analysis of the depth of the demarcation line by means of IVCM and AS-OCT [196]. The “M Nomogram” is designed to preoperatively estimate the depth of treatment according to the thinnest pachymetry and ensure the safety of the corneal endothelium [196]. Treatment with A-CXL 9 mW/cm^2, 10 minutes is also included as it is found to be comparable with S-CXL with ensured stabilization over 24 months and a safe procedure for the preservation of the integrity of the corneal endothelium [196].

3.8. Pediatric keratoconus and CXL – Particularities

KC in patients under 18 years of age exhibits a more aggressive pattern with faster progression rate and may present already in advanced stages with severe visual impairment at first diagnosis [15,177]. KC is a disease which appears mainly within puberty and it seems to have an accelerated rhythm of progression at younger ages [37,245]. The youngest patient diagnosed with KC as documented in the literature is a four-year old girl with Down’s syndrome [252]. The prevalence of KC in pediatric population is estimated 0.16 % according to the Intelligence Research in Sight Registry of the American Academy of Ophthalmology [211], with strong variation according to ethnicity [232,302]. Patients of Asian origin, including Indians, Pakistani and Bangladeshi who lived in the English Midlands were found to be significantly younger than white subjects not only at the time of diagnosis but also at the time of surgical treatment and had a 4.4 times higher incidence of KC [232]. An epidemiological study

in Saudi Arabia detected an estimated prevalence of 4.79 % among subjects aged 6-21 years [302]. Because of the visual impairment, the possible contact lens intolerance due to difficulty in using them and/or atopy, and advanced KC findings, the risk for corneal transplantation can be high [15]. Younger age is considered as an independent risk factor for corneal transplantation [304], and corneal transplantations for KC in pediatric patients are estimated at about 15-20 %, while the procedure at a young age is related to a higher risk of graft rejection and worse visual prognosis [228]. At these ages, especially with asymmetrical findings between the two eyes present, a CXL for stabilization should be conducted without waiting for evident progression. In younger age, the frequent existence of vernal keratoconjunctivitis and atopy must be also considered as a factor that can lead to quicker and more aggressive course of KC [15,304]. The higher progression rate of KC in young age compared to adults can be also attributed to the higher rate of corneal collagen remodeling in association with ocular allergy, while the risk of acute hydrops is high because of eye rubbing [15,218]. A French epidemiological study showed a predominance of male sex at pediatric KC population compared to adult KC subjects, with existence of atopy as well as eye rubbing at a percentage of 91.84 % [177]. Several studies have noted an asymmetrical KC based on eye rubbing and atopy, being responsible for microtrauma and alteration of the inflammatory status of the cornea [112,135,140].

Treating young patients with KC can be challenging because of the different level of compliance and the age particularities. The whole family should participate in a thorough counseling that includes participation in long-term follow ups, treatment of atopy and halt of eye rubbing [15]. CXL should be offered as early as possible without waiting for progression of the disease, especially at existence of asymmetrical findings, advanced stage of KC and visual impairment [15,112,112]. An inverse relationship has been described between the age of the KC patient and the progression tendency of the disease, with pediatric KC being more likely to deteriorate, leading even to corneal hydrops [4]. It is also already underlined that CXL for pediatric KC may be not as efficient as for adult KC patients, with risk of keratometric progression at about 22 % compared to 2-10 % found in adult patients [101,228]. In another study, where several

age groups with KC were treated with the S-CXL protocol, it was found that the topographic cone of pediatric corneas (aged < 18 years) was located more centrally compared to adolescent (aged 18-26 years) and adult groups (> 26 years, age groups as specifically described in this study), and more postoperative flattening was observed at the first age group compared to the other two groups [285]. Caporossi et al. published encouraging results ("Siena CXL pediatrics") with stabilization of KC in patients under 18 years of age even after 3 years and observed a faster and better functional recovery at treated corneas with pachymetry < 450 μm at 3 months postoperatively [38]. Because of the duration of the S-CXL procedure, the postoperative pain and risk of infection, the epi-on CXL technique has been proposed for younger patients. However, as it has been already explained, the preservation of the epithelium through the CXL process is leading to inferior results compared to S-CXL [14,220], thus the shortening of the duration of the procedure with use of an effective A-CXL protocol should be preferred. Similarly to treatment of adult KC, the A-CXL protocol of 9 mW/cm^2, 10 minutes offers comparable results at the long-term with the S-CXL protocol [279,305].

3.9 Indications and contraindications for collagen corneal crosslinking for keratoconus

3.9.1 Indications

CXL is indicated in younger patients without evident progression by whom the risk of possible corneal transplantation is higher [245], as will be discussed below, and in every case of evident progression. Nevertheless, even in older age groups, where KC tends to stabilize without interventions, a CXL can be conducted in order to achieve a reduction of topographic values and thus corneal flattening, which enables better CL-tolerance. An improvement of visual acuity is also documented, though this is slight and the patients should be thoroughly informed about the procedure and the expected outcomes [37].

An interesting finding at KC corneas by means of IVCM is the presence of extracellular reticular striae deep in the corneal stroma in more progressive KC, with

different orientation and thickness compared to normal corneas and the anterior stroma. That finding, according to Mazzotta et al., independently of the presence or not of Vogt's striae, is correlated with late stromal corneal scarring after CXL and should be considered as limitation for conducting the procedure, when present [191].

In cases of present risk factors such as young age, atopy, significantly high astigmatism and borderline thin corneas, the need of re-treatment may be necessary [270].

3.9.2 Contraindications

Contraindications for CXL exist in patients with prior ocular herpetic infection, as explained before, patients with active ocular inflammation, existence of severe scarring, positive history of autoimmune diseases and epithelial healing problems [330]. Other exclusion criteria were ocular malformations, and previous ocular trauma [17]. A corneal thickness of > 400 μm is proposed for the safety of the procedure, although this can be also considered as relative contraindication, considering the evolution of CXL as explained above [330].

3.10 Complications of corneal collagen crosslinking

Postoperative pain

The first step before begin with application of RF is corneal debridement and at the end of the procedure a contact lens may be used to relieve patients' pain and accelerate reepithelialization. The postoperative pain is more evident at the day of the surgery and the next day and is soon reduced. Artificial tears and systemical anti-inflammatory drugs are of help [78]. The use of topical anti-inflammatory eye drops has been reported to cause of corneal melting and is not advised to be admitted postoperatively [209].

Postoperative infectious keratitis

At the first postoperative period the possibility of infectious keratitis may be high [63]. The use of a bandage contact lens and topical steroids prior to complete epithelialization post-CXL are considered as significant risk factors [306]. The cause is

mostly bacteria, including gram positive bacteria (several species of *staphylococci* and *streptococci* such as *staphylococcus epidermidis, staphylococcus aureus, streptococcus salivarius, streptococcus oralis*) and gram negative bacteria (*escherichia coli* and *pseudomonas aeruginosa*) [78,280]. Moreover, infection with acanthamoeba and fungi has been also documented [63,78]. *Pseudomonas aeruginosa* and acanthamoeba can produce severe inflammation with corneal melting and deep corneal scarring [78,280]. Infections with herpes simplex virus have been also reported as well as reactivation of an infection, thus, history of herpes simplex infection is considered as a contraindication for CXL [78,169].

Postoperative healing problems, corneal melting, sterile keratitis

Epithelial healing after epi-off CXL has been reported to have a mean duration of four days, with use of a bandage contact lens [193]. Delay at the reepithelialization process has been reported to 3-8 % [3]. Kanellopoulos et al. published a delayed reepithelialization in nine of twenty one eyes, four of them treated with A-CXL and five with S-CXL protocols [145]. The background of the delay of the healing process post-CXL may be attributed to keratocyte damage and increase of MMP levels at the cornea and tear film [3]. Under these inflammatory circumstances, sterile keratitis may occur weeks or even years after CXL [43], which can include sterile infiltrates or even peripheral ulcerative keratitis and shield ulcers [3,18,43] and can lead to corneal melting, a most severe complication of CXL [3]. Acute non-infectious corneal melting with corneal perforation, which led to PKP has been also described [298]. Increased corneal curvature of > 60 D and corneal thickness < 425 μm are found to be significant risk factors for developing postoperative sterile keratitis [160,174]. Positive history of atopy or, in younger patients vernal keratoconjunctivitis may be also present [3,18]. In these cases, other than topical antibiotics, the use of topical steroids and even cyclosporine eyedrops are indicated. The two latter can be administered even 2-4 weeks prior to surgery, when positive history exists [3,78].

Postoperative corneal haze

Haze formation at the corneal stroma is a diffuse corneal opacity which may be observed at the first postoperative period of CXL as a result of corneal edema and decrease of keratocytes, even at the first 4 weeks postoperatively, and does not seem to affect visual acuity [163,191]. It differs from the haze observed after photorefractive keratectomy (PRK) which is located subepithelially [163]. By means of IVCM at the clinical cite of haze, at a depth of about 170-200 μm, the extracellular matrix is more dense because of increase of the number of keratocytes [192,193]. Changes of the stromal swelling pressure, the PG and collagen reorganization and the GAG hydration also play a role at the haze formation post-CXL [107]. In the long term study of Raiskup et al., persistent haze formation was observed at 38.2 % of the treated cases without effect on visual acuity [244]. As explained before, the preoperative reticular formation of stromal microstriae observed with ICVM can be considered as risk factor for postoperative persistent haze formation and eventually corneal scarring [191–193]. At advanced KC stages, where corneal thinning and high corneal curvature is observed, the risk of haze development post-CXL is higher [63,243].

Postoperative corneal edema

Corneal edema is a rare complication after CXL and can be attributed to endothelial damage and depending on the grade of damage it can require a corneal transplantation. It can be attributed to the intraoperative delivery of an exceeded amount of irradiation, inaccurate preoperative pachymetry measurements and intraoperative corneal thinning either because of the corneal debridement or because of the lid-speculum remaining at its place for the whole duration of the operation [275]. We thus advise intraoperative corneal thickness measurements during the CXL procedure in order to ensure the maintenance of the safety of the procedure. Hypotonic solution may be instilled if the thickness of the cornea falls below 350 μm [275].

3.11 Other therapeutic applications of corneal collagen crosslinking

The applications of CXL are not restricted only in treating corneal ectasia. Wollensak et al. presented the use of CXL in patients with bullous keratopathy, meaning, cornea with stromal and epithelial edema with formation of hydrated epithelial cysts because of endothelial insufficiency. Glycose 40 % was administered for 1 day for preoperative corneal dehydration and after corneal debridement, the Dresden CXL protocol was performed. Postoperative thinning was observed even since 3 days postoperatively and until 8 months postoperatively, with resolution of bullous changes thus improving patients' discomfort and with improvement of visual acuity [328]. CXL has been also proposed for the treatment of bullous keratopathy after cataract surgery [97]. The application of a modified CXL at Fuchs' endothelial corneal dystrophy, a corneal disease characterized by swelling of the cornea, led to reduction of the corneal thickness with stability at 3-months follow-up [114].

A significant application of CXL is related to treatment of infectious keratitis, and was given the term PACK-CXL: Photo Activated Chromophore for Keratitis at the 9th Annual International CXL Congress in Dublin, Ireland [116]. It relies on the concept that the photoactivation of a chromophore (eg. RF) can have disinfectant properties because of: 1) the production of ROS which is essential for the damage of the pathogen's cell walls, 2) the interference of the chromophore with the nucleic acids of the pathogens and the inhibition of their proliferation and 3) the changes happening at the structure of the stromal collagen fibers, which make the deposition and function of collagenases difficult [116]. The first published application for that cause has been conducted in 2008 [137]. Several studies have proved its efficacy against bacterial keratitis and the healing time of small corneal ulcers (up to 4 mm), either as adjuvant or standalone treatment [116,118,330] but the results concerning fungal keratitis remain controversial [239,330]. PACK-CXL can be helpful in stabilizing the cornea in case of corneal melting of various infectious origin (bacterial, fungal, Acanthamoeba keratitis) and lead to corneal integrity, preventing a corneal perforation [213].

3.12 Questions

Considering the importance of CXL in the field of KC treatment and the need to minimalize the possible complications and discomfort that this minimal invasive method can cause, but with preservation of the efficacy of the procedure, we examined retrospectively the tomographic and visual outcomes of epi-off A-CXL with irradiation 9 mW/cm^2 for 10 minutes in adult and underaged patients, as well as the reliability of successive biomechanical measurements in KC patients treated with the same A-CXL protocol and untreated KC corneas. For the first part of the study, we included 151 eyes of 124 patients ≥ 18 years of age and 41 eyes of 30 patients less than 18 years of age, who received A-CXL treatment 9 mW/cm^2, 10 minutes for KC between May 2015 and December 2019, conducted at the Department of Ophthalmology at Saarland University Medical Center (UKS) in Homburg/Saar [332,334].

For the second part of the study, we compared the reliability of three successive measurements of Corvis® ST of 20 KC corneas of 14 patients at least 2 years after A-CXL treatment with the same protocol, with those of 20 untreated KC corneas of 20 patients, who were matched according to Belin's ABCD KC grading system [333], everything conducted at the Department of Ophthalmology at Saarland University Medical Center (UKS) in Homburg/Saar.

In this dissertation the following questions have been examined and answered:

1. Did the epi-off A-CXL protocol with irradiation 9 mW/cm^2 for 10 minutes provide stable tomographic and visual outcomes with deep demarcation line in both age groups?

2. Was the procedure safe for both age groups?

3. Is Corvis ST® capable of assessing reliably treated and untreated KC corneas?

4. Can this specific A-CXL protocol provide a positive effect on the biomechanics of KC corneas?

4. Patients and methods

4.1 Study design and examined variables

The first part of the study comprised a retrospective monocentric study performed at the Department of Ophthalmology at Saarland University Medical Center (UKS) in Homburg/Saar, Germany. All patient charts of KC patients who underwent A-CXL 9 mW/cm^2, 10 minutes, during the period May 2015 until December 2019, split in two age groups, < 18 years of age and ≥ 18 years of age, were reviewed and enrolled from the Homburg Keratoconus Center (HKC) which was established in 2010 [88,332,334].

Diagnosis of KC was based on: *(1) clinical features such as the Fleischer ring, Vogt striae, corneal thinning on slit lamp examination and/or (2) tomographic pathological features detected within the Belin/Ambrósio-enhanced ectasia screening display within the Pentacam® HR software (Pentacam High Resolution (HR), Oculus, Wetzlar, Germany).*

The criteria of KC progression were: *(1) an increase of corneal astigmatism ≥ 1 D and/or (2) an increase of the maximal anterior keratometric power (Kmax) of the corneal tomography (Pentacam® HR) ≥ 1 D and/or (3) a decrease of the thinnest corneal thickness (TCT) ≥ 30 µm within 12 months* [332–334].

In adult patients CXL was performed only for progressive KC, while in the young patients, CXL was performed after evident progression but also without waiting for progression, either in case asymmetrical findings with already advanced KC in the partner eye or due to a progressed stage of KC already at first presentation [334].

The A-CXL treatment (9 mW/cm^2, 10 minutes, 5.4 J/cm^2) was performed by use of Avedro KXL® crosslinking system (Avedro, Waltham, Massachusetts, USA) and RF VibeX Rapid™ 0.1 % solution (Avedro, Waltham, MA, USA).

All patients were asked to stop wearing contact lenses at least 3 days prior to all visits and measurements.

Whenever possible, the following parameters were evaluated for each eye at 2 years, 1 year and 6 months preoperatively, directly prior to surgery, as well as 6 weeks, 6 months, 1 year, 2 years and > 2 years postoperatively: best spectacle-corrected distance visual acuity (BCVA, in LogMAR), the steep (K1), flat (K2), mean (Kmean) keratometry values and astigmatism of the anterior and posterior corneal curvature (anterior: K1a, K2a, Kma, Astia; posterior: K1p, K2p, Kmp, Astip), maximal anterior keratometric power (Kmax), apex pachymetry (ACT) and pachymetry at thinnest point (TCT), measured by corneal tomography (Pentacam® HR). Only Pentacam measurements with an "OK" score were included in the study. Intraoperatively, the pachymetry (CT) of the treated corneas was measured four times: CT1 prior to corneal debridement, CT2 after corneal debridement, CT3 prior to irradiation and CT4 after irradiation) using the ultrasound pachymeter SP-3000® (Tomey, Nagoya, Japan). The demarcation line was evaluated based on AS-OCT measurements (Tomey SS-1000® and Tomey Casia 2®, Tomey, Nagoya, Japan). The measurement was conducted from the corneal epithelium to the detectable hyper-refractive line at the corneal center within the Tomey software (Tomey, Nagoya, Japan).

The medical history of the patients was controlled for the presence of atopic eczema, trisomy 21, hypothyroidism, history of premature birth.

The possible postoperative complications, including haze, corneal scarring, infection and corneal melting were assessed and the follow-up visits took place from 6 weeks post-CXL and were repeated every 6 months [332,334]. Haze evaluation was performed by slit-lamp examination and was based on the grading scale according to Fantes et al.: Grade 0 – clear cornea with no opacity observed by any means with microscopic slit-lamp examination; grade 0.5 – trace or faint haze seen only by indirect, broad tangential illumination (considered clear); grade 1: haze or minimal opacification traced with difficulty with direct or diffuse slit-lamp examination; grade 2: mild haze formation easily observed with direct focal slit lamp illumination; grade 3: moderate corneal opacification with partial obscurity of iris details; grade 4: severe corneal opacification which completely hides the visibility of intraocular structures [81,179].

For the second part of the study, the biomechanical analysis, a retrospective monocentric cross-sectional cohort study was performed, including patients ≥ 18 years of age with diagnosed KC with the upper explained diagnosis criteria from the HKC [333].

A "crosslinking group" (CXLG) consisted of 20 KC corneas of 16 KC patients who underwent epi-off A-CXL (9 mW/cm^2, 10 minutes, 5.4 J/cm^2) two or more years before enrollment with the Avedro KXL® system using RF VibeX Rapid™ 0.1 % solution after evident KC progression, according to the KC progression criteria as listed above. A second "control group" for biomechanical measurements was formed consisting of 20 untreated stable KC corneas of 20 KC patients (controls), chosen as ABC-stage-matched controls according to Belin's ABCD KC grading system [333].

The patients from both groups underwent three successive CST measurements during one regular follow-up examination. All patients were asked to stop wearing contact lenses at least 3 days prior to measurements.

For the matching of patients, firstly, the ABC parameters were collected for the CXLG from the "topometric/KC staging" display of the Pentacam software. Then, ABC stage-matched controls were enrolled from the HKC, so that, each CXL-treated cornea could be paired with an untreated KC cornea of the same ABC stage as a control. The ABC staging was derived from Pentacam measurements, which were always conducted before the CST measurements in order to avoid tomographic changes caused by the air puff system of CST. Both the Pentacam and CST measurements were only included with an "OK" score (in advanced stages, "model deviations" were also accepted) and the three measurements were independently reviewed by two physicians (Kassandra Xanthopoulou KX, Elias Flockerzi, EF). The maximal keratometry (Kmax) and the Belin/Ambrósio-Enhanced-Ectasia-Deviation-Index (BAD-D) were analyzed to determine tomographic KC severity in addition to the ABC severity stage.

-The main outcome DCR parameters included the ones included in CBI: (1) A1 velocity, which is the speed of the corneal apex at inward applanation, (2) the ratio

between the deformation amplitude at the apex and 2 mm away from the center (DA ratio 2 mm), (3) the sum of the inverse radii of the concave state between the first and second applanation (integrated radius), (4) the Ambrósio's relational thickness to the horizontil profile (ARTh) and (5) the stiffness parameter at inward applanation A1 (SP-A1), and the Corvis Biomechanical Factor (CBiF, the linearized term of the Corvis Biomechanical Index, CBI) which serves as a basis for the Homburg biomechanical E-staging [333].

Important for our conducted study is to note that:

1) All patient and legal guardians of the underaged patients signed an informed consent form for their data analysis and participation in the HKC observational clinical study, which was approved by the local ethics committee (Ethikkommission bei der Ärztekammer des Saarlandes, reference number 121/20, trial number NCT03923101, U.S. National Institutes of Health, ClinicalTrials.gov), respecting the principles of the Declaration of Helsinki [332–334].

2) CXL was only performed in KC eyes without central corneal scarring, severe Vogt lines, excessive corneal thinning or severe atopic eczema. None of the included female patients was pregnant at the time of surgery [332–334].

3) The presented data have been recently published (see page 4 and 166) [332–334].

4.2 Crosslinking procedure

A-CXL was conducted in the operating rooms under high-standard sterile conditions. Prior to surgery, every patient received topical anesthesia (Oxybuprocain eyedrops, Conjucain® EDO®, Bausch & Lomb, New York, USA) at least 3 times before treatment, as well as oral acetaminophen (500 mg) in order to relieve possible postoperative pain.

Firstly, the corneal thickness CT1) was measured, followed by epithelial abrasion and the next pachymetric measurement (CT2).

After that, the instillation of RF solution (VibeX Rapid™ 0.1 % solution, Avedro Waltham, Massachusetts, USA) every 2 minutes for 20 minutes with closure of the treated eye between the instillation followed, in order to prevent the dryness of the ocular surface. The next step was a further pachymetric measurement (CT3) to ensure that the thickness value was more than 400 μm immediately before radiation.

For the following irradiation the Avedro KXL® CXL system was used, for 10 minutes with an irradiance of 9 mW/cm^2 and a fluence of 5.4 J/cm^2 (epi-off A-CXL, 9 mW/cm^2, 10 minutes). Throughout the irradiation process, one drop of VibeX Rapid™ was instilled every 2 minutes.

A last pachymetric measurement (CT4) took place at the end of irradiation and then the cornea was extensively washed up, followed by application of a 17 mm bandage contact lens, in order to relieve the patient from pain. Non-preserved ofloxacin eye drops (Floxal® EDO®, Bausch & Lomb, New York, USA) were instilled immediately thereafter.

The postoperative therapy consisted of non-preserved ofloxacin eye drops (Floxal® EDO®, Bausch & Lomb, New York, USA) 5 times daily and non-preserved lubricating eye drops with hyaluronic acid (Protagent®, Alcon, Freiburg, Switzerland) 8 times per day until complete healing of the epithelium. After epithelial closure, the bandage contact lens could be removed and the treatment included the continuation of the non-preserved lubricating eye drops 6 times daily and the instillation of non-preserved dexamethasone eye-drops (Dexa-sine®, Novartis, Basel, Switzerland) 6 times daily, with weekly reduction by one drop to minimize the appearance of postoperative haze [332–334].

4.3 Data recruitment and statistical methods

The data recruitment was first held in a preset Microsoft Excel data collection form. The statistical analysis was performed with SPSS software (version 27, SPSS/IBM, Inc. Chicago, USA).

For the **first part of the study**, the parameters analyzed were calculated as mean ± standard deviation (SD). Statistical analysis included: 1) the repeated multivariate analysis of variance (MANOVA) and 2) the pair-wise comparison (paired t-test) for the different time periods. The MANOVA checks the totality of the values for significance at different time points of examination and includes the degrees of freedom (df) as well as the F-Value. The paired t-test examines the development of the parameters over time for the individual eye and summarizes these individual results for the entire collective included in the study.

Results with p-values (p) < 0.05 were considered as statistically significant. Due to the fact that this part of the study was based on KC patients' retrospective chart reviews, patients who did not attend the planned follow-up visits led to missing data. The number of eyes in each follow-up for the different age groups are reported in the following descriptive tables and figures in order to keep being as exact as possible and reduce bias (**Tables 4, 6, 11, 14**, **Figures 12, 13, 14, 15**) [332,334].

For the **second part of the study**, the parameters analyzed were calculated as mean ± SD. The outcome measures were first analyzed for normal distribution using the Shapiro–Wilk test and assuming a normal distribution with $p \geq 0.05$. The parameters resulting from three measurements per eye per patient were subsequently compared between the control group and the CXLG using the two-tailed paired t-test (if normally distributed) or the Wilcoxon matched-pairs test (if not normally distributed) assuming significant differences with $p \geq 0.05$. The parameters resulting from three measurements per eye per patient were subsequently compared between the control group and the CXLG using the two-tailed paired t-test (if normally distributed) or the Wilcoxon matched-paired t-test (if not normally distributed) assuming significant differences with $p < 0.05$. The paired tests were used to obtain the most accurate comparison between the respective crosslinked and staged matched, non-treated control-corneas. The coefficients of repeatability were calculated as the within-subject standard deviation Sw x $\sqrt{2}$ x 1.96. The intraclass correlation coefficients (ICC) that correlate successive measurements carried out on the same subject or a collective of

patients with the same underlying disease and Cronbach’s alpha (CA) were calculated to determine the reliability of the biomechanical measurements [333].

5. Results

5.1. First part of the study: visual and tomographic results > 2 years after A-CXL for KC patients ≥ 18 years and < 18 years of age

5.1.1 Description of the study population

Included in the study were 151 eyes of 124 patients ≥ 18 years of age, 102 males (82.3 %) and 22 females (17.7 %), with a mean age of 31.4 ± 19.0 years at the time of CXL and 41 eyes of 30 underaged (< 18 years of age) patients, 25 males, 5 females with mean age of 15.3 ± 1.2 years at the time of treatment (**Table 3**).

The > 2 years follow-up for the adult population included: 4 eyes with 3 years follow-up, 20 eyes with 4 years follow-up, 12 eyes with 5 years follow-up and 9 eyes with 6 years follow-up (n = 45, mean 4.6 ± 0.9 years, minimum 3, maximum 6 years).

For the underaged patients, the > 2 years follow-up consisted of 1 eye with 3 years follow-up, 6 eyes with 4 years follow-up, 8 eyes with 5 years follow-up and 1 eye with 6 years follow-up (n = 16, mean 4.6 ± 3.0 years, minimum 3, maximum 6 years).

As far as the medical history is concerned, hypothyroidism was documented in 12 out of the 124 adults (9.7 %) and in 3 out of the 30 underaged patients (10.0 %). Atopic eczema was found in 7 adults (5.6 %) and 4 underaged patients (13.3 %) and trisomy 21 was documented in 1 adult (0.8 %) and in 1 young patient (3.3 %). History of eye rubbing was found to be positive in 7 adult patients (5.6 %) and 2 underaged patients (6.7 %). Premature birth was documented at two adult patients (1.6 %) and at none of the group of underaged patients (**Table 3**).

In the case of adult patients, all eyes were treated with CXL because of progressive KC according to the described criteria at section 4.1 “Study design and examined variables”. However, in the case of underaged patients CXL treatment was conducted in 16 eyes of 9 patients because of increasing Kmax and/or corneal astigmatism and/or decreasing corneal pachymetry values, even if the previously mentioned KC progression criteria were not fully met, or because of advanced KC in the partner eye,

because of more aggressive KC pattern. Therefore, there were only 9 eyes with preoperative data covering the period of 2 years preoperatively [332,334].

Table 3: Descriptives	Patients ≥ 18 years of age	Patients < 18 years of age
Gender	102 male, 22 female, 151 eyes	25 male, 5 female, 41 eyes
Age (years)	31.4 ± 10	15.3 ± 1.2
Hypothyreodism (patients)	12 (9.7 %)	3 (10.0 %)
Trisomy 21	1 (0.8 %)	4 (13.3 %)
Atopic eczema	7 (5.6 %)	4 (13.3 %)
Premature birth	2 (1.6 %)	0 (0 %)
Eye rubbing	7 (5.6 %)	2 (6.7 %)
Epithelial closure (days)	5.7 ± 1.8	6.1 ± 2.7
CT1	492 ± 50	477 ± 52
CT2	435 ± 45	425 ± 44
CT3	472 ± 42	469 ± 43
CT4	460 ± 50	454 ± 33
Demarcation line depth	(81 out of 151 eyes) 242 ± 62 (53.6 %)	(36 out of 41 eyes) 237 ± 66 (52.1 %)
Infection	4 eyes	0 eyes
Haze	60 eyes	7 eyes
Progression of KC	3 eyes	0 eyes

Table 3: *Listed descriptives of* ***adult*** *and* ***underaged*** *patients of the first part of the study including gender, age, medical history, time until epithelial closure (days) postoperatively, intraoperative corneal thickness values, demarcation line depth and complications.*

5.1.2 Tomographic results in adult patients

Anterior curvature: steep (K1a), flat (K2a) and mean (Kma) anterior keratometry, maximal anterior keratometry (Kmax) (Pentacam® HR, Oculus, Wetzlar, Germany)

According to the MANOVA analysis, there was no statistically significant difference over time between the different follow-up examinations of the steep keratometry of the anterior curvature (K1a: df(8) = 1.541, p = 0.139). The paired t-test comparisons showed a statistically significant increase from pre-CXL to 6 weeks post-CXL (**p < 0.0001**) and a statistical significant decrease from the 6 weeks follow-up on until > 2 years post-CXL (**p < 0.0001**) for all comparisons, **Tables 4** and **5**, **Figure 12**) [332] .

Table 4: Adult group - Means ± Standard Deviations (SD) for anterior and posterior keratometries						
	K1a (D)	**K2a (D)**	**Kma (D)**	**K1p (D)**	**K2p (D)**	**Kmp (D)**
2 years pre-CXL (n = 52)	45.2 ± 2.7	48.1 ± 3.2	46.8 ± 3.2	-6.2 ± 0.6	-7.2 ± 0.7	-6.9 ± 0.8
1 year pre-CXL (n = 62)	45.9 ± 3.4	49.0 ± 3.9	47.3 ± 3.5	-6.6 ± 0.8	-7.3 ± 0.8	-6.9 ± 0.7
6 months pre-CXL (n = 74)	46.5 ± 4.0	49.7 ± 4.3	48.0 ± 4.0	-6.8 ± 0.8	-7.4 ± 9.9	-7.1 ± 0.8
pre-CXL (n = 151)	46.8 ± 4.0	50.2 ± 4.3	48.4 ± 4.0	-6.8 ± 0.8	-7.5 ± 0.8	-7.1 ± 0.8
6 weeks post-CXL (n= 128)	47.0 ± 4.1	50.6 ± 4.6	48.9 ± 4.2	-6.9 ± 0.8	-7.6 ± 0.9	-7.2 ± 0.8
6 months post-CXL (n = 104)	46.4 ± 3.8	49.7 ± 4.4	48.0 ± 3.9	-7.0 ± 0.8	-7.7 ± 0.9	-7.3 ± 0.8
1 year post-CXL (n = 91)	46.2 ± 3.9	49.5 ± 4.2	47.5 ± 4.8	-6.9 ± 0.8	-7.6 ± 0.8	-7.2 ± 0.7
2 years post-CXL (n = 73)	46.3 ± 3.9	49.9 ± 4.2	47.4 ± 5.0	-6.9 ± 0.8	-7.7 ± 0.7	-7.3 ± 0.7
>2 years post-CXL (n = 45)	46.2 ± 3.8	49.8 ± 3.7	48.2 ± 3.8	-6.9 ± 0.8	-7.8 ± 0.8	-7.5 ± 0.7

Table 4: *Mean ± standard deviation (SD) values of steep, flat, mean keratometries of the anterior (K1a, K2a, Kma) and the posterior cornea (K1p, K2p, Kmp) for the time lines 2 years, 1 year, 6 months preoperatively, directly prior to corneal crosslinking (CXL), as well as 6 weeks, 6 months, 1 year, 2 years, > 2 years post-CXL for the* ***adult*** *patients. An increase of the means for all anterior and posterior keratometric values from preoperatively to 6 weeks post-CXL, followed by a progressive decrease of the anterior keratometric values until > 2 years post-CXL was noted. No similar decrease of the posterior corneal parameters after the* 6^{th} *postoperative week was observed [332].*

Table 5: Adult group - Mean differences ± Standard Deviations and p-values for K1a, K2a, Kma (paired t-test)									
	pre-CXL - 6 weeks post-CXL (n = 129)	pre-CXL - 6 months post-CXL (n = 106)	pre-CXL - 1 year post-CXL (n = 93)	pre-CXL - 2 years post-CXL (n = 75)	pre-CXL - >2 years post-CXL (n = 49)	6 weeks post-CXL - 6 months post-CXL (n = 89)	6 weeks post-CXL - 1 year post-CXL (n = 76)	6 weeks post-CXL - 2 years post-CXL (n = 59)	6 weeks post-CXL - >2 years post-CXL (n = 38)
K1a (D)									
Δ ± SD	-0.4 ± 0.1	0.7 ± 0.2	0.9 ± 0.2	1.1 ± 0.3	1.7 ± 0.4	1.1 ± 0.2	1.2 ± 0.2	1.6 ± 0.3	2.6 ± 0.5
p-value	**p < 0.0001**	**p < 0.0001**	**p < 0.0001**	**p < 0.0001**	**p < 0.0001**	**p < 0.0001**	**p < 0.0001**	**p < 0.0001**	**p < 0.0001**
K2a (D)									
Δ ± SD	-0.7 ± 0.2	0.7 ± 0.2	0.9 ± 0.2	1.2 ± 0.4	2.3 ± 0.4	1.4 ± 0.2	1.4 ± 0.3	1.8 ± 0.4	3.0 ± 0.5
p-value	**p < 0.0001**	**p < 0.0001**	**p < 0.0001**	**p = 0.001**	**p < 0.0001**	**p < 0.0001**	**p < 0.0001**	**p < 0.0001**	**p < 0.0001**
Kma (D)									
Δ ± SD	-0.7 ± 0.2	0.5 ± 0.1	1.0 ± 0.3	1.5 ± 0.4	1.3 ± 0.2	1.3 ± 0.2	1.8 ± 0.5	2.5 ± 0.6	2.5 ± 0.3
p-value	**p < 0.0001**	**p < 0.0001**	**p = 0.003**	**p = 0.001**	**p < 0.0001**	**p < 0.0001**	**p < 0.0001**	**p < 0.0001**	**p < 0.0001**

Table 5: *Mean differences ± standard deviation (SD) values and corresponding p-values for steep (K1a), flat (K2a) and mean (Kma) anterior keratometry values between prior to corneal crosslinking (CXL) and all postoperative follow-up periods, as well as between 6 weeks post-CXL compared to the rest postoperative follow-up examinations for the* ***adult*** *patients. Statistically significant increase of K1a, K2a, Kma 6 weeks post-CXL compared to pre-CXL values, followed by a progressive statistically significant decrease until > 2 years post-CXL* [332].

The flat keratometry of the anterior curvature (df(8) = 2.165, p = 0.028) K2a showed no statistically significant decrease from 6 months post-CXL until > 2 years post-CXL, considering MANOVA. The analysis with paired t-test revealed a statistically significant increase from pre-CXL to 6 weeks post-CXL (**p < 0.0001**) and a statistically significant decrease for the remaining follow-up examinations (**p < 0.0001**, **Tables 4** and **5**, **Figure 12**).

The anterior mean keratometry Kma showed a statistically significant decrease from 6 weeks post-CXL to 1 and 2 years post-CXL (**p < 0.05**) as determined by MANOVA. The paired t-test comparisons showed a statistically significant increase between the pre-CXL and 6 weeks post-CXL values (**p < 0.0001**), followed by a statistically significant decrease for the remaining follow-ups, apart from > 2 years (**p < 0.05**, **Tables 4** and **5**, **Figure 12**) [332].

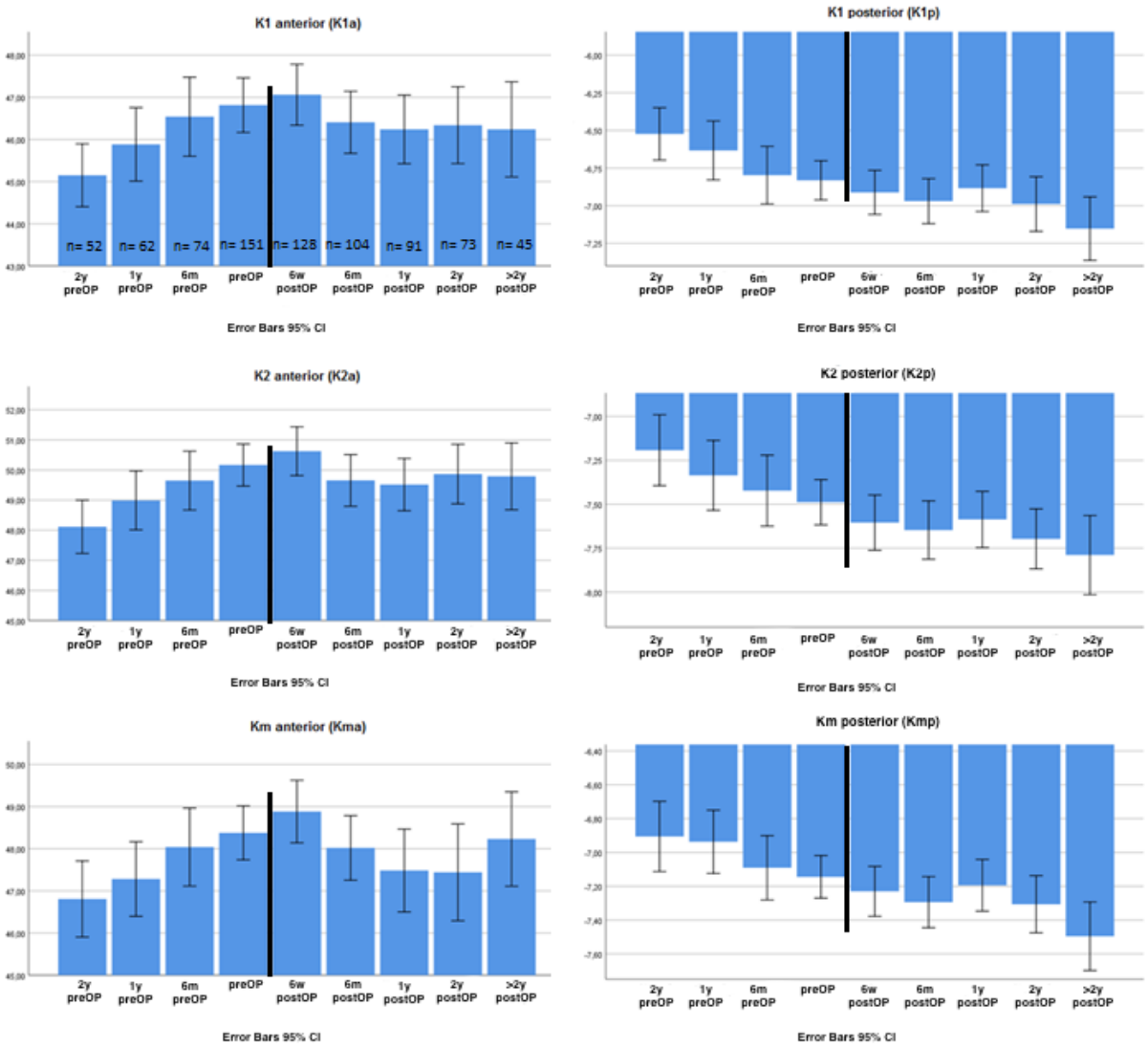

***Figure 12**: Mean ± standard deviation (SD) values of anterior and posterior corneal tomography measurements for the **adult** patients. Progressive increase with corneal steepening for K1a (= anterior steep keratometry), K2a (anterior flat keratometry) and Kma (= anterior mean keratometry) until 6 weeks after corneal crosslinking (CXL), followed by decrease (corneal flattening) and stabilization until > 2 years postoperatively. No statistically significant changes observed for the posterior corneal tomographic parameters K1p (= posterior steep keratometry), K2p (= posterior flat keratometry), Kmp (= posterior mean keratometry)* [332].

Kmax increased significantly from 2 years pre-CXL until 6 weeks postoperatively (df(8) = 3.450, **p = 0.01**, MANOVA) and decreased significantly from 6 weeks post-CXL until > 2 years post-CXL (**p = 0.034**, **Tables 6 and 7**, **Figure 13**). The paired t-

test showed a statistically significant increase from pre-CXL to 6 weeks post-CXL (**p = 0.001**), then Kmax decreased statistically significantly from 6 weeks post-CXL until > 2 years post-CXL (**p < 0.005**, **Tables 6 and 7**, **Figure 13**) [332].

Table 6: Adult group - Means and Standard Deviations (SD) for Kmax, BCVA, anterior and posterior astigmatism, thinnest and apex pachymetry

	Kmax (D)	BCVA (LogMAR)	Astia (D)	Astip (D)	TCT (µm)	ACT (µm)
2 years pre-CXL (n = 52)	53.3 ± 5.0	0.19 ± 0.04	3.1 ± 1.8	-6.5 ± 0.6	478 ± 30	490 ± 30
1 year pre-CXL (n = 62)	55.4 ± 6.0	0.27 ± 0.03	3.2 ± 2.0	-6.6 ± 0.8	470 ± 36	482 ± 35
6 months pre-CXL (n = 74)	57.1 ± 7.2	0.32 ± 0.03	3.2 ± 2.1	-6.8 ± 0.8	460 ± 38	474 ± 38
pre-CXL (n = 151)	57.6 ± 6.8	0.35 ± 0.02	3.4 ± 1.9	-6.8 ± 0.8	459 ± 39	474 ± 36
6 weeks post-CXL (n= 128)	58.3 ± 6.8	0.39 ± 0.02	3.6 ± 2.1	-6.9 ± 0.8	444 ± 42	456 ± 39
6 months post-CXL (n = 104)	57.1 ± 6.7	0.31 ± 0.03	3.4 ± 1.9	-7.0 ± 0.8	442 ± 41	455 ± 40
1 year post-CXL (n = 91)	56.6 ± 6.6	0.30 ± 0.03	3.3 ± 2.0	-6.9 ± 0.8	447 ± 47	463 ± 41
2 years post-CXL (n = 73)	56.7 ± 6.8	0.22 ± 0.03	3.6 ± 2.0	-6.9 ± 0.8	449 ± 42	466 ± 39
>2 years post-CXL (n = 45)	55.9 ± 5.5	0.18 ± 0.04	3.4 ± 2.0	-6.9 ± 0.8	447 ± 46	462 ± 41

Table 6: *Mean ± standard deviation (SD) values of the maximal anterior keratometry (Kmax), the best spectacle-corrected distance visual acuity (BCVA), the astigmatism of the anterior (Astia) and posterior cornea (Astip), the thinnest corneal thickness (TCT), the pachymetry of the apex (ACT) for the **adult** patients. Decrease of TCT and ACT 6 weeks and 6 months after corneal crosslinking (CXL) followed by a stabilization until > 2 years post-CXL. Increase of the Astia 6 weeks post-CXL and fluctuations until > 2 years post-CXL compared to the pre-CXL values. Progressive deterioration of BCVA from 2 years preoperatively to 6 weeks postoperatively, followed by a stepwise improvement until > 2 years postoperatively* [332].

Table 7: Adult group - Mean differences ± Standard Deviations and p-values for Kmax (paired t-test)

Kmax (D)	pre-CXL - 6 weeks post-CXL (n = 129)	pre-CXL - 6 months post-CXL (n = 106)	pre-CXL - 1 year post-CXL (n = 93)	pre-CXL - 2 years post-CXL (n = 75)	pre-CXL - > 2 years post-CXL (n = 49)
Δ ± SD	-0.8 ± 0.2	0.9 ± 0.3	1.5 ± 0.3	2.2 ± 0.3	3.8 ± 0.6
p-value	**p = 0.001**	**p = 0.001**	**p < 0.0001**	**p < 0.0001**	**p < 0.0001**
	6 weeks post-CXL - 6 months post-CXL (n = 89)	6 weeks post-CXL - 1 year post-CXL (n = 76)	6 weeks post-CXL - 2 years post-CXL (n = 59)	6 weeks post-CXL - >2 years post-CXL (n = 38)	
Δ ± SD	1.7 ± 0.3	2.3 ± 0.3	2.9 ± 0.4	4.9 ± 0.8	
p-value	**p < 0.0001**	**p < 0.0001**	**p < 0.0001**	**p < 0.0001**	

Table 7: *Mean differences (Δ) ± standard deviation (SD) values and corresponding p-values for maximal anterior keratometry (Kmax) for the* ***adult*** *patients. Statistically significant increase of Kmax 6 weeks after corneal crosslinking (CXL) compared to prior to-CXL, followed by statistically significant decrease at all further postoperative follow-ups* [332].

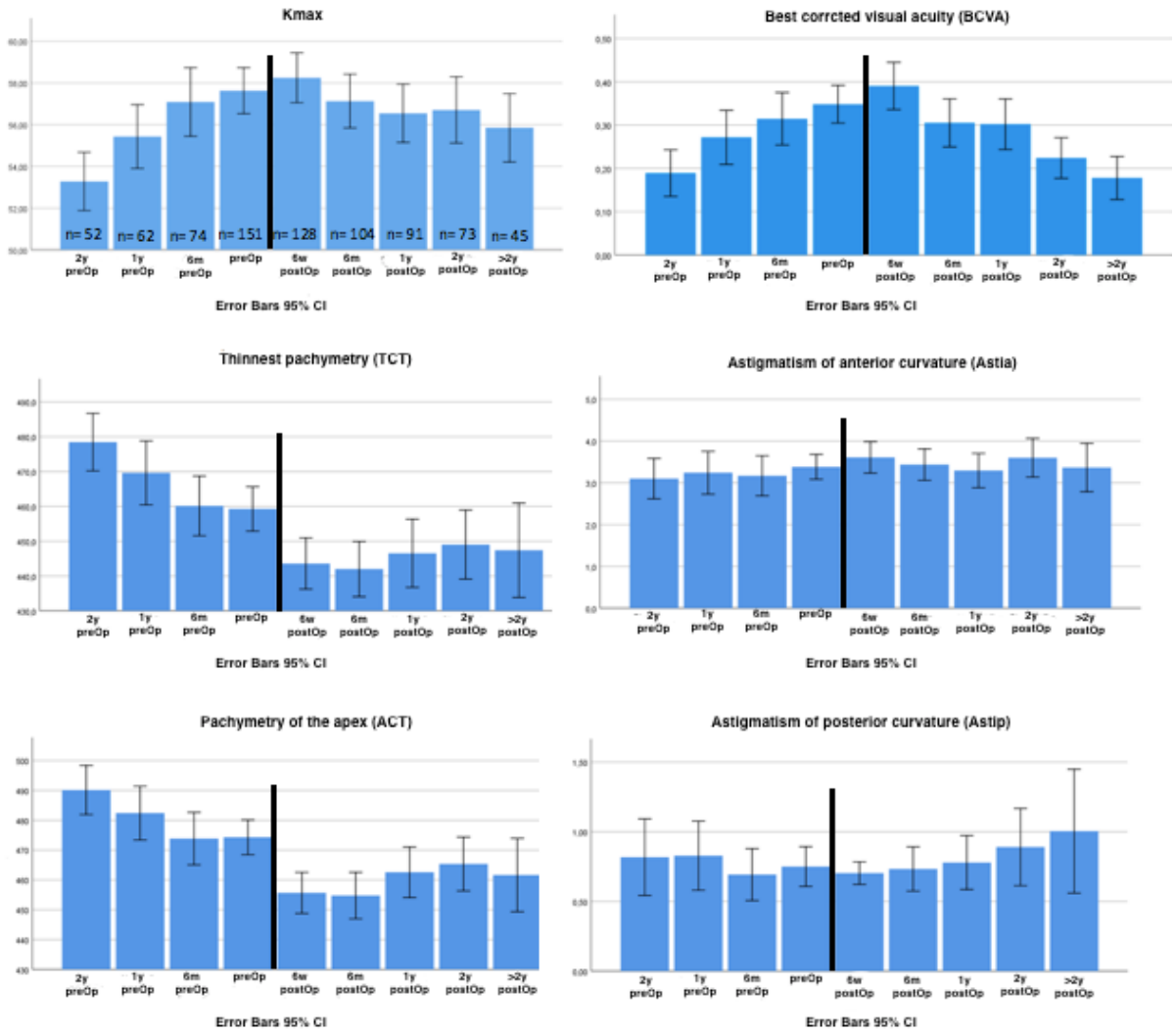

***Figure 13**: Mean ± standard deviation (SD) values of Kmax (= maximal anterior keratometry), TCT (= thinnest corneal pachymetry), ACT (= apex corneal pachymetry), BCVA (= best spectacle-corrected distance visual acuity), Astia (= anterior astigmatism), Astip (= posterior astigmatism), for the **adult** patients. Increasing Kmax, decreasing BCVA, TCT and ACT over 2 years before corneal crosslinking (CXL). Progressive Kmax increase 6 weeks post-CXL, followed by a decrease and stabilization. Continuous decrease of TCT and ACT 6 weeks and 6 months post-CXL. Deterioration of the BCVA corresponding to the corneal steepening and thinning 6 weeks post-CXL, followed by continuous improvement. Fluctuations of Astia and increase of Astip* [332].

Posterior curvature: steep (K1p), flat (K2p) and mean (K2p) (Pentacam® HR, Oculus, Wetzlar, Germany)

MANOVA revealed a statistically significant change for all steep, flat and mean posterior corneal curvature overtime (K1p: df(8) = 3.367, **p = 0.0001**, K2p: df(8) = 3.197, **p = 0.0001**, Kmp: df(8) = 3.313, **p < 0.0001**). A long-term increase of those values was observed from 2 years pre-CXL to all postoperative follow-ups (**Table 4**, **Figure 12**). However, the paired t-test comparison for K1p showed stability from pre-CXL to all post-CXL time points and a statistically significant increase for K2p from pre-CXL to 6 weeks, 1 year and 2 years post-CXL (**p < 0.0001, p = 0.012 and p = 0.031** respectively) and for Kmp until 6 months post-CXL (**p ≤ 0.045**, **Table 8**, **Figure 13**) [332]. Compared to 6 weeks post-CXL again no statistical significant changes were observed for all posterior keratometric values apart from the 1 year comparison for K1p and for the > 2 years comparison for K2p (**p = 0.039** and **p = 0.033** respectively), indicating a weak effect of CXL at the posterior keratometry (**Table 8, Figure 13**).

Table 8: Adult group - Mean differences ± Standard Deviations and p-values for K1p, K2p, Kmp (paired t-test)

	pre-CXL - 6 weeks post-CXL (n = 129)	pre-CXL - 6 months post-CXL (n = 106)	pre-CXL - 1 year post-CXL (n = 93)	pre-CXL - 2 years post-CXL (n = 75)	pre-CXL - >2 years post-CXL (n = 49)	6 weeks post-CXL - 6 months post-CXL (n = 89)	6 weeks post-CXL - 1 year post-CXL (n = 76)	6 weeks post-CXL - 2 years post-CXL (n = 59)	6 weeks post-CXL - >2 years post-CXL (n = 38)
K1p (D)									
Δ ± SD	0.2 ± 0.1	0.2 ± 0.1	0.2 ± 0.2	0.0 ± 0.3	0.4 ± 0.3	0.0 ± 0.3	-0.0 ± 0.0	-0.3 ± 0.3	-0.1 ± 0.1
p-value	p = 0.067	p = 0.069	p = 0.298	p = 0.902	p = 0.182	p = 0.969	**p = 0.039**	p = 0.284	p = 0.335
K2p (D)									
Δ ± SD	0.1 ± 0.0	-0.0 ± 0.2	0.1 ± 0.0	0.1 ± 0.0	0.0 ± 0.1	-0.2 ± 0.2	0.0 ± 0.0	-0.1 ± 0.1	-0.2 ± 0.1
p-value	**p < 0.0001**	p = 0.945	**p = 0.012**	**p = 0.031**	p = 0.442	p = 0.338	p = 0.179	p = 0.122	**p = 0.033**
Kmp (D)									
Δ ± SD	0.2 ± 0.1	0.2 ± 0.1	0.2 ± 0.1	0.2 ± 0.2	0.1 ± 0.1	0.0 ± 0.0	-0.1 ± 0.0	-0.1 ± 0.1	-0.0 ± 0.1
p-value	**p = 0.038**	**p = 0.045**	p = 0.229	p = 0.226	p = 0.096	p = 0.859	p = 0.175	p = 0.312	0.466

Table 8: *Mean differences (Δ) ± standard deviation (SD) values and corresponding p-values for steep (K1p), flat (K2p) and mean (Kmp) posterior keratometries between prior to corneal*

*crosslinking-(CXL) and all postoperative periods, as well as 6 weeks post-CXL compared to 6 months / 1 year / 2 years and > 2 years post-CXL for the **adult** patients* [332].

Pachymetry of the thinnest corneal thickness (TCT) and pachymetry of the apex (ACT) (Pentacam® HR, Oculus, Wetzlar, Germany)

The thinnest corneal pachymetry (TCT) showed a statistically significant difference over time as measured with MANOVA (df(8) = 6.838, **p = 0.0001**). There was a significant decrease from pre-CXL to 6 weeks and 6 months post-CXL (**p < 0.05**), followed by stability until the latest follow-up (**Table 6**, **Figure 13**). The paired t-test analysis showed also a statistically significant decrease of TCT from preoperatively up to 2 years post-CXL (**p ≤ 0.036**) and it remained stable at > 2years follow-up (**Table 9**, **Figure 13**).

The apex corneal pachymetry (ACT) again presented with statistically significant differences overtime as evaluated with MANOVA (df(8) = 7.668, **p < 0.0001**). We observed a decrease from preoperatively to 6 weeks and 6 months post-CXL (**p < 0.05**) and non-significant statistical differences until the latest follow-up (**Table 6**, **Figure 13**). The paired t-test showed a statistically significantly lower ACT until 1 year post-CXL compared to values pre-CXL (**p < 0.0001**, **Table 9**, **Figure 13**) [332].

Table 9: Adult group - Mean differences ± Standard Deviations and p-values for TCT, ACT (paired t-test)

	pre-CXL - 6 weeks post-CXL (n = 129)	pre-CXL - 6 months post-CXL (n = 106)	pre-CXL - 1 year post-CXL (n = 93)	pre-CXL - 2 years post-CXL (n = 75)	pre-CXL - >2 years post-CXL (n = 49)
TCT (µm)					
Δ ± SD	16 ± 3	13 ± 3	9 ± 4	8 ± 4	3 ± 6
p-value	**p < 0.0001**	**p < 0.0001**	**p = 0.017**	**p = 0.036**	p = 0.578
ACT (µm)					
Δ ± SD	19 ± 2	20 ± 5	10 ± 3	6 ± 3	6 ± 5
p-value	**p < 0.0001**	**p < 0.0001**	**p < 0.0001**	**p < 0.0001**	p = 0.257

Table 9: *Mean Differences (Δ) ± standard deviation (SD) values and corresponding p-values for thinnest and apex corneal pachymetry (TCT, ACT) for the **adult** patients. Statistically*

significant decrease 6 weeks, 6 months, 1 and 2 years post-CXL for TCT and 6 weeks, 6 months and 1 year post-CXL for ACT compared to pre-CXL [332].

Astigmatism of the anterior (Astia) and posterior corneal curvature (Astip) (Pentacam® HR, Oculus, Wetzlar, Germany)

Both MANOVA (Astia: df(8) = 0.635, p = 0.749, Astip: df(8) = 0.755, p = 0.643) and paired t-test showed no statistically significant differences for the astigmatism changes of the anterior and posterior corneal curvature (**Table 6**, **Figure 13**) [332].

5.1.3 Visual results on adult patients

Best spectacle-corrected visual acuity (BCVA) (in LogMAR)

MANOVA analysis showed a statistically significant difference of BCVA overtime (df(8) = 6.015, **p < 0.0001**). There was a non-significant decrease 6 weeks post-CXL compared to pre-CXL and an improvement from the 6-month postoperative follow-up on, with statistically significant difference at 2 years and > 2 years follow-up, compared with the pre-CXL and 6-week post-CXL values (**p < 0.05**, **Table 6**). The paired t-test showed statistically significant differences for all time periods from pre-CXL until > 2 years post-CXL (**p < 0.05**), except for the comparison between the 6 weeks and 6 months post-CXL with p > 0.05 (**Table 10**, **Figure 13**) [332].

Table 10: Adult group - Mean differences ± Standard Deviations and p-values for BCVA (paired t-test)					
BCVA (LogMAR)	pre-CXL - 6 weeks post-CXL (n = 129)	pre-CXL - 6 months post-CXL (n = 106)	pre-CXL - 1 year post-CXL (n = 93)	pre-CXL - 2 years post-CXL (n = 75)	pre-CXL - >2 years post-CXL (n = 49)
Δ ± SD	-0.04 ± 0.02	0.04 ± 0.02	0.06 ± 0.02	0.13 ± 0.03	0.19 ± 0.03
p-value	p = 0.087	p = 0.053	**p = 0.023**	**p < 0.0001**	**p < 0.0001**
	6 weeks post-CXL - 6 months post-CXL (n = 89)	6 weeks post-CXL - 1 year post-CXL (n = 76)	6 weeks post-CXL - 2 years post-CXL (n = 59)	6 weeks post-CXL - >2 years post-CXL (n = 38)	
Δ ± SD	0.09 ± 0.03	0.13 ± 0.03	0.17 ± 0.03	0.20 ± 0.03	
p-value	**p = 0.002**	**p < 0.0001**	**p < 0.0001**	**p < 0.0001**	

Table 10: *Mean differences (Δ) ± standard deviation (SD) values and corresponding p-values (paired t-test) for best spectacle-corrected distance visual acuity (BCVA) for the* ***adult*** *patients. Decrease of BCVA 6 weeks after corneal crosslinking (CXL) compared to pre-CXL, followed by an increase with statistically significance 1 year, 2 years and > 2 years post-CXL compared to pre-CXL as well as 6 months post-CXL* [332].

5.1.4 Tomographic results on patients under 18 years of age

Belin-Ambrósio deviation value (BAD-D) (Pentacam® HR, Oculus, Wetzlar, Germany)

According to the MANOVA analysis, a statistically significant difference overtime occurred for the total deviation value (BAD-D: df(8) = 2.982, **p = 0.03**, **Table 11**). The paired t-test showed a statistically significant increase from 6 months pre-CXL to pre-CXL (**p = 0.028**) and, in comparison to all postoperative follow-up time points until 2 years post-CXL (**p < 0.0001**), but with a progressive decrease of the difference from the 6 months follow-up on (**Table 12**). Compared to pre-CXL values, there was a statistically significant increase 6 weeks post-CXL (**p = 0.007**) and 6 months post-CXL (**p= 0.042**) but with no statistically significant differences compared to all the other time points (**Table 12**) [334].

Table 11: Underaged group - Mean ± Standard Deviation (SD) for anterior and posterior keratometries and total deviation value

	K1a (D)	K2a (D)	Kma (D)	K1p (D)	K2p (D)	Kmp (D)	BAD-D
2 years pre-CXL (n = 9)	44.8 ± 3.1	48.9 ± 3.2	47.0 ± 3.1	-6.4 ± 0.7	-7.5 ± 0.7	-6.9 ± 0.6	6.8 ± 3.1
1 year pre-CXL (n = 16)	44.8 ± 2.3	50.2 ± 4.2	47.3 ± 2.9	-6.5 ± 0.4	-7.6 ± 0.8	-7.0 ± 0.5	7.6 ± 2.3
6 months pre-CXL (n = 25)	44.7 ± 3.0	49.8 ± 3.2	47.1 ± 2.9	-6.5 ± 0.6	-7.6 ± 0.7	-7.0 ± 0.6	7.5 ± 2.9
pre-CXL (n = 41)	47.2 ± 5.1	52.7 ± 5.4	49.8 ± 5.0	-7.0 ± 1.0	-8.1 ± 1.0	-7.5 ± 0.9	9.8 ± 4.4
6 weeks post-CXL (n = 33)	48.5 ± 5.2	53.8 ± 5.8	51.0 ± 5.2	-7.1 ± 0.9	-8.2 ± 1.0	-7.6 ± 0.9	10.9 ± 4.5
6 months post-CXL (n = 34)	47.2 ± 4.9	52.6 ± 5.2	49.7 ± 4.9	-7.0 ± 1.1	-8.2 ± 1.0	-7.6 ± 0.9	10.5 ± 4.1
1 year post-CXL (n = 36)	46.6. ± 5.2	51.8 ± 6.0	49.1 ± 5.3	-6.9 ± 0.9	-8.0 ± 1.0	-7.5 ± 0.9	9.8 ± 4.1
2 years post-CXL (n = 26)	46.0 ± 4.9	52.3 ± 5.7	49.4 ± 5.1	-7.0 ± 0.9	-8.1 ± 0.9	-7.5 ± 0.9	10.6 ± 4.4
>2 years post-CXL (n = 16)	47.5 ± 4.3	53.2 ± 4.4	50.3 ± 3.9	-7.1 ± 0.7	-8.2 ± 0.8	-7.7 ± 0.7	10.9 ± 3.6

Table 11: *Mean ± standard deviation (SD) values of anterior steep (K1a), flat (K2a), mean (Kma) and posterior steep (K1p), flat (K2p) mean (Kmp) keratometry and total deviation value (BAD-D) 2 years, 1 year, 6 months before corneal crosslinking (pre-CXL) prior to surgery (pre-CXL) and 6 weeks, 6 months, 1 year, 2 years, > 2 years after CXL for the* ***underaged*** *patients. A stepwise increase of all anterior keratometry values is observed until 6 weeks post-CXL, followed by a decrease until >2 years post-CXL. The posterior keratometry values increase until pre-CXL and remain unaffected post-CXL. The total deviation value increases prior to CXL and post-CXL compared to the preoperative values; the post-CXL values from the 6 weeks-post CXL onwards fluctuate, but seem at a comparable level until > 2 years post-CXL* [334].

Table 12: Underaged patients - Mean differences ± Standard Deviations and p-values for BAD-D (paired t-test)

BAD-D	6 months pre-CXL - pre-CXL (n = 25 eyes)	6 months pre-CXL - 6 weeks post-CXL (n = 19 eyes)	6 months pre-CXL - 6 months post-CXL (n = 22 eyes)	6 months pre-CXL- 1 year post-CXL (n = 23 eyes)	6 months pre-CXL- 2 years post-CXL (n = 15 eyes)	6 months pre-CXL- >2 years post-CXL (n = 10 eyes)
Δ ± SD	-0.5 ± 0.2	-1.3 ± 0.3	-1.2 ± 0.3	-1.0 ± 0.3	-0.9 ± 0.4	-0.5 ± 0.5
p-value	**p = 0.028**	**p = 0.0001**	**p = 0.002**	**p = 0.003**	**p = 0.038**	p = 0.414
	pre-CXL - 6 weeks post-CXL (n = 33 eyes)	pre-CXL - 6 months post-CXL (n = 34 eyes)	pre-CXL - 1 year post-CXL (n = 36 eyes)	pre-CXL - 2 years post-CXL (n = 26 eyes)	pre-CXL - >2 years post-CXL (n = 16 eyes)	
Δ ± SD	-0.7 ± 0.2	-0.5 ± 0.2	-0.3 ± 0.2	-0.3 ± 0.2	-0.2 ± 0.3	
p-value	**p = 0.007**	**p = 0.012**	p = 0.169	p = 0.094	p = 0.382	

Table 12: *Mean Differences (Δ) ± standard deviation (SD) values and corresponding p-values for total deviation values (BAD-D) after comparing measurements 6 months before CXL (6 months pre-CXL) with prior to surgery (pre-CXL) and with 6 weeks, 6 months, 1 year, 2 years, > 2 years after corneal crosslinking (post-CXL) as well as after comparing the prior to surgery values to the postoperative follow-up measurements for the* ***underaged*** *patients. Statistically significant increase of the values from 6 months pre-CXL to pre-CXL as well as 6 weeks, 6 months, 1 year and 2 years post-CXL followed by a not statistically significant increase until > 2 years post-CXL. Statistically significant increase of the values 6 weeks and 6 months post-CXL compared to prior to CXL with following not statistically significant increase until > 2 years post-CXL* [334].

Anterior curvature: steep (K1a), flat (K2a) and mean (Kma) anterior keratometry, maximal anterior keratometry (Kmax) (Pentacam® HR, Oculus, Wetzlar, Germany)

The steep anterior keratometry K1a did not change significantly over time according to MANOVA (K1a: df(8) = 1.906, p = 0.06, **Table 11**). The paired t-test showed a statistically significant increase from pre-CXL to 6 weeks post-CXL (**p = 0.014**) and a following decrease with statistical significance at 1 year (**p = 0.038**) and 2 years post-CXL (**p = 0.024, Table 13**). Furthermore, compared to the 6-week follow-up, there was a statistically significant decrease of K1a values until the latest follow-up (**p < 0.0001, Tables 11** and **13**). In the follow-up of > 2 years post-CXL, there seemed to be a slight increase of mean K1a (**Figure 14**), however, the paired t-test showed further decrease of the value without statistical significance compared to pre-CXL

(**Table 13**). This could be considered as a bias due to a dropout of follow-up at > 2 years postoperatively (n = 16, **Table 11**).

The flat anterior keratometry K2a showed a statistically significant change over time according to MANOVA (df(8) = 1.995, **p = 0.048**), but without statistically significant changes prior to CXL compared to the postoperative follow-up values (**Table 11**). The comparisons with paired t-test showed a statistically significant increase of K2a from prior to CXL to 6 weeks post-CXL (**p = 0.031**, **Table 13**, **Figure 14**), followed by a statistically significant decrease 1 year post-CXL (**p = 0.022, Table 13**, **Figure 14**). Compared to 6 weeks postoperatively, the K2a values decreased statistically significantly until > 2 years post-CXL (**p < 0.05**, **Table 13**, **Figure 14**). Again, mean K2a was higher at > 2 years follow-up than prior to CXL, which could be attributed to the lower number of follow-up examinations at this time point (n = 16). Nevertheless, the mean difference remained negative, implying a decreasing tendency of K2a, without statistical significance (**Table 11** and **13**, **Figure 14**).

The MANOVA analysis revealed a statistically significant change of mean anterior keratometry Kma over time df(8) = 2.159, **p = 0.032**). No statistically significant changes were observed post-CXL compared to before CXL and only the decrease from 6 weeks post-CXL in comparison to 1 year post-CXL was close to statistical significance (p = 0.088, **Table 11**). Using the paired t-test, a statistically significant increase was revealed 6 weeks post-CXL (**p = 0.011**), followed by a statistically significant decrease even at the 2-year follow-up, compared to pre-CXL (**p ≤ 0.035**, **Table 13**, **Figure 3**). Compared to 6 weeks post-CXL, there was a statistically significant decrease of Kma until the latest follow-up (p < 0.0001, **Table 13**, **Figure 14**). No statistically significant changes were observed between the remaining follow-up visits, indicating stability post-CXL (p > 0.05) [334].

Table 13: Underaged group - Mean differences ± Standard Deviations and p-values for K1a, K2a, Kma (paired t-test)									
	pre-CXL - 6 weeks post-CXL (n = 33 eyes)	pre-CXL - 6 months post-CXL (n = 34 eyes)	pre-CXL - 1 year post-CXL (n = 36 eyes)	pre-CXL - 2 years post-CXL (n = 26 eyes)	pre-CXL - >2 years post-CXL (n = 16 eyes)	6 weeks post-CXL - 6 months post-CXL (n = 28 eyes)	6 weeks post-CXL - 1 year post-CXL (n = 28 eyes)	6 weeks post-CXL - 2 years post-CXL (n = 21 eyes)	6 weeks post-CXL - >2 years post-CXL (n = 16 eyes)
K1a (D)									
Δ ± SD	-0.8 ± 0.3	0.4 ± 0.3	0.5 ± 0.2	0.8 ± 0.3	0.8 ± 0.5	1.1 ± 0.2	1.2 ± 0.2	1.6 ± 0.3	1.6 ± 0.3
p-value	**p = 0.014**	**p = 0.184**	**p = 0.038**	**p = 0.024**	p = 0.137	**p < 0.0001**	**p < 0.0001**	**p < 0.0001**	**p = 0.0001**
K2a (D)									
Δ ± SD	-0.7 ± 0.3	0.6 ± 0.3	0.9 ± 0.4	0.8 ± 0.4	0.9 ± 0.7	1.1 ± 0.4	1.4 ± 0.4	1.3 ± 0.3	1.5 ± 0.4
p-value	**p = 0.031**	p = 0.053	**p = 0.022**	p = 0.067	p = 0.220	**p = 0.013**	**p = 0.004**	**p < 0.0001**	**p = 0.004**
Kma (D)									
Δ ± SD	-0.7 ± 0.3	0.6 ± 0.3	0.6 ± 0.2	0.9 ± 0.3	1.0 ± 0.6	1.2 ± 0.2	1.2 ± 0.2	1.5 ± 0.2	1.8 ± 0.3
p-value	**p = 0.011**	**p = 0.035**	**p = 0.009**	**p = 0.019**	p = 0.114	**p < 0.0001**	**p < 0.0001**	**p < 0.0001**	**p < 0.0001**

Table 13: *Mean differences (Δ) ± standard deviation (SD) values for anterior steep (K1a), flat (K2a) and mean (Kma) keratometry values after comparing measurements prior to surgery with 6 weeks, 6 months, 1 year, 2 years, > 2 years after corneal crosslinking (CXL) as well as after comparing the measurements of the 6-week follow-up with the measurements of the rest follow-up examinations for the* ***underaged*** *patients. Statistically significant increase of all keratometry values 6 weeks post-CXL followed by a statistically significant decrease until 2 years post-CXL, even after 2 years post-CXL* [334].

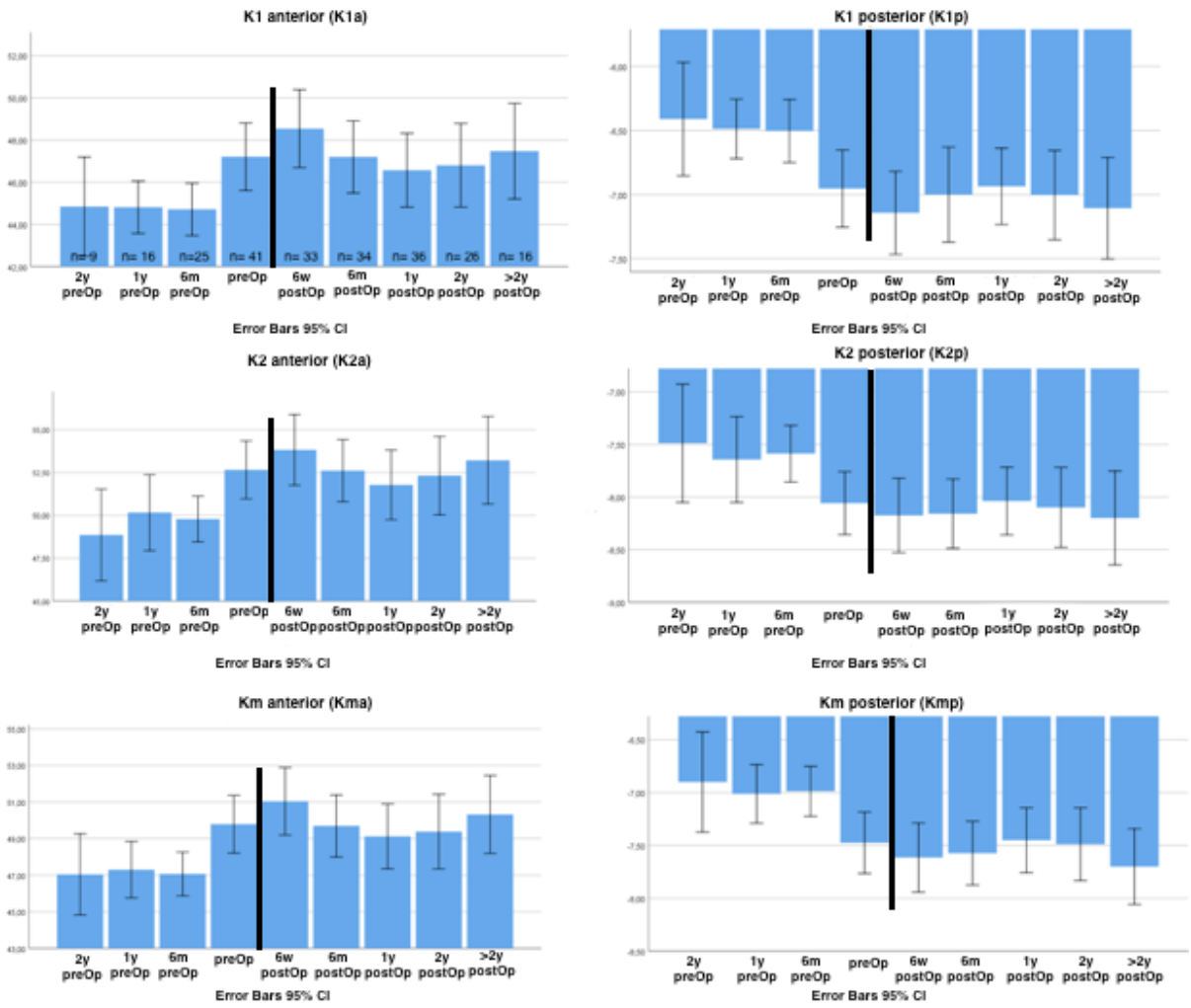

Figure 14: *Mean ± standard deviation (SD) values of K1a (= anterior steep keratometry), K2a (anterior flat keratometry), Kma (= anterior mean keratometry), K1p (= posterior steep keratometry), K2p (= posterior flat keratometry), Kmp (=posterior mean keratometry) for the* ***underaged*** *patients. Progressive increase of K1a, K2a, Kma until 6 weeks after corneal crosslinking (CXL), followed by a decrease and stabilization until > 2 years post-CXL. Progressive increase for the posterior keratometry values followed by fluctuations postoperatively, indicating no effect of CXL on the posterior corneal curvature* [334].

The maximal anterior keratometry Kmax showed statistically significant changes over time as determined by MANOVA (df(8) = 2.629, **p = 0.009**). There was a statistically significant increase until 6 weeks post-CXL, followed by a decrease without statistical significance (**Table 14**). The paired t-test comparisons revealed again an increase of Kmax at 6 weeks post-CXL compared to prior to CXL followed by a statistically

significant decrease until > 2 years postoperatively (**p < 0.05**, **Tables 14 and 15**, **Figure 15**). A similar statistically significant decrease of Kmax was observed until the latest follow-up, compared to 6 weeks post-CXL (**p < 0.05**, **Tables 14** and **15**, **Figure 15**). The other paired t-test comparisons showed a statistically non-significant decrease of Kmax, with exception the comparison between the values 2 years post-CXL to > 2 years post-CXL (mean difference ± standard deviation, p value: 0.5 ± 0.2, **p = 0.024**). Once more, the increased mean Kmax value > 2 years post-CXL could be due to the reduced number of follow-ups at this time point (n = 16, **Table 14**) [334].

Table 14: Underaged group - Mean ± Standard Deviation (SD) for Kmax, BCVA, anterior and posterior astigmatism, thinnest and apex pachymetry

	Kmax (D)	BCVA (LogMAR)	Astia (D)	Astip (D)	TCT (µm)	ACT (µm)
2 years pre-CXL (n = 9)	53.7 ± 5.5	0.31 ± 0.08	4.0 ± 1.8	1.0 ± 0.4	486 ± 32	515 ± 38
1 year pre-CXL (n = 16)	56.5 ± 5.5	0.25 ± 0.07	5.3 ± 2.4	1.2 ± 0.6	476 ± 22	488 ± 21
6 months pre-CXL (n = 25)	56.1 ± 5.9	0.29 ± 0.05	5.1 ± 2.4	1.1 ± 0.4	474 ± 32	483 ± 32
pre-CXL (n = 41)	61.5 ± 8.5	0.44 ± 0.04	5.6 ± 3.2	1.1 ± 0.6	460 ± 37	468 ± 37
6 weeks post-CXL (n = 33)	62.6 ± 8.0	0.48 ± 0.05	5.4 ± 3.3	1.1 ± 0.5	439 ± 36	447 ± 34
6 months post-CXL (n = 34)	60.3 ± 7.8	0.33 ± 0.04	5.4 ± 2.8	1.1 ± 0.6	447 ± 48	460 ± 41
1 year post-CXL (n = 36)	59.2 ± 8.4	0.30 ± 0.03	5.5 ± 3.0	1.3 ± 0.9	452 ± 44	461 ± 41
2 years post-CXL (n = 26)	60.0 ± 8.3	0.26 ± 0.05	5.4 ± 3.0	1.1 ± 0.5	447 ± 43	457 ± 37
>2 years post-CXL (n = 16)	60.8 ± 7.9	0.21 ± 0.06	5.4 ± 3.5	1.2 ± 0.6	437 ± 46	447 ± 33

Table 14: *Mean ± Standard deviation (SD) values of maximal anterior keratometry (Kmax), best spectacle corrected visual acuity (BCVA) in LogMAR, anterior (Astia) and posterior (Astip) astigmatism, thinnest (TCT) and apex (ACT) corneal pachymetry 2 years, 1 year, 6*

*months before corneal crosslinking (pre-CXL), prior to surgery (pre-CXL), as well as 6 weeks, 6 months, 1 year, 2 years and > 2 years post-CXL for the **underaged** patients. Continuous increase of Kmax values until 6 weeks post-CXL, followed by a stepwise decrease until 1 year post-CXL. Deterioration of BCVA until 6 weeks post-CXL, followed by improvement until >2 years post-CXL. Fluctuations of Astia and Astip before and after CXL. Continuous decrease of TCT and ACT, especially until the 6-week follow-up* [334].

Table 15: Underaged group - Mean differences ± Standard Deviations and p-values for Kmax (paired t-test)

Kmax (D)	pre-CXL - 6 weeks post-CXL (n = 33 eyes)	pre-CXL - 6 months post-CXL (n = 34 eyes)	pre-CXL - 1 year post-CXL (n = 36 eyes)	pre-CXL - 2 years post-CXL (n = 26 eyes)	pre-CXL - >2 years post-CXL (n = 16 eyes)
Δ ± SD p-value	-0.2 ± 0.5 p = 0.675	1.7 ± 0.5 **p = 0.001**	1.8 ± 0.5 **p = 0.001**	1.8 ± 0.5 **p = 0.001**	2.1 ± 0.5 **p = 0.001**
	6 weeks post-CXL - 6 months post-CXL (n = 28 eyes)	6 weeks post-CXL - 1 year post-CXL (n = 28 eyes)	6 weeks post-CXL - 2 years post-CXL (n = 21 eyes)	6 weeks post-CXL - >2 years post-CXL (n = 16 eyes)	
Δ ± SD p-value	1.6 ± 0.5 **p = 0.002**	1.8 ± 0.5 **p = 0.001**	1.8 ± 0.6 **p = 0.007**	1.9 ± 0.7 **p = 0.018**	

***Table 15:** Mean Differences (Δ) ± standard deviation (SD) values and corresponding p-values for maximal anterior keratometry (Kmax) for the comparisons of the measurements prior to corneal crosslinking (pre-CXL) to postoperative values 6 weeks, 6 months, 1 year, 2 years, > 2 years postoperatively (post-CXL) as well as for the comparisons of the measurements 6 weeks post-CXL to the medium-term follow-up measurements for the **underaged** patients. Increase of Kmax without statistical significance 6 weeks post-CXL, followed by statistically significant decrease even until > 2 years post-CXL. Statistically significant decrease of Kmax comparing the 6 week post-CXL values to the medium-term follow-up measurements, until > 2 years post-CXL* [334].

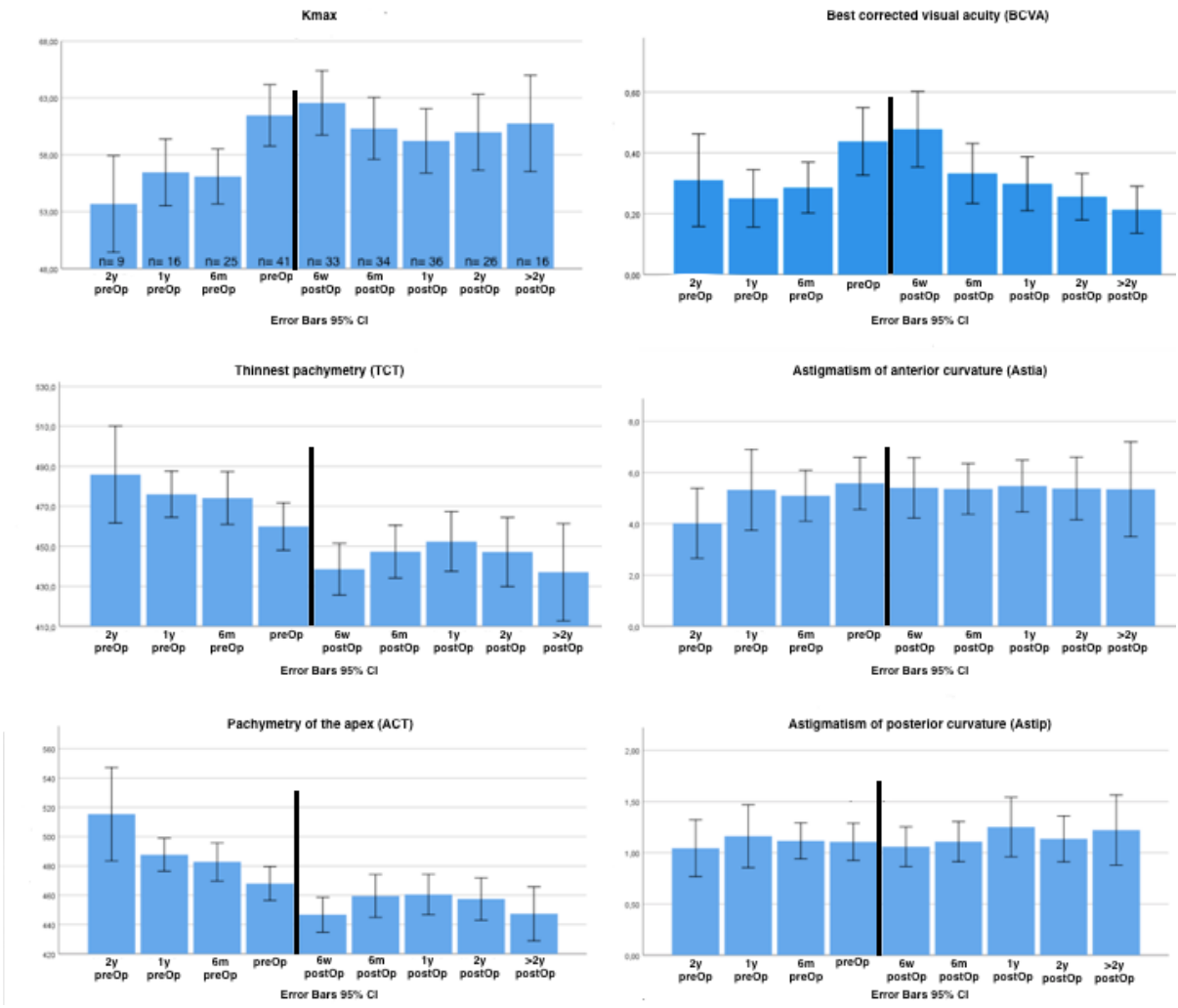

Figure 15: *Mean ± standard deviation (SD) values of Kmax (= maximal anterior keratometry), TCT (= thinnest corneal pachymetry), ACT (= apex corneal pachymetry), BCVA (= best spectacle-corrected distance visual acuity), Astia (= anterior astigmatism), Astip (= posterior astigmatism), for the* ***underaged*** *patients. Deterioration of Kmax and BCVA until 6 weeks postoperatively, followed by improvement and stabilization. Progressive reduction of TCT and ACT until 6 weeks and 6 months postoperatively, with following stabilization. Fluctuations of Astia and Astip* [334].

Posterior curvature: steep (K1p), flat (K2p) and mean (K2p) (Pentacam® HR, Oculus, Wetzlar, Germany)

The posterior steep (K1p) and mean (Kmp) corneal keratometry values showed statistically significant differences preoperatively with higher values indicating KC

progression (K1p: df(8) = 0.041, Kmp: df(8) = 2.446, **p = 0.015**), without statistically significant differences prior to CXL and at postoperative follow-ups (p > 0.05), according to MANOVA (**Table 11**). The flat posterior keratometry did not show statistically significant changes overtime (df(8) = 1.779, p ≥ 0.082). The paired t-test showed no statistically significant differences for the postoperative comparisons for all posterior keratometry values, indicating an unaffected posterior keratometry (**Tables 11** and **18**, **Figure 14**) [334].

Table 16: Underaged group - Mean differences ± Standard Deviations and p-values for K1p, K2p, Kmp (paired t-test)

	pre-CXL - 6 weeks post-CXL (n = 33 eyes)	pre-CXL - 6 months post-CXL (n = 34 eyes)	pre-CXL - 1 year post-CXL (n = 36 eyes)	pre-CXL - 2 years post-CXL (n = 26 eyes)	pre-CXL - >2 years post-CXL (n = 16 eyes)	6 weeks post-CXL - 6 months post-CXL (n = 28 eyes)	6 weeks post-CXL - 1 year post-CXL (n = 28 eyes)	6 weeks post-CXL - 2 years post-CXL (n = 21 eyes)	6 weeks post-CXL - >2 years post-CXL (n = 16 eyes)
K1p (D)									
Δ ± SD	-0.2 ± 0.4	-0.0 ± 0.1	0.0 ± 0.00	0.0 ± 0.1	0.0 ± 0.1	0.2 ± 0.4	0.3 ± 0.4	0.4 ± 0.5	-0.1 ± 0.1
p-value	p = 0.508	p = 0.757	p = 0.864	p = 1.000	p = 0.865	p = 0.576	p = 0.433	p = 0.442	p = 0.381
K2p (D)									
Δ ± SD	0.1 ± 0.1	-0.0 ± 0.1	-0.0 ± 0.1	-0.0 ± 0.1	-0.1 ± 0.1	-0.1 ± 0.1	-0.0 ± 0.1	-0.1 ± 0.1	-0.1 ± 0.1
p-value	p = 0.312	p = 0.852	p = 0.688	p = 0.516	p = 0.427	p = 0.589	p = 0.754	p = 0.294	p = 0.273
Kmp (D)									
Δ ± SD	0.8 ± 0.6	0.0 ± 0.1	-0.0 ± 0.0	-0.0 ± 0.1	-0.0 ± 0.1	-0.1 ± 0.1	-0.1 ± 0.5	-0.2 ± 0.1	-0.1 ± 0.1
p-value	p = 0.177	p = 1.000	p = 0.591	p = 0.443	p = 0.927	p = 0.241	p = 0.200	**p = 0.036**	p = 0.243

Table 16: *Mean Differences (Δ) ± standard deviation (SD) values and corresponding p-values of comparisons for posterior steep (K1p), flat (K2p) and mean (Kmp) keratometry values prior to corneal crosslinking (CXL) to 6 weeks, 6 months, 1 year, 2 years, > 2 years post-CXL, as well as 6 weeks post-CXL to all the rest follow-up measurements with paired t-test, for the* ***underaged*** *patients. No significant fluctuations of all posterior keratometry values except for the comparison of the 6 weeks post-CXL to the 2 years post-CXL (p = 0.036), without obvious clinical relevance, indicating no effect of CXL on posterior keratometry* [334].

Pachymetry of the thinnest corneal thickness (TCT) and pachymetry of the apex (ACT) (Pentacam® HR, Oculus, Wetzlar, Germany)

The thinnest (TCT) and apex corneal pachymetry (ACT) showed statistically significant changes over time according to MANOVA analysis (TCT: df(8) = 3.750, **p**

< 0.0001, ACT: df(8) = 5.334, **p < 0.0001**). Both values decreased without statistical significance from pre-CXL to 6 weeks and 6 months post-CXL and without significant differences compared to the remaining follow-up visits (p > 0.05). The mean values of TCT and ACT are presented in **Table 14**. The paired t-test comparison revealed a statistically significant decrease 6 weeks (**p = 0.049**) and 6 months post-CXL (**p = 0.033**) compared to pre-CXL, followed by further decrease without statistical significance post-CXL (p ≥ 0.065), indicating stability after the CXL procedure (**Tables 14** and **17**, **Figure 15**). Similarly, ACT decreased significantly 6 weeks, and 1 year post-CXL (**p < 0.0001** and **p = 0.0003**, **Table 17**, **Figure 15)** and further decreased until > 2 years post-CXL without statistical significance (p > 0.05), which is again indicative of stability post-CXL (**Tables 14** and **17**, **Figure 15**) [334].

Table 17: Underaged group - Mean differences ± Standard Deviations and p-values for TCT, ACT (paired t-test)

	pre-CXL - 6 weeks post-CXL (n = 33 eyes)	pre-CXL - 6 months post-CXL (n = 34 eyes)	pre-CXL - 1 year post-CXL (n = 36 eyes)	pre-CXL - 2 years post-CXL (n = 26 eyes)	pre-CXL - >2 years post-CXL (n = 16 eyes)
TCT (µm)					
Δ ± SD	15 ± 2	8 ± 2	8 ± 9	6 ± 3	8 ± 6
p-value	**p = 0.049**	**p = 0.033**	p = 0.655	p = 1.000	p = 1.000
ACT (µm)					
Δ ± SD	15 ± 2	4 ± 5	7 ± 2	4 ± 2	4 ± 6
p-value	**p < 0.0001**	p = 0.469	**p = 0.003**	p = 0.121	p = 0.577

Table 17: *Mean Differences (Δ) ± standard deviation (SD) values and corresponding p-values for the thinnest (TCT) and apex (ACT) corneal pachymetry values after comparison of the measurements prior to corneal crosslinking (CXL) to 6 weeks, 6 months, 1 year, 2 years and > 2 years postoperatively for the* ***underaged*** *patients. Statistically significant decrease of both TCT and ACT until 6 months post-CXL, followed by continuous but non-significant decrease until the longest follow-up, indicating a postoperative long-term stability* [334].

Astigmatism of the anterior (Astia) and posterior corneal curvature (Astip) (Pentacam® HR, Oculus, Wetzlar, Germany)

Neither MANOVA analysis overtime (Astia: df(8) = 0.281, p = 0.972, Astip: df(8) = 0.322, p = 0.957) nor the paired t-test for the assessment at different time points showed statistically significant changes of astigmatism of the anterior (Astia) and posterior corneal curvature (Astip, **Table 15**, **Figure 15**) [334].

5.1.5 Visual results on patients under 18 years of age

Best spectacle-corrected visual acuity (BCVA) (in LogMAR)

The best spectacle-corrected visual acuity (BCVA) in logMAR was found with statistical significant changes within the assessed timeline, as detected with MANOVA analysis (df(8) = 3.003, **p = 0.003**). A statistically significant visual improvement of BCVA was documented 1 year, 2 years and > 2 years post-CXL compared to pre-CXL values, and 6 months, 1 year, 2 years and > 2 years post-CXL compared to the values 6 weeks post-CXL. The mean BCVA values are presented in **Table 12**. The paired t-test showed a slight deterioration of BCVA at 6 weeks post-CXL compared to prior to CXL with statistically significant improvement at 1 year, 2 years and > 2 years post-CXL (**p = 0.017**, **p = 0.002** and **p = 0.003** respectively, **Tables 14** and **18**, **Figure 15**). Compared to 6 weeks post-CXL BCVA improved statistically significantly at all further follow-up visits (**p ≤ 0.01**, **Tables 14** and **18**, **Figure 15**). Statistical significant improvement was also found at the comparison of 2 years post-CXL to > 2 years post-CXL (**p = 0.003**) [334].

Table 18: Underaged group - Mean differences ± Standard Deviations and p-values for BCVA (paired t-test)					
BCVA (LogMAR)	pre-CXL - 6 weeks post-CXL (n = 33 eyes)	pre-CXL - 6 months post-CXL (n = 34 eyes)	pre-CXL - 1 year post-CXL (n = 36 eyes)	pre-CXL - 2 years post-CXL (n = 26 eyes)	pre-CXL - >2 years post-CXL (n = 16 eyes)
Δ ± SD	-0.03 ± 0.05	0.11 ± 0.06	0.13 ± 0.05	0.19 ± 0.06	0.25 ± 0.07
p-value	p = 0.087	p = 0.068	**p = 0.017**	**p = 0.004**	**p = 0.003**
	6 weeks post-CXL - 6 months post-CXL (n = 28 eyes)	6 weeks post-CXL - 1 year post-CXL (n = 28 eyes)	6 weeks post-CXL - 2 years post-CXL (n = 21 eyes)	6 weeks post-CXL - >2 years post-CXL (n = 16 eyes)	
Δ ± SD	0.16 ± 0.06	0.20 ± 0.07	0.31 ± 0.07	0.35 ± 0.09	
p-value	**p = 0.010**	**p = 0.007**	**p < 0.0001**	**p = 0.001**	

Table 18: *Mean Differences (Δ) ± standard deviation (SD) values and corresponding p-values) for LogMAR best-spectacle-corrected visual acuity (BCVA) comparing the prior to corneal crosslinking (pre-CXL) values to 6 weeks, 6 months, 1 year, 2 years, > 2 years postoperatively (post-CXL) as well as comparing the values 6 weeks post-CXL to medium-term postoperative follow-up measurements for the* ***underaged*** *patients. Deterioration of BCVA 6 weeks post-CXL without statistical significance, followed by continuous improvement with statistical significance from 1 year post-CXL until the latest follow-up. Continuous improvement of BCVA even after > 2 years post-CXL compared to 6 weeks post-CXL measurements* [334].

5.1.6 Demarcation line depth at adult population and patients under 18 years of age

The demarcation line was measured at 6 weeks post-CXL.

Patients ≥ 18 years of age

In patients ≥ 18 years of age it was observed in 81 out of 151 eyes, with a mean depth 242 ± 62 μm out of a mean central corneal thickness 454 ± 49 μm, corresponding to a percentage of 53.6 % (**Table 3**). The reason for missing data at the remaining 70 eyes was the lack of measurement with anterior segment optical coherence tomography (A-OCT) examination at the 6-week follow up, therefore, an analysis of the demarcation line was not possible [332].

Patients < 18 years of age

In patients < 18 years of age, the demarcation line was measured at 36 out of the 41 eyes using the A-OCT at a mean depth of 237 ± 66 μm out of a total mean corneal

thickness 455 ± 66 μm, corresponding to a depth percentage of 52.1 % (**Table 3**). At the remaining 5 eyes no A-OCT was available at the 6 week follow-up visit, so that no analysis of the demarcation line depth was possible [334].

5.1.7 Intraoperative pachymetry measurements and postoperative complications at adult population and patients under 18 years of age

Patients ≥ 18 years of age

For the adult patients, the mean values of the intraoperative pachymetry measurements were all above 400 μm and without statistically significant differences between each other: CT1: 492 ± 50 μm, CT2: 435 ± 45 μm, CT1: 472 ± 42 μm, CT1: 460 ± 50 μm (**Table 3**). No intraoperative complications occurred. Postoperatively, bacterial corneal infection occurred in 4 eyes post-CXL and could be successfully treated with use of local antibiotics. The mean time until epithelial closure was 5.7 ± 1.8 days. Haze of grade > 0.5 according to Fantes haze grading scale as previously described in the methods section [81,179] occurred in 60 eyes post-CXL and was treated with extensive use of topical dexamethasone eye drops after closure of the corneal epithelium (6 times daily, with weekly reduction by 1 drop). Further KC progression, as this is defined in paragraph 4.1 “Study design and examined variables”, was observed in 3 patients and in one patient, a penetrating keratoplasty had to be performed due to reduced visual acuity and contact lens intolerance (**Table 3**) [332].

Patients < 18 years of age

Similarly, for the underaged patients, the mean intraoperative pachymetry values exceeded 400 μm without statistically significant differences between each other: CT1: 477 ± 52 μm, CT2: 425 ± 44 μm, CT1: 469 ± 43 μm, CT1: 454 ± 33 μm (**Table 3**). No intraoperative complications were documented. The epithelial healing was observed after 6.1 ± 2.7 days (**Table 3**). Postoperatively, haze formation was documented at 7 out of 41 eyes and in all cases, it was successfully treated with the previously explained topical therapy. No postoperative infections were documented

and none of the treated eyes of the underage group showed further KC progression post-CXL (**Table 3**) [334].

5.2. Second part of the study: reliability analysis of successive biomechanical measurements at least 2 years after A-CXL compared to untreated KC corneas

5.2.1 Description of the study population

As far as **the second part of our study** is concerned, the CXLG comprised 12 right eyes and 8 left eyes. A-CXL (9 mW/cm^2, 10 minutes) was performed on average 48 ± 19 months before enrollment. The mean age of the patients of this group was 31 ± 11 years. The control group consisted of 11 right eyes and 9 left eyes and the mean age of the control patients was 39 ± 14 years. The age of the patients of both groups was normally distributed (CXLG: p = 0.111, controls: p = 0.805, Shapiro-Wilk test) without significant statistical difference between the groups (p = 0.065, paired t-test). Both CXLG and control group were found to be tomographically comparable as shown from the mean Kmax value and mean BAD-D from Pentacam® HR respectively: mean Kmax: 60.5 ± 7.2|60.7 ± 7.7 D, controls|CXLG, p = 0.868 and mean BAD-D: 11.5 ± 4.7|11.2 ± 3.6, controls|CXLG, p = 0.682. Other tomographic parameters examined were the anterior and posterior radii of curvature (ARC, PRC) and the thinnest corneal thickness (TCT) which were similarly found to be comparable between the two groups (mean ARC: 6.2 ± 0.6|6.3 ± 0.6, controls|CXLG, p = 0.344, mean PRC 4.6 ± 0.6|4.5 ± 0.4, controls|CXLG, p = 0.605, mean TCT 456 ± 34|452 ± 27 mm, controls|CXLG, p = 0.401). The upper results are summarized in **Table 19** [333].

Table 19: Descriptives	Controls	CXLG	P-value
Gender	13 male, 7 female	13 male, 3 female	
Age (years)	39 ± 14	31 ± 11	0.065^{T}
Kmax (D)	60.5 ± 7	60.7 ± 8	0.868^{T}
ARC (mm)	6.2 ± 0.6	6.3 ± 0.6	0.344^{T}
PRC (mm)	4.6 ± 0.6	4.5 ± 0.4	0.605^{T}
TCT (µm)	456 ± 34	452 ± 2.7	0.401^{T}
BAD-D	11.5 ± 5	11.3 ± 4	0.682^{T}

Table 19: *Comparison of the control group and the crosslinking group (CXLG). ABC-stage-matched non operated KC controls were paired with KC corneas at least 2 years after accelerated corneal crosslinking (9 mW/cm², 10 minutes, 5.4 J/cm²). Kmax (= maximal anterior keratometry), ARC (= anterior radius of curvature), PRC (= posterior radius of curvature), TCT (= thinnest corneal pachymetry), BAD-D (= Belin/Ambrósio-Enhanced-Ectasia-Deviation-Index, P-values calculated by paired t-test (^{T}), if normally distributed* [333].

5.2.2 Reliability analysis of biomechanic measurements using CORVIS® ST

A1 velocity, DA ratio 2 mm, ARTh, integrated radius, SP-A1 and CBiF of three consecutive CST measurements were evaluated.

The mean values for A1 velocity, DA ratio 2 mm, integrated radius and CBiF were found to be comparable between controls and CXLG. Mean ARTh was statistically significantly higher in controls than in the CXLG (controls|CXLG: 177.1 ± 59|155.21 ± 65, **p = 0.0062**, **Table 20**). Mean SP-A1 was statistically significantly higher post-CXL than in controls (controls|CXLG: 52.2 ± 16|59.2 ± 13, **p = 0.0018**, **Table 20**). Bland-Altman plots were created for these two parameters that differed significantly between the two groups showing the mean difference and the 95 % limits of agreement (**Figure 16**).

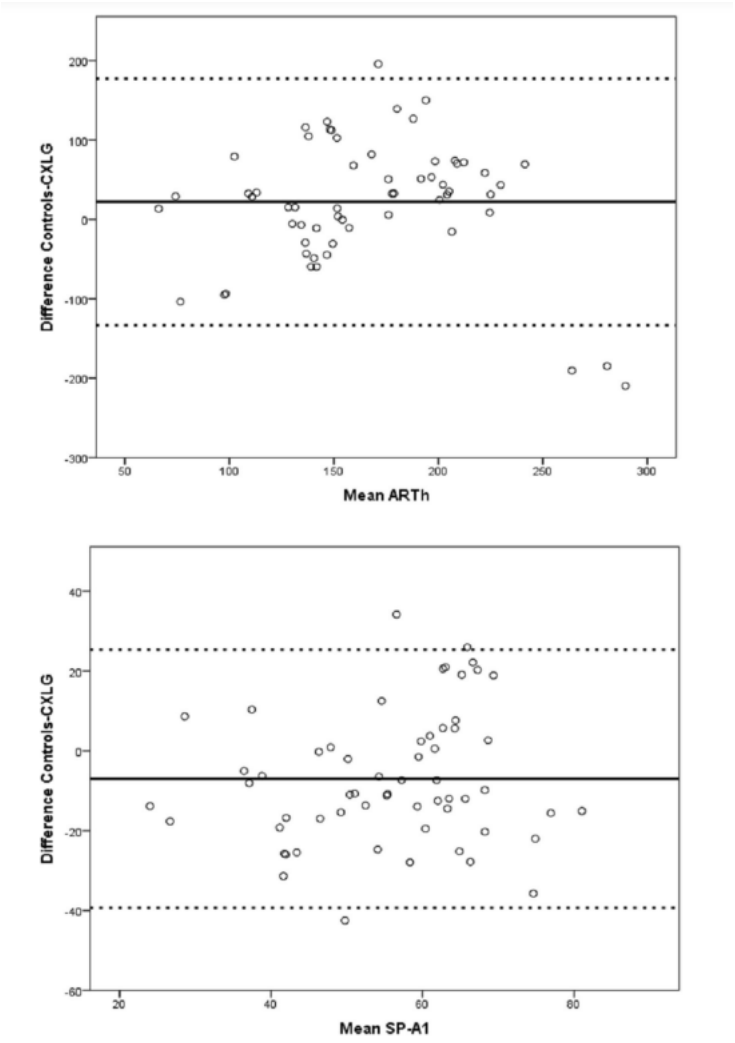

Figure 16: *Bland-Altman plots presenting the mean difference (solid black line) between controls and CXLG for ARTh (= Ambrósio's relational thickness to the horizontal profile) and SP-A1 (= stiffness parameter A1) and the 95 % limits of agreement (dotted lines)* [333].

The coefficients of repeatability were lower in controls compared to the CXLG for A1 velocity, SP-A1 and CBiF but higher for DA ratio 2 mm, integrated radius and ARTh, as summarized in **Table 20**. The intraclass correlation coefficients and Cronbach's alpha (CA) values were found to be the same for both groups and were indicative of excellent reliability of the biomechanical measurements for both untreated KC corneas and crosslinked KC corneas (CA ≥ 0.912, **Table 20**) [333].

Table 20: Means ± Standard Deviations, p-values, coefficients of repeatability and ICC for CORVIS® ST biomechanical measurements for controls and CXLG

Parameter	Controls Mean ± SD	CXLG Mean ± SD	P-value	Controls Coefficient of repeatability	CXLG Coefficient of repeatability	Controls and CXLG ICC	Controls and CXLG CA
A1 velocity	0.176 ± 0.02	0.183 ± 0.02	0.090^{T}	0.01	0.02	0.956	0.960
DA ratio 2 mm	6.04 ± 1.13	6.14 ± 1.03	0.490^{W}	0.97	0.82	0.952	0.967
Integrated radius	12.08 ± 2.5	12.42 ± 1.90	0.450^{W}	2.07	1.28	0.969	0.976
ARTh	177.1 ± 59	155.21 ± 65	**0.0062^{W}**	33.12	25.00	0.991	0.993
SP-A1	52.2 ± 16	59.2 ± 13	**0.0018^{T}**	12.31	16.46	0.894	0.912
CBiF	4.62 ± 0.6	4.62 ± 0.4	0.830^{W}	0.27	0.39	0.955	0.965

Table 20: *Main outcome measures in the control group and the crosslinking group (CXLG). Mean ± standard deviation (SD) values, resulting out of three measurements per eye, ICC (= intraclass correlation coefficient), CA (Cronbach's alpha), DA (= deformation amplitude) ratio 2 mm, ARTh (Ambrósio's relational thickness to the horizontal profile), SP-A1 (= stiffness parameter A1), CBiF (= Corvis Biomechanical Factor, the linearized term of the Corvis Biomechanical Index, CBI). Mean ± standard deviation (SD) values are comparable in controls and CXLG except for ARTh and SP-A1. P-values calculated by paired two-tailed t-test (^{T}), if normally distributed, or by Wilcoxon matched-pairs test (^{W}) if not normally distributed, as determined by the Shapiro-Wilk test. Coefficients of repeatability for each parameter in controls and CXLG calculated as the within-subject standard deviation Sw x √2 x 1.96. Identical ICCs and CA values in the CXLG and controls, with CA ≥ 0.912, indicative of excellent reliability* [333].

6. Discussion

6.1.1 Effectivity of A-CXL (9 mW/cm^2, 10 minutes, 5.4 J/cm^2) for adult and underaged KC patients

KC is a corneal disease with increasing incidence that can lead to severe visual impairment [241,258]. Diagnosis of KC at a young age as well as steep keratometry values and short duration of the disease are considered risk factors for corneal transplantation [177,245] and in children it can be a rare cause of amblyopia, with a range of visual impairment between 0.08 % and 12 % [177]. Progression of KC in pediatric patients has been associated with a 7 times higher risk of corneal transplantation [177] and at this age group the risk of developing corneal hydrops is higher [68].

CXL represents a revolution in the treatment of corneal ectasias, including KC, as it is a minimally invasive method that can provide stability of the disease and prevent severe visual impairment and the need for more drastic methods, meaning a corneal transplantation [273]. The S-CXL protocol has been proven to be successful and provide safe and stable tomographic, biomechanical [256,329,341] and visual results with deep demarcation lines that can be preserved for even 10 and more years postoperatively [124,243]. Similarly, S-CXL can achieve successful tomographic, visual results and deep demarcation line with safety, even after a decade, for patients under 18 years of age [100,197]. In case of younger patients, the need of intervention can be imperative and without waiting for evident progression of the disease, as the course of KC is faster and more aggressive, leading to advanced findings already at first presentation as well as to asymmetrical findings [15,19,177].

Considering the time consuming S-CXL procedure and the possible complications from the prolonged irradiation such as corneal infection, haze formation and corneal infiltration, the A-CXL treatment seems to be preferred especially in case of younger patients, as it promises similar results compared to S-CXL in a faster and, therefore, less dangerous way [39,279,281,301,319]. The A-CXL protocol with a fluence of 9 mW/cm^2, for 10 minutes, with an irradiance of 5.4 J/cm^2 has been proven to be

superior over other accelerated protocols in terms of topo/-tomographic results and demarcation line depth (30 mW/cm^2, 3 minutes, 18 mW/cm^2, 5 minutes) [155,281], and to provide similar tomographic and refractive results with S-CXL, with ability of preservation of these results in the long term [224,225,315]. Furthermore, a 1 year-follow up study of our center proved that this A-CXL protocol can provide biomechanical stability postoperatively [84]. Mazzotta et al. presented 5-year results of A-CXL 9 mW/cm^2 for 10 minutes and demonstrated a statistically significant improvement of uncorrected and best corrected visual acuity, corneal curvature values and high-order aberrations which remained preserved in the long-term. The conclusion of this study was that this protocol can be considered as a natural evolution of the epi-off S-CXL protocol for the management and treatment of early progressive corneal ectasia, which also improves the everyday practice [200].

6.1.2 Visual and tomographic results of A-CXL (9 mW/cm^2, 10 minutes, 5.4 J/cm^2) on adult patients

In the first part of our study, we present a visual and tomographic analysis of the anterior and posterior keratometry values from 2 years preoperatively until > 2 years postoperatively after A-CXL treatment (9 mW/cm^2, 10 minutes) for progressive KC in 151 eyes of 124 adult patients, at the Ophthalmology Department of Saarland University Medical Center UKS. A significant corneal steepening (K1a, K2a, Kma, Kmax, paired t-test) was found in the 6-week follow-up examination post-CXL, compared to the values pre-CXL. This steepening, according to the KC progression criteria (paragraph 4.1 “Study design and examined variables”) could be interpreted as an early ***postoperative “pseudoprogression”*** as we named it [332]. These findings are in agreement with those of the Siena Eye-Cross Study 2 where a deterioration of the uncorrected and best corrected visual acuity, high-order aberrations and Kmax occurred at the first follow-up of 4 weeks after A-CXL (9 mW/cm^2, 10 minutes), followed by statistically significant improvement until 5 years post-CXL [200].

This first “peak” phenomenon, a “***pseudoprogression***” as we called it, was not indicative of the following course, as decrease of these values from 6 months on with meaning corneal flattening occurred [200,332,334]. In a study of Vinciguerra et al. it

was observed that the epithelial removal led to significant elevation of the steepest, flattest and mean values of the corneal topography, until the fourth week of follow-up, compared to preoperative values [308]. This observation is essential as it shows that the corneal epithelium has a tremendous effect on the corneal power and corneal astigmatism and can mask the true corneal curvature in KC corneas as well [308,340]. In another study, a deterioration of visual acuity at the first month postoperatively was demonstrated again, followed by a transient improvement from the third month on. The study underlined the presence of excessive epithelial thinning one month after treatment especially in the apex region followed by improvement at the third postoperative month and normalization until 6 months postoperatively [194]. The epithelium analysis showed postoperative stratification and smoothing effect of the irregularities of the corneal surface, especially at the corneal apex which seemed to be time-dependent. The epithelial analysis was accompanied by increased stromal density of the extracellular matrix, increased number of keratocyte nuclei and the formation of new structured fibers at the anterior-middle stroma, as well as a more edematous, hyperreflective deep stroma to normoreflective deeper stroma with apoptotic keratocyte bodies [191,193,194].

The same author demonstrated a postoperative corneal thinning at TCT until the first postoperative year which agrees with our study results where TCT had a decreasing tendency until the latest follow-up with statistical significance until 2 years postoperatively and ACT did also decrease until > 2 years postoperatively with statistical significance until 1 year post-CXL [194]. Greenstein et al. also presented a similar decrease of corneal thickness values at the 3-month and 6-month follow-up [108].

Although in our study the anterior corneal curvature values, including the steep, flat, mean and maximal keratometry presented a progressive improvement after the 6-week follow-up, the posterior corneal curvature values did not seem to be affected after CXL. This implies that CXL has a limited effect upon the posterior part of the cornea as it was also morphologically detected by Mazzotta et al. [194,332]. This difference between the changes of the anterior and posterior corneal stroma could

result from a difference of the corneal stiffness of the anterior and posterior stroma. A study of corneal elastography could show that the posterior stroma has an increased corneal stiffness whereas the anterior stroma has a decreased corneal stiffness in case of KC [60]. Thus, the anterior stroma may be more affected after CXL.

Our study presents a combination of increase of the anterior corneal curvature including Kmax, along with the decrease of the corneal pachymetry 6 weeks post-CXL, which can be again interpreted as a postoperative KC progression. We propose to apply to this progression phenomenon the term **"*pseudoprogressio*n"**, going similarly along with an increase of K1m, Kmax and a decrease of the TCT, which, however is not permanent and does not agree with the further long term postoperative results. Therefore, the immediate postoperative period after CXL must not be evaluated for KC progression as it shows transient changes which are similar to the KC progression criteria that are set, but again, these are not indicative of the long term postoperative results which are showing stability [332,334].

The BCVA showed a deterioration 6 weeks post-CXL, which could happen due to the ***"pseudoprogression"*** and haze taking place, meaning the corneal steepening and thinning at the first postoperative period. From the sixth month post-CXL and on, the BCVA improves and stays stable until the latest follow-up [332]. The results agree with the Siena Eye-Cross Study 2 where the BCVA improved statistically even 5 years postoperatively after A-CXL of 9 mW/cm^2 for 10 minutes [200]. Karaca et al. studied the effect of the A-CXL 9 mW/cm^2 for 10 minutes at the visual outcomes according to the severity of KC and found that this protocol leads to improvement of BCVA, which is better at steeper corneas (> 51 D), and is correlated to spherical equivalent and high order aberrations [148]. The morphological changes that were presented by Mazzotta et al. may also explain the deterioration of the visual acuity at the first postoperative period [194]. Long term studies show the improvement of the visual acuity after A-CXL even after 13 years postoperatively [76,200,244].

6.1.3 Visual and tomographic results of A-CXL (9 mW/cm^2, 10 minutes, 5.4 J/cm^2) for patients under 18 years of age

In the case of treatment of KC at younger ages, the challenge of aggressiveness and high rate of KC progression can be more difficult to manage compared to adult patients [15,19,35,177,228]. Studies on pediatric KC demonstrated that at the time of diagnosis 27.8 % were already at an advanced stage and 88 % were progressing [44,228]. Therefore the CXL intervention should be conducted as early as needed and be accurate but also tolerable from the patients [15,19,177,228]. The S-CXL protocol remains until today the gold standard method for treatment of KC and several studies have proven the efficacy of this protocol in the long term [197,309]. The potentially safer and more tolerable solution of epi-on CXL at patients with a range of age 11 to 26 years could not provide stability postoperatively as it failed to stop the keratometric progression and gradual corneal thinning and made a revision of treatment with epi-off CXL procedure for achievement of stabilization necessary at 50 % of the patients [34]. Iqbal et al. compared the results of S-CXL, A-CXL (18 mW/cm^2 for 5 minutes) and T-CXL for pediatric KC population and showed that the A-CXL protocol can be a safe and effective alternative for S-CXL but does not reach the improvement of S-CXL and that T-CXL is inferior than both A-CXL and S-CXL treatment methods [136]. A three-year follow-up study of S-CXL versus A-CXL for pediatric KC could show that A-CXL can be as effective as the S-CXL treatment with a decrease of Kmax by a mean 0.98 ± 0.56 D after S-CXL ($p = 0.02$) and 1.48 ± 8.4 D after A-CXL (9 mW/cm^2, 10 minutes, $p = 0.015$ at 3-year follow-up) [74]. A large meta-analysis comparing the results of S-CXL versus A-CXL and T-CXL for pediatric KC could show that A-CXL can provide similar stabilizing keratometric and visual improvement results as the S-CXL method and again inferior results as far as T-CXL is concerned [82]. Shetty et al. showed in a retrospective analysis that A-CXL of 9 mW/cm^2 for 10 minutes is a safe and successful method that stops the progression of KC and improves the visual acuity even in children of age 11-14 years until 2 years post-CXL [279].

In our study, we proved that a shorter epi-off CXL treatment protocol, A-CXL of 9 mW/cm^2 for 10 minutes can provide safe and effective results and be used for the treatment of KC in adult patients. There are few publications that examined the effect of this A-CXL protocol at underaged patients and this has been a goal in our study as well. Given the most aggressive course of KC at young ages, in our study, 16 out of 41 patients less than 18 years of age were treated without waiting for evident progression of KC. This fact could create a bias, but, considering the upper explained facts of pediatric KC and the clinical findings of these patients we conducted CXL in order to halt the further KC progression. We, therefore, evaluated the BAD-D in the young patients' population and found a statistically significant increase compared to the values 6 months pre-CXL. The BAD-D continued to increase after CXL but without statistical significant difference compared to 6 months pre-CXL at the latest follow-up and compared to pre-CXL from 1 year on [334]. Considering the study of Shajari et al., who demonstrated the BAD-D as a predictor for KC progression, our results indicate a stabilizing effect of A-CXL from the first year postoperatively and on even until > 2 years post-CXL [274,334].

An interesting point of our study is the preoperative keratometric measurements that ranged among the highest preoperative values that have been published until today (Kmax pre-CXL 61.5 ± 8.5 D) [39,44,197,230,279,309,334]. A large study of Padmanabhan et al. which included 377 eyes of KC patients aged 8-18 years (mean age: 15 ± 2.5 years) that received S-CXL, presented similarly Kmax values pre-CXL 61.65 ± 7.04 D [230]. In our study we could show that A-CXL could effectively lead to stabilization of the anterior curvature values, including Kmax, even after 2 years postoperatively, similarly to the upper study of Padmanabhan et al. where S-CXL was used and results of ≥ 2 years post-CXL are also presented. This fact proves once more a comparable effectivity of A-CXL 9 mW/cm^2, 10 minutes with that of S-CXL even at underaged groups. At the first 6 weeks post-CXL, an increase of the anterior curvature values (K1a, K2a, Kma, Kmax) along with a decrease of the corneal pachymetry (ACT, TCT) and BCVA is observed, a fact which, according to our findings at the adult population, as analyzed above and already published, and the KC

progression criteria presented (paragraph 4.1 “Study design and examined variables”), could, once more be characterized as a ***“pseudoprogression”*** [334]. Similar results were also published by Padmanabhan et al., [230] and, as previously explained, could be attributed to the effect of epithelial removal during the CXL procedure and its gradual restoration postoperatively along with the reorganization of the corneal stroma [194,308,340]. This deterioration, similarly to the adult group, is not permanent and not indicative of the long-term effect of A-CXL, as a further decrease of the anterior curvature values is observed even after 2 and > 2 years post-CXL. The ACT and TCT show also stabilization from the first postoperative year on, while the BCVA shows an improvement from the 6th postoperative month and until 2 and > 2 years post-CXL. We acknowledge that at the > 2-year follow-up the number of examined eyes is smaller (n = 16) than preoperatively (n = 41) which represents a limitation of our study. Our results, nevertheless, remain consistent to the ones of the published studies we previously referred to [39,200,230,279,334].

The posterior curvature values in our study seem to remain unaffected after A-CXL in the underaged group as well, as the steep, flat and mean posterior keratometry continue to fluctuate until > 2 years post-CXL without statistically significant differences [334]. As presented previously, in the adult population the posterior keratometry values show a slight further increase without statistical significance even after > 2 years post-CXL, which indicates that A-CXL does not have a significant effect on the posterior curvature of the cornea. In an analysis of the postoperative posterior curvature values after A-CXL of 10 mW/cm^2 for 9 minutes on underaged KC patients, Badawi et al. found no effect of this protocol on the posterior curvature values [21]. In this study there an increase of the anterior curvature values including Kmax until the 3rd postoperative month and a decrease of these values compared to preoperatively from the 6th postoperative month on up until one year postoperatively was also documented. The corneal thickness showed a significant decrease that continued until the latest follow-up of 1 year post-CXL [21]. Interestingly, the study of Mazzotta et al. where S-CXL was conducted in 62 eyes of 47 pediatric KC patients, a deterioration of the topographic data was observed in 9 eyes of 7 patients between

the 2- and 3-year follow-up examinations, which was attributed to the more aggressive course of KC at these ages as well as the positive history of allergy, atopy and eye rubbing in these specific patients, which led to re-treatment. Again a regression of Kmax was documented in 13 eyes but without deterioration of the visual acuity, leading to re-treatment in 2 patients who were both under 15 years of age [200]. Similarly in our study, the Kmax appears to have an escalation at the > 2 year-follow-up but without increase of the mean values, which could be also attributed to the nature of these patients. However, the reduced number of follow-up examinations of this time point (n = 16) could be considered as bias [334]. As Mazzotta et al. also underlined a corneal collagen turnover happens at 6 to 7 years post-CXL and this should be taken into consideration for possible regression especially for young patients less than 15 years of age at the time of inclusion [200].

6.1.4 Demarcation line characteristics

At the adult population of our study, we present a deep demarcation line with a depth of 242 ± 62 μm out of 454 ± 49 μm (53.6 % percentage depth) and a similar depth was observed in the underaged patients as well: 237 ± 66 μm out of a total mean corneal thickness 455 ± 66 μm (52.1 % percentage depth). To our knowledge the demarcation line depth is documented for the first time after A-CXL 9 mW/cm^2, 10 minutes for patients less than 18 years of age [332,334].

The demarcation line is indicative of the depth of penetration of CXL in the corneal stroma [198,272,286]. Several studies proved a similar demarcation line depth between A-CXL (9 mW/cm^2, 10 minutes) and the Dresden protocol [281,287]. Spadea et al. compared the demarcation line depth after S-CXL and A-CXL (10 mW/cm^2, 9 minutes) and found values of 275 ± 42 μm and 279 ± 33 μm respectively, without significant statistical difference [287]. Similarly Shetty et al. found values of 280 ± 47 μm and 292 ± 73 μm in a comparative study of S-CXL and A-CXL (9 mW/cm^2, 10 minutes), respectively [281]. Our results for both age groups are comparable with these findings. The Siena Eye-Cross Study 2 provided a demarcation line depth of 332.6 ± 23.6 μm after A-CXL 9 mW/cm^2, 10 minutes [200]. Moreover, Toker et al. showed that the demarcation line depth after A-CXL (9 mW/cm^2, 10

minutes) did not differ significantly from the values after S-CXL and that the 9mW/cm^2, 10 minutes protocol could provide similar visual and keratometric results compared to S-CXL which were also superior compared to a 30 mW continuous and pulsed A-CXL protocol [300]. The demarcation line depth at the 30 mW protocols was also significantly shallower compared to S-CXL [300]. The same author underlined that the duration of CXL has a linear relationship with the depth of the demarcation line, based on a 3D surface model, and that higher irradiance might not provide a deeper depth of demarcation line because of inadequate oxygen diffusion in the corneal stroma [300]. The upper studies prove that the A-CXL of 9 mW/cm^2 can provide a similar demarcation line depth as the standard method [281,287,300]. A-CXL was found to provide a more superficial demarcation line at higher intensities and it has been concluded that "the deeper the better" and that the most important aim was the achievement of biomechanical stability after CXL [95,198]. Several studies proposed a differentiation of the CXL protocol in order to achieve a deeper demarcation line. Mazzotta et al. compared the 1-year results of pulsed-light versus continuous-light A-CXL at (30 mW/cm^2 for 8 minutes on, 1 minute off and 30 mW/cm^2 for 4 minutes) and found a deeper demarcation line depth with the pulsed CXL method [195] while in another study a higher fluence of 7.2 J/cm^2 instead of 5.4 J/cm^2 was proposed [199]. Kymionis et al. proposed a modification of A-CXL of 9 mW/cm^2 by increasing the time setting by 40 % in order to achieve a deeper demarcation line [173]. Lin et al. proposed a protocol termed "RF concentration-controlled method (CCM)", according to which extra RF is applied to the cornea at every crosslink time during irradiation with a frequency determined by a specific algorithm, thus an optimized CXL protocol of higher intensity and/or lower RF concentration, where higher frequency of RF instillation is required in order to decrease the faster depletion of RF compared to S-CXL [181]. Mazzotta outlined as well the role of RF administration and concentration during CXL at the depth of the demarcation line [200]. This fact may be the reason for the deeper demarcation line presented in the Siena Eye-Cross Study 2 compared to our study, as, in our study the RF soaking time was 20 minutes compared to 10 minutes in the Siena Eye-Cross Study 2 and the dropping interval of RF was every 2 minutes in our study compared

to 2.5 minutes in the Siena Eye-Cross Study 2, which may be created a RF shield effect [200].

6.2 Safety of A-CXL (9 mW/cm^2, 10 minutes, 5.4 J/cm^2) for adult and underaged KC patients

Large studies of S-CXL have shown the safety of the procedure even after 13 years of follow-up with non-significant changes of the endothelium and no adverse events [76,159,200,224]. In our study, intraoperative measurements were performed to ensure the preservation of an adequate postoperative corneal pachymetry and safety of the corneal endothelium and the procedure was held for both age groups without intraoperative complications [332–334]. Knutsson et al. included 886 KC eyes treated with S-CXL in a safety analysis and observed a KC progression in 5 cases, a mild haze in all eyes which was only persistent as anterior corneal opacity in 9 eyes, and in 11 eyes, severe corneal opacities and scarring occurred which led to a decrease of visual acuity and in 10 eyes peripheral sterile corneal infiltrates were observed 1 week postoperatively that could be treated with topical steroid therapy [159]. In our study, mild haze formation was observed in 60 out of the 151 eyes of the adult population and in 7 out of 41 eyes of the underaged patients, which could be successfully treated in all cases with the use of topical steroids [332,334]. As haze formation is attributed to the repopulation of the keratocytes and reorganization of corneal collagen fibers intrastromally post-CXL [193], it is a direct and expected complication which can completely resolve under therapy with topical steroids [192]. Shetty et al. reported haze formation in almost all treated KC eyes of underaged patients after A-CXL (9 mW/cm^2, 10 minutes) [279], whereas the Siena Eye-Cross study 2 (A-CXL 9 mW/cm^2, 10 minutes) reported about 14 % of mild haze [200]. Although in our study, the underaged group showed high anterior curvature values pre-CXL which are associated with higher risk of corneal scarring [63,243], no severe cases of persistent haze or/and corneal scarring occurred. The lack of sterile keratitis in our study could be attributed to the fact that the patients were carefully selected and these with severe and/or uncontrolled atopy or uncontrolled systemic autoimmune disorders were not

considered as eligible for the CXL treatment, although, especially in the underaged group, highly steepened corneas were treated (preoperative mean Kmax: 61.5 ± 8.5 D) [160,174]. Infectious keratitis was observed only in 3 eyes in the group of adult patients which could be successfully treated with topical antibiotic eye drops. This could be a negative aspect of the epi-off procedure compared to the epi-on CXL in terms of safety. However, as we already stated, the epi-on CXL has been found to be inferior in terms of effectiveness not only in comparison to the S-CXL procedure but also compared to A-CXL [34,40,136]. As far as the further progression of KC is concerned, it was observed in 3 eyes of the adult group (1.98 %) [332]. In all these three cases, the preoperative keratometric values were high preoperatively. No progression was found for the underaged patients, where, however, we recognize the possible bias of reduced follow-ups until > 2 years post-CXL (n = 16) [334]. Koller et al. concluded that preoperative reading values < 58.0 D can reduce the regression of KC by 3 %, and age < 35 years can restrict the complication rates by 1 % [163]. Ting et al. correlated KC progression after A-CXL (9 mW/cm^2, 10 minutes) with higher preoperative Kmean and Kmax, although no statistical significance could be reached [299]. Caporossi et al. in the Siena Eye-Cross Study of 5 years follow-up reported an increase of the keratometric values to baseline between the 2nd and 3rd follow-up postoperative year without deterioration of the visual acuity and all of the patients had positive history of eye rubbing and atopy [37]. Considering all the above, in our study in both groups, we could show that the A-CXL of 9 mW/cm^2, 10 minutes can provide an all in all stability, with safety, with low percentage of regression, and that is essential especially in the underaged group where the preoperative anterior curvature values were very high [332,334].

6.3 Effect of A-CXL (9 mW/cm^2, 10 minutes, 5.4 J/cm^2) on the biomechanics of KC corneas

In our study we also analyzed the reliability of biomechanical CST measurements in KC corneas ≥ 2 years after A-CXL treatment (9 mW/cm^2, 10 minutes) compared to untreated KC corneas of the same ABC stage of Belin's KC ABCD grading system.

The examined values were the parameters that the CBI consists of: (1) A1 velocity, (2) DA ratio 2 mm, (3) integrated radius, (4) ARTh and (5) SP-A1, and the CBiF, the linearized term of the CBI which serves as a basis for the Homburg biomechanical E-staging [89,333]. Through this evaluation and taking into consideration the evolution of the ABCD grading system with the inclusion of the biomechanical E staging based on the CBiF [89,90], there is the need to clarify whether CXL affects the corneal biomechanics in the long term and if the stiffening and stabilizing effect, that we have already discussed above and proved through the first part of our study, has an effect on the reliability of CST as a device available to assess the corneal biomechanics [333].

CXL has been proved to improve the corneal biomechanical properties and provide stability by stiffening the cornea mostly in the anterior part of the stroma than in the posterior part of it [162]. This depth-dependent effect may be attributed to the absorption analogy of UVA light in the corneal stroma soaked with RF. Schumacher et al. conducted stress-strain measurements on porcine corneas after A-CXL (10 mW/cm^2, 9 minutes), S-CXL and without CXL treatment and could show that the stiffening effect did not significantly differ between the two treatment protocols, a fact that indicates that the A-CXL protocol can lead to similar stiffening as the S-CXL procedure [265]. CST is a device available since 2010 which aims at the detection of corneal ectasia [11].

Several studies have examined the CST response at measuring normal and KC corneas [5,311]. A combination of DCR parameters, the former CBI, consisting of deformation amplitude ratio at 1 and 2 mm, applanation 1 velocity, standard deviation of deformation amplitude at highest concavity, Ambrósio's Relational Thickness to the horizontal profile were found to show excellent reliability at detecting KC from normal corneas [311]. DA was found to be significantly higher in KC patients compared to healthy eyes and is advised to be used for monitoring of KC and treatment for KC such as CXL [5]. KC corneas have been found to show lower stiffness parameter values, thinner pachymetry, shorter applanation length values, greater absolute values of applanation velocities, earlier A1 applanation time and later

A2 applanation time values and greater DA, which means that they show less resistance to deformation compared to normal eyes with similar IOP values [249].

There are few published studies that present a biomechanical analysis after CXL for KC patients using the CST [84,127,141,269,291,301,312], one of them referring to pediatric KC patients [141]. Jian et al. examined the biomechanical responses of CST 1 year after TE-CXL for pediatric KC and reported an increase of the first applanation time which represents the time when the cornea reached the first applanation, and which is expected to be longer when a cornea is stiffer [141]. Furthermore, the DA, the total displacement of the corneal from the original position at the highest corneal concavity time, which is expected to have lower values at stiffer corneas, was found to show no significant changes 1 year post-TE-CXL at the same study [141], which does not agree with the results of Tomita et al., where a significant decrease of DA after S-CXL on adult KC eyes was presented [301]. Interestingly, a study of Sedaghat et al., that evaluated the biomechanical measurements with CST until 4 years after S-CXL for KC eyes, showed that other than a significant change of the radius at highest concavity and integrated inverse radius, compatible with corneal stiffening, no statistically significant changes were noted of the majority of CBI parameters at the latest follow-up, which shows the necessity of larger follow-up studies [269]. Early analysis 1 month post-S-CXL from Vinciguerra et al. demonstrated a significant increase of SP-A1 and highest concavity and significant decrease of DA ratio [312].

A study of Hashemi et al. where a biomechanical evaluation was conducted until 2 years after A-CXL of 18 mW/cm^2, 5 minutes and A-CXL of 9 mW/cm^2, 10 minutes for KC eyes, showed a statistical significant reduction of integrated radius and borderline increase of SP-A1 without statistical significance at the shorter A-CXL protocol, compared to statistical significant decrease of DA ratio 2 mm and integrated radius and statistical significant increase of SP-A1 values at the 10 minute protocol [127], which indicates a stronger improving effect of biomechanics with the 10 minute A-CXL protocol which we also conducted in our study.

In the current study we detected no significant differences between the CXLG and control group for the parameters consisting CBI: A1 velocity, DA ratio 2 mm,

integrated radius and the CBiF (**Table 20**). The patients of CXLG were always present at their follow-up examinations and no further progression or need of re-treatment was detected in any of them and the untreated KC control corneas were corneas without signs of KC progression (see KC progression criteria, paragraph 4.1 “Study design and examined variables”). This non-significant difference of these values, especially the CBiF, compared to the ABC-staged KC controls indicates that the stabilization ≥ 2 years post-CXL can match the non-progressive KC corneas of the same stage [333].

On the other side, a highly significant statistical difference is observed for the SP-A1, with mean values found to be higher in the CXLG and a statistically significant difference for ARTh, with values found to be lower at the CXLG compared to controls (Table 18) [333], which comes to contrast with the 4-year follow-up results of Sedaghat et al., where no significant difference values were noted [269]. It is appropriate, in order to evaluate this result, to understand the meaning of these two values. The SP-A1 is the stiffness parameter at inward applanation and is expected to increase with increased corneal stiffening. In case of KC, SP-A1 shows decreasing values compared to healthy eyes and with increasing KC severity and decreasing corneal thickness [338]. After CXL, an increase of SP-A1 is expected compared to non-treated corneas. Indeed, in our department, we could show a slight, but not statistically significant increase of SP-A1 6 months and 1 year after A-CXL 9 mW/cm^2, 10 minutes for KC [84], while other studies could show a statistically significant increase of SP-A1 6 months after S-CXL [138] and A-CXL (9 mW/cm^2, 10 minutes) [233]. This result comes along with the borderline increase of SP-A1 after A-CXL 18 mW/cm^2, 5 minutes and a statistically significant increase after the A-CXL protocol 9 mW/cm^2, 10 minutes, presented by Hashemi et al., as previously reported, which seems to provide higher stability compared to the other A-CXL protocol and is more comparable to S-CXL [127,281]. Sedaghat et al. did observe an increase of SP-A1 post S-CXL but without statistical significance [269]. We could show, that, despite the relatively small sample size of our study and the ABC-

matching, there are biomechanical differences that can be measured even more than 2 years post-CXL (average 48 ± 19 months) [333].

The ARTh mean values in our study were found to be lower in the CXLG compared to KC controls with statistical significance (**p = 0.0062**, **Table 20**) [333]. A statistically significant decrease of ARTh was found 6 months and one year after A-CXL 9 mW/cm^2, 10 minutes for KC in the retrospective study of our department [84]. The study of Hashemi et al. did show a decrease of ARTh 2 years after two different A-CXL protocols (18 mW/cm^2, 5 minutes and 9 mW/cm^2, 10 minutes), but without statistical significance [127]. In the study of Sedaghat et al. however, the results after S-CXL on 18 KC eyes showed slightly higher ARTh values 4 years post-S-CXL but without statistical significance compared to preoperative values [269]. This could be attributed to a thicker central cornea with lower increase of corneal pachymetry peripherally. The conflicting results found between the above referred studies including our results create the need to determine in what extent and for how long after CXL treatment, thickness-related tomographic and biomechanical Scheimpflug-measured parameters are prone to measurements artifacts, which may result in contradictory values [333].

6.4 Capability of Corvis ST® of reliably assessing crosslinked A-CXL (9 mW/cm^2, 10 minutes, 5.4 J/cm^2) and untreated KC corneas

There are several studies that prove the reliable assessment of corneal biomechanics in healthy corneas and KC corneas, as well as in different KC stages [5,91,183,336]. Flockerzi et al. demonstrated a high reliability of CST evaluating different biomechanical parameters after 5 successive CST measurements, independently of the KC stage according to Belin's ABCD KC Grading System [91]. Yang et al. evaluated the reliability of three successive CST measurements on 77 healthy and 77 mild to moderate KC corneas and found high reliability values for all parameters, and exceptionally high with ICC > 0.900 for A1 velocity and DA ratio 2 mm [336]. In the current study, we recorded for the first time reliability measurements of CST for crosslinked corneas and for that cause, we applied three successive CST

measurements at 20 KC corneas treated at least 2 years earlier with A-CXL (9 mW/cm^2, 10 minutes, CST group) and at 20 untreated KC controls which were ABC-stage matched. The calculated ICC values and CA values, were found to be the same for both CXLG and control groups, ranging from 0.894 (SP-A1) to 0.969 (Integrated radius) and 0.912 (SP-A1) to 0.967 (DA ratio 2 mm) respectively. These results indicate that CST shows excellent reliability in assessing both CXL-treated and untreated KC corneas. The fact that the reliability analysis results are identical for both groups could indicate that the A-CXL can achieve similar stabilizing biomechanical effect with KC corneas which do not show progression. Furthermore, the excellent reliability of the CBiF parameter (CA: 0.965 for both CXLG and controls) indicates that this parameter can be used for the assessment of KC severity, and, as an extension, to the assessment of biomechanical stability [333].

6.5 Limitations of the study

We acknowledge the following limitations in our study:

<u>For the first part of our study:</u>

- Our study is retrospective and therefore there are drop-outs during the follow-up examinations pre-and postoperatively which are more evident in the underaged group. Thus, we used not only the paired t-test comparisons but also the MANOVA analysis in order to avoid bias and strengthen the statistical results.

- We acknowledge the limited number of patients of the underage group of the first part of our study, compared to the adult KC group, also considering the limiting number of remaining eyes at the postoperative follow-up visits, this is once more attributed to the retrospective character of our study [332,334].

<u>For the second part of the study:</u>

- We acknowledge also in this part of our study the moderate sample size and the majority of KC eyes being intermediate to advanced stages, as seen in **Table 17**, as well as the choice of selecting a control group. Ideally, patients would have been

followed up with three successive measurements prior to CXL and two years and more after CXL. As this was not available, an ABC-stage-matched control group was created and the selected eyes were tomographically comparable with the ones of CXLG (**Table 19)** at the time of comparison, but, this matching does not have correspondence to the duration of the KC disease. As the aim of the study was the analysis of reliability of biomechanical CST measurements in KC corneas ≥ 2 years after A-CXL (9 mW/cm^2, 10 minutes), the corneas in this group were progressive before treatment, the CXLG group consisted of progressive KC corneas that received CXL treatment, whereas the control group comprised stable ABC-matched KC corneas. The KC progression within the CXLG should have been halted by the CXL effect, which should, in a way, equilibrate the aspect of different progression rates in both groups [333].

- Another limitation of this part of our study could be the inclusion of two eyes per patient in eight cases in the CXLG, which could lead to bias, as two eyes of one patient are not considered to be independent [333].

6.6 Conclusions

In summary, CXL is a revolutionary and necessary method that halts the progression of KC in a minimally invasive way and can postpone and/or avoid the necessity of a corneal transplantation. Our study assessed (1) the visual and tomographic efficacy as well as safety of an accelerated CXL protocol of 9 mW/cm^2 for 10 minutes. It was demonstrated that a protocol of same energy but reduced duration, compared to the standard Dresden CXL method, can lead to improvement of vision and tomographic stability, long term positive results (latest follow-up 6 years) and less disturbance for the patients. These conclusions were proven to be applicable not only in adult KC patients but also in underaged KC patients, who are characterized by more aggressive pattern of KC course and less compliance in terms of “eye rubbing”. We could also show a transient deterioration of the visual and tomographic results limited to the earliest follow-up of 6 weeks post-CXL, which we suggest to entitle as

"pseudoprogression", and which, however, is not indicative of the long term results of CXL.

Furthermore, we evaluated (2) the biomechanical assessment and reliability of CST in corneas treated at least 2 years before with the same A-CXL protocol compared to ABC-matched untreated KC controls and could also prove that the biomechanical assessment of KC corneas treated at least 2 years before with that A-CXL protocol is excellent and comparable to untreated KC corneas of the same stage. The study indicates that the biomechanical effects of CXL can remain measurable far beyond 2 years after treatment (48 ± 19 months on average). The CST parameters ARTh and SP-A1 which present statistically significant differences between both CXLG and KC controls.

Larger scale studies with comparison of different A-CXL protocols with the S-CXL protocol and longer follow-up visits are expected to establish a new "standard" of an A-CXL protocol which can ensure long-term stability with safety and without the need for a revision of the procedure. Moreover, future studies with bigger samples are required in order to define when biomechanical stabilization after CXL begins and how long it lasts postoperatively.

7. List of figures

8. List of tables

9. List of references

1. Abahussin M, Hayes S, Knox Cartwright NE, Kamma-Lorger CS, Khan Y, Marshall J, Meek KM (2009) 3D Collagen orientation study of the human cornea using X-ray diffraction and femtosecond laser technology. Invest Ophthalmol Vis Sci 50:5159-5164

2. Ackroyd R, Kelty C, Brown N, Reed M (2007) The history of photodetection and photodynamic therapy. Photochem Photobiol 74:656–669

3. Agarwal R, Jain P, Arora R (2022) Complications of corneal collagen cross-linking. Indian J Ophthalmol 70:1466-1474

4. Al Suhaibani AH, Al-Rajhi AA, Al-Motowa S, Wagoner MD (2007) Inverse relationship between age and severity and sequelae of acute corneal hydrops associated with keratoconus. Br J Ophthalmol 91:984–985

5. Ali NQ, Patel DV, McGhee CNJ (2014) Biomechanical responses of healthy and keratoconic corneas measured using a noncontact Scheimpflug-based tonometer. Invest Ophthalmol Vis Sci 55:3651–3659

6. Alió JL, Piñero DP, Alesón A, Teus MA, Barraquer RI, Murta J, Maldonado MJ, De Luna GC, Gutiérrez R, Villa C, Uceda-Montanes A (2011) Keratoconus-integrated characterization considering anterior corneal aberrations, internal astigmatism, and corneal biomechanics. J Cataract Refract Surg 37:552–568

7. Allison RR, Moghissi K (2013) Photodynamic therapy (PDT): PDT mechanisms. Clin Endosc 46:24-29

8. Ambrósio R, Ramos I, Luz A, Faria FC, Steinmueller A, Krug M, Belin MW, Roberts CJ (2013) Dynamic ultra high speed Scheimpflug imaging for assessing corneal biomechanical properties. Rev Bras Oftalmol 72:99–102

9. Ambrósio R, Belin MW (2010) Imaging of the cornea: Topography vs tomography. J Refract Surg 26:847–849

10. Ambrósio R, Valbon BF, Faria-Correia F, Ramos I, Luz A (2013) Scheimpflug imaging for laser refractive surgery. Curr Opin Ophthalmol 24:310–320

11. Ambrósio R, Correia FF, Lopes B, Salomão MQ, Luz A, Dawson DG, Elsheikh A, Vinciguerra R, Vinciguerra P, Roberts CJ (2017) Corneal biomechanics in ectatic diseases: Refractive surgery implications. Open Ophthalmol J 11:176–193

12. Amsler M (1938) Le kératocône fruste au Javal. Ophthalmologica 96:77–83

13. Anayol MA, Güler E, Yağc R, Şekeroğlu MA, Ylmazoğlu M, Trhş H, Kulak AE, Ylmazbaş P (2014) Comparison of central corneal thickness, thinnest corneal thickness, anterior chamber depth, and simulated keratometry using Galilei, Pentacam, and Sirius devices. Cornea 33:582–586

14. Angelo L, Gokul Boptom A, McGhee C, Ziaei M (2022) Corneal crosslinking: Present and future. Asia Pac J Ophthalmol 11:441–452

15. Anitha V, Vanathi M, Raghavan A, Rajaraman R, Ravindran M, Tandon R (2021) Pediatric keratoconus - Current perspectives and clinical challenges. Indian J Ophthalmol 69:214

16. Antonios R, Dirani A, Fadlallah A, Chelala E, Hamade A, Cherfane C, Jarade E (2015) Safety and visual outcome of visian toric ICL implantation after corneal collagen cross-linking in keratoconus: Up to 2 years of follow-up. J Ophthalmol 2015:1–8

17. Antunes-Foschini R, Doná H, De Mello PHS, Pereira RB, Marqueis IM, Rocha EM, De Faria-e-Sousa SJ, Perdona GC (2023) Natural history and predictors for progression in pediatric keratoconus. Sci Rep 13:4940

18. Arora R, Jain P, Gupta D, Goyal JL (2012) Sterile keratitis after corneal collagen crosslinking in a child. Cont Lens Anterior Eye 35:233–235

19. Arora R, Gupta D, Goyal JL, Jain P (2012) Results of corneal collagen cross-linking in pediatric patients. J Refract Surg 28:759–762

20. Asbell PA, Uçakhan ÖÖ (2001) Long-term follow-up of Intacs from a single center. J Cataract Refract Surg 27:1456–1468

21. Badawi AE (2017) Accelerated corneal collagen cross-linking in pediatric keratoconus: One year study. Saudi J Ophthalmol 31:11–18

22. Baptista PM, Ambrosio R, Oliveira L, Meneres P, Beirao JM (2021) Corneal biomechanical assessment with Ultra-High-Speed Scheimpflug Imaging during non-contact tonometry: A prospective review. Clin Ophthalmol 15:1409–1423

23. Basu S, Vaddavalli PK, Ramappa M, Shah S, Murthy SI, Sangwan VS (2011) Intracameral perfluoropropane gas in the treatment of acute corneal hydrops. Ophthalmology 118:934–939

24. Battaglia Parodi M, Da Pozzo S, Toto L, Saviano S, Ravalico G (2001) Photodynamic therapy for choroidal neovascularization associated with choroidal osteoma. Retina 21:660–661

25. Battaglia Parodi M, La Spina C, Berchicci L, Petruzzi G, Bandello F (2016) Photosensitizers and photodynamic therapy: Verteporfin. Dev Ophthalmol 2016:55:330-336

26. Belin M, Kundu G, Shetty N, Gupta K, Mullick R, Thakur P (2020) ABCD: A new classification for keratoconus. Indian J Ophthalmol 68:2831-2834

27. Belin MW, Khachikian SS (2007) Keratoconus: It is hard to define, but … Am J Ophthalmol 143:500–503

28. Belin MW, Duncan JK (2016) Keratoconus: The ABCD Grading System. Klin Monbl Augenheilkd 233:701–707

29. Belin MW, Alizadeh R, Torres-Netto EA, Hafezi F, Ambrósio R, Pajic B (2020) Determining progression in ectatic corneal disease. Asia Pac J Ophthalmol (Phila) 9:541–548

30. Bonanno JA (2012) Molecular mechanisms underlying the corneal endothelial pump. Exp Eye Res 95:2–7

31. Bourne WM (1998) Clinical estimation of corneal endothelial pump function. Trans Am Ophthalmol Soc 96:229–242

32. Bunsen R, Roscoe H (1859) Photochemische Untersuchungen. Annalen der Physik 184:193–273

33. Burris TE (1998) Intrastromal corneal ring technology: results and indications. Curr Opin Ophthalmol 9:9–14

34. Buzzonetti L, Petrocelli G (2012) Transepithelial corneal cross-linking in pediatric patients: Early results. J Refract Surg 28:763–767

35. Buzzonetti L, Bohringer D, Liskova P, Lang S, Valente P (2020) Keratoconus in children: A literature review. Cornea 39:1592–1598

36. Caporossi A, Baiocchi S, Mazzotta C, Traversi C, Caporossi T (2006) Parasurgical therapy for keratoconus by riboflavin–ultraviolet type A rays induced cross-linking of corneal collagen: Preliminary refractive results in an Italian study. J Cataract Refract Surg 32:837–845

37. Caporossi A, Mazzotta C, Baiocchi S, Caporossi T (2010) Long-term results of riboflavin ultraviolet a corneal collagen cross-linking for keratoconus in Italy: The Siena eye cross study. Am J Ophthalmol 149:585–593

38. Caporossi A, Mazzotta C, Baiocchi S, Caporossi T, Denaro R (2011) Age-related long-term functional results after riboflavin UV A corneal cross-linking. J Ophthalmol 2011:1–6

39. Caporossi A, Mazzotta C, Baiocchi S, Caporossi T, Denaro R, Balestrazzi A (2012) Riboflavin-UVA-induced corneal collagen cross-linking in pediatric patients. Cornea 31:227–231

40. Caporossi A, Mazzotta C, Paradiso AL, Baiocchi S, Marigliani D, Caporossi T (2013) Transepithelial corneal collagen crosslinking for progressive keratoconus: 24-month clinical results. J Cataract Refract Surg 39:1157–1163

41. Cassagne M, Laurent C, Rodrigues M, Galinier A, Spoerl E, Galiacy SD, Soler V, Fournié P, Malecaze F (2016) Iontophoresis transcorneal delivery technique for transepithelial corneal collagen crosslinking with riboflavin in a rabbit model. Invest Ophthalmol Vis Sci 57:594-603

42. Chan CCK, Sharma M, Wachler BSB (2007) Effect of inferior-segment Intacs with and without C3-R on keratoconus. J Cataract Refract Surg 33:75–80

43. Chanbour W, Mokdad I, Mouhajer A, Jarade E (2019) Late-onset sterile peripheral ulcerative keratitis post-corneal collagen crosslinking. Cornea 38:338–343

44. Chatzis N, Hafezi F (2012) Progression of keratoconus and efficacy of pediatric corneal collagen cross-linking in children and adolescents. J Refract Surg 28:753–758

45. Chen X, Stojanovic A, Eidet JR, Utheim TP (2015) Corneal collagen cross-linking (CXL) in thin corneas. Eye and Vis 2:15

46. Chong J, Dupps WJ (2021) Corneal biomechanics: Measurement and structural correlations. Exp Eye Res 205:108508

47. Cohen KL, Tripoli NK, Pellom AC, Kupper LL, Fryczkowski AW (1984) A new photogrammetric method for quantifying corneal topography. Invest Ophthalmol Vis Sci 25:323–330

48. Colin J, Cochener B, Savary G, Malet F (2000) Correcting keratoconus with intracorneal rings. J Cataract Refract Surg 26:1117–1122

49. Collin J, Queen R, Zerti D, Bojic S, Dorgau B, Moyse N, Molina MM, Yang C, Dey S, Reynolds G, Hussain R, Coxhead JM, Lisgo S, Henderson D, Joseph A, Rooney P, Ghosh S, Clarke L, Connon C, Haniffa M, Figueiredo F, Armstrong L, Lako M (2021) A single cell atlas of human cornea that defines its development, limbal progenitor cells and their interactions with the immune cells. Ocul Surf 21:279–298

50. Collomb E, Yang Y, Foriel S, Cadau S, Pearton DJ, Dhouailly D (2013) The Corneal epithelium and lens develop independently from a common pool of precursors: Multistep induction of corneal epithelium. Dev Dyn 242:401–413

51. Conde Penedo A, Díaz Tomé V, Fernández Ferreiro A, González Barcia M, Otero Espinar FJ (2021) Enhancement in corneal permeability of riboflavin using cyclodextrin derivates complexes as a previous step to transepithelial cross-linking. Eur J Pharm Biopharm 162:12–22

52. Correia JH, Rodrigues JA, Pimenta S, Dong T, Yang Z (2021) Photodynamic therapy review: Principles, photosensitizers, applications, and future directions. Pharmaceutics 13:1332

53. Crawford AZ, Patel DV, McGhee CNJ (2013) Comparison and repeatability of keratometric and corneal power measurements obtained by Orbscan II, Pentacam, and Galilei corneal tomography systems. Am J Ophthalmol 156:53–60

54. Cullen JF, Butler HG (1963) Mongolism (Down's Syndrome) and keratoconus. Br J Ophthalmol 47:321–330

55. Davanger M, Evensen A (1971) Role of the pericorneal papillary structure in renewal of corneal epithelium. Nature 229:560–561

56. Dawson DG, Watsky MA, Geroski DH, Edelhauser HF (2009) Chapter 4 Cornea and Sclera. Duane's Clinical Ophthalmology Lipincott Williams and Wilkins

57. Dawson DG, Edelhauser HF (2010) Corneal edema. In: Levin LA, Albert DM (eds) Ocular Disease. Mechanisms and management Elsevier Ltd. pp 64-73

58. De la Parra-Colín P, Garza-León M, Barrientos-Gutierrez T (2014) Repeatability and comparability of anterior segment biometry obtained by the Sirius and the Pentacam analyzers. Int Ophthalmol 34:27–33

59. De Oliveira RC, Wilson SE (2020) Descemet’s membrane development, structure, function and regeneration. Exp Eye Res 197:108090

60. De Stefano VS, Ford MR, Seven I, Dupps WJ (2020) Depth-dependent corneal biomechanical properties in normal and keratoconic subjects by optical coherence elastography. Transl Vis Sci Technol 9:4

61. DelMonte DW, Kim T (2011) Anatomy and physiology of the cornea. J Cataract Refract Surg 37:588–598

62. Deshmukh R, Hafezi F, Kymionis G, Kling S, Shah R, Padmanabhan P, Sachdev M (2019) Current concepts in crosslinking thin corneas. Indian J Ophthalmol 67:8-15

63. Dhawan S, Rao K, Natrajan S (2011) Complications of corneal collagen cross-linking. J Ophthalmol 2011:1–5

64. Dingeldein SA (1989) The topography of normal corneas. Arch Ophthalmol 107:512

65. Doctor K, Vunnava KP, Shroff R, Kaweri L, Lalgudi VG, Gupta K, Kundu G (2020) Simplifying and understanding various topographic indices for keratoconus using Scheimpflug based topographers. Indian J Ophthalmol 68:2732–2743

66. Doss JD, Hutson RL, Rowsey JJ, Brown DR (1981) Method for calculation of corneal profile and power distribution. Arch Ophthalmol 99:1261–1265

67. Dougherty TJ (1984) Photodynamic therapy (PDT) of malignant tumors. Crit Rev Oncol Hematol 2:83–116

68. Downie LE (2014) The necessity for ocular assessment in atopic children: Bilateral corneal hydrops in an 8 year old. Pediatrics 134:596–601

69. Du Y, Funderburgh ML, Mann MM, SundarRaj N, Funderburgh JL (2005) Multipotent stem cells in human corneal stroma. Stem Cells 23:1266–1275

70. Dua HS, Faraj LA, Said DG, Gray T, Lowe J (2013) Human corneal anatomy redefined. Ophthalmology 120:1778–1785

71. Dua HS, Freitas R, Mohammed I, Ting DSJ, Said DG (2023) The pre-Descemet's layer (Dua's layer, also known as the Dua-Fine layer and the pre-posterior limiting lamina layer): Discovery, characterisation, clinical and surgical applications, and the controversy. Prog Retin Eye Res 97:101161

72. Edwards M, McGhee CN, Dean S (2001) The genetics of keratoconus. Clin Exp Ophthalmol 29:345–351

73. Efron N, Hollingsworth JG (2008) New perspectives on keratoconus as revealed by corneal confocal microscopy. Clin Exp Optom 91:34–55

74. Einan-Lifshitz A, Achiron A, Hed S, Hecht I, Dubinsky-Pertzov B, Knyazer B (2023) Three-year follow-up of accelerated versus standard corneal cross-linking in paediatric keratoconus. Eye 37:1219–1224

75. El-Husseiny M, Daas L, Langenbucher A, Seitz B (2016) Intracorneal ring segments to treat keratectasia - interim results and potential complications. Klin Monbl Augenheilkd 233:722–726

76. Enders C, Vogel D, Dreyhaupt J, Wolf W, Garip-Kuebler A, Hall J, Neuhann L, Werner JU (2023) Corneal cross-linking in patients with keratoconus: up to 13 years of follow-up. Graefes Arch Clin Exp Ophthalmol 261:1037–1043

77. Esporcatte LPG, Salomão MQ, Lopes BT, Vinciguerra P, Vinciguerra R, Roberts C, Elsheikh A, Dawson DG, Ambrósio R (2020) Biomechanical diagnostics of the cornea. Eye and Vis 7:9

78. Evangelista CB, Hatch KM (2018) Corneal collagen cross-linking complications. Semin Ophthalmol 33:29–35

79. F abre EJ, Bureau J, Pouliquen Y, Lorans G (1991) Binding sites for human interleukin 1 α, gamma interferon and tumor necrosis factor on cultured fibroblasts of normal cornea and keratoconus. Curr Eye Res 10:585–592

80. Fan R, Chan TC, Prakash G, Jhanji V (2018) Applications of corneal topography and tomography: a review. Clin Exp Ophthalmol 46:133–146

81. Fantes FE (1990) Wound healing after excimer laser keratomileusis (photorefractive keratectomy) in monkeys. Arch Ophthalmol 108:665-675

82. Fard AM, Reynolds AL, Lillvis JH, Nader ND (2020) Corneal collagen cross-linking in pediatric keratoconus with three protocols: a systematic review and meta-analysis. J AAPOS 24:331–336

83. Fehrenbacher L, Gospodarowicz D, Shuman MA (1979) Synthesis of plasminogen activator by bovine corneal endothelial cells. Exp Eye Res 29:219–228

84. Feld S, Flockerzi E, Daas L, Xanthopoulou K, Sideroudi H, Langenbucher A, Seitz B (2023) Die Biomechanik der Hornhaut vor und nach Crosslinking bei Patienten mit Keratokonus. Ophthalmologie 120:940–946

85. Fine BS, Yanoff M (1979) Ocular histology: a text and atlas. 2d ed edition. Medical Dept., Harper & Row, Hagerstown, Md

86. Fischbarg J (2003) On the mechanism of fluid transport across corneal endothelium and epithelia in general. J Exp Zool A Comp Exp Biol 300:30–40

87. Flockerzi E, Daas L, Seitz B (2020) Structural changes in the corneal subbasal nerve plexus in keratoconus. Acta Ophthalmol 98:928-932

88. Flockerzi E, Xanthopoulou K, Goebels SC, Zemova E, Razafimino S, Hamon L, Jullien T, Klühspies U, Eppig T, Langenbucher A, Seitz B (2020) Keratoconus staging by decades: a baseline ABCD classification of 1000 patients in the Homburg Keratoconus Center. Br J Ophthalmol 105:1069-1075

89. Flockerzi E, Vinciguerra R, Belin MW, Vinciguerra P, Ambrósio R, Seitz B (2021) Combined biomechanical and tomographic keratoconus staging: Adding a biomechanical parameter to the ABCD keratoconus staging system. Acta Ophthalmol 100:1135-1142

90. Flockerzi E, Vinciguerra R, Belin MW, Vinciguerra P, Ambrósio R, Seitz B (2021) Correlation of the Corvis Biomechanical Factor CBiF with tomographic parameters in keratoconus. J Cataract Refract Surg 48:215–221

91. Flockerzi E, Häfner L, Xanthopoulou K, Daas L, Munteanu C, Langenbucher A, Seitz B (2021) Reliability analysis of successive Corneal Visualization Scheimpflug Technology measurements in different keratoconus stages. Acta Ophthalmol 100:83-90

92. Fraenkel D, Hamon L, Daas L, Flockerzi E, Suffo S, Eppig T, Seitz B (2020) Tomographically normal partner eye in very asymmetrical corneal ectasia: biomechanical analysis. J Cataract Refract Surg 47:366-372

93. Funderburgh JL, Funderburgh ML, Du Y (2016) Stem cells in the limbal stroma. Ocul Surf 14:113–120

94. Gajecka M, Nowak D (2011) The genetics of keratoconus. Middle East Afr J Ophthalmol 18:2

95. Gatzioufas Z, Balidis M, Kozeis N (2016) Is the corneal stromal demarcation line depth a true indicator of corneal collagen crosslinking efficacy? J Cataract Refract Surg 42:804

96. Georgiou T, Funnell CL, Cassels-Brown A, O'Conor R (2004) Influence of ethnic origin on the incidence of keratoconus and associated atopic disease in Asians and white patients. Eye 18:379–383

97. Ghanem RC, Santhiago MR, Berti TB, Thomaz S, Netto MV (2010) Collagen crosslinking with riboflavin and ultraviolet-A in eyes with pseudophakic bullous keratopathy. J Cataract Refract Surg 36:273–276

98. Ghezzi CE, Rnjak-Kovacina J, Kaplan DL (2015) Corneal tissue engineering: Recent advances and future perspectives. Tiss Eng Part B Rev 21:278–287

99. Glass DH, Roberts CJ, Litsky AS, Weber PA (2008) A viscoelastic biomechanical model of the cornea describing the effect of viscosity and elasticity on hysteresis. Invest Ophthalmol Vis Sci 49:3919–3926

100. Godefrooij DA, Soeters N, Imhof SM, Wisse RPL (2016) Corneal cross-linking for pediatric keratoconus: Long-term results. Cornea 35:954–958

101. Godefrooij DA, de Wit GA, Uiterwaal CS, Imhof SM, Wisse RPL (2017) Age-specific incidence and prevalence of keratoconus: A nationwide registration study. Am J Ophthalmol 175:169–172

102. Godefrooij DA, Galvis V, Tello A (2018) Von Helmholtz's ophthalmometer: historical review and experience with one of the last surviving original devices. Acta Ophthalmol 96:314–320

103. Gokul A, Patel DV, McGhee CNJ (2016) Dr John Nottingham's 1854 landmark treatise on conical cornea considered in the context of the current knowledge of keratoconus. Cornea 35:673–678

104. Gomes JAP, Tan D, Rapuano CJ, Belin MW, Ambrósio R, Guell JL, Malecaze F, Nishida K, Sangwan VS (2015) Global consensus on keratoconus and ectatic diseases. Cornea 34:359–369

105. Gomes JAP, Rodrigues PF, Lamazales LL (2022) Keratoconus epidemiology: A review. Saudi J Ophthalmol 36:3–6

106. Gordon-Shaag A, Millodot M, Shneor E, Liu Y (2015) The genetic and environmental factors for keratoconus. Biomed Res Int 2015:795738

107. Greenstein SA, Fry KL, Bhatt J, Hersh PS (2010) Natural history of corneal haze after collagen crosslinking for keratoconus and corneal ectasia: Scheimpflug and biomicroscopic analysis. J Cataract Refract Surg 36:2105–2114

108. Greenstein SA, Shah VP, Fry KL, Hersh PS (2011) Corneal thickness changes after corneal collagen crosslinking for keratoconus and corneal ectasia: One-year results. J Cataract Refract Surg 37:691–700

109. Grentzelos MA, Liakopoulos DA, Siganos CS, Tsilimbaris MK, Pallikaris IG, Kymionis GD (2019) Long-term comparison of combined t-PTK and CXL (Cretan Protocol) versus CXL with mechanical epithelial debridement for keratoconus. J Refract Surg 35:650–655

110. Grzybowski A, Kanclerz P (2018) Beginnings of astigmatism understanding and management in the 19th century. Eye Contact Lens 44:22–29

111. Gullstrand A (1924) Appendix II. In Southall JPC (ed): Helmholtz's treatise on physiological optics. Vol. I. The Optical Society of America, Rochester, NY

112. Gupta Y, Sharma N, Maharana PK, Saxena R, Sinha R, Agarwal T, Jhanji V, Titiyal JS (2021) Pediatric keratoconus: Topographic, biomechanical and aberrometric characteristics. Am J Ophthalmol 225:69–75

113. Hafezi F, Mrochen M, Iseli HP, Seiler T (2009) Collagen crosslinking with ultraviolet-A and hypoosmolar riboflavin solution in thin corneas. J Cataract Refract Surg 35:621–624

114. Hafezi F, Dejica P, Majo F (2010) Modified corneal collagen crosslinking reduces corneal oedema and diurnal visual fluctuations in Fuchs dystrophy. Br J Ophthalmol 94:660–661

115. Hafezi F (2011) Limitation of collagen cross-linking with hypoosmolar riboflavin solution: Failure in an extremely thin cornea. Cornea 30:917–919

116. Hafezi F, Randleman JB (2014) PACK-CXL: Defining CXL for infectious keratitis. J Refract Surg 30:438–439

117. Hafezi F, Kling S, Gilardoni F, Hafezi N, Hillen M, Abrishamchi R, Gomes JAP, Mazzotta C, Randleman JB, Torres-Netto EA (2021) Individualized corneal cross-linking with riboflavin and UV-A in ultrathin corneas: The Sub400 Protocol. Am J Ophthalmol 224:133–142

118. Hafezi F, Hosny M, Shetty R, Knyazer B, Chen S, Wang Q, Hashemi H, Torres-Netto EA, the PACK-CXL Working Group, Zhang H, Bora'i A, Tawfeek M, Nagaraja H, D'Souza S, Asgari S, Mirsalim A, Chorny A, Krakauer Y, Pajic B, Gilardoni F, Hafezi N, Hillen M, Liu N, Boldi MO, Tabibian D, Torgerson PR,

Zbinden R, Koliwer-Brandl H, Randleman JB (2022) PACK-CXL vs. antimicrobial therapy for bacterial, fungal, and mixed infectious keratitis: a prospective randomized phase 3 trial. Eye and Vis 9:2

119. Hahnel C, Somodi S, Weiss DG, Guthoff RF (2000) The keratocyte network of human cornea: A three-dimensional study using confocal laser scanning fluorescence microscopy: Cornea 19:185–193

120. Hamilton KE, Pye DC (2008) Young's modulus in normal corneas and the effect on applanation tonometry. Optom Vis Sci 85:445–450

121. Hammerstein W (1974) Zur Genetik des Keratoconus. Albrecht von Graefes Arch Klin Ophthalmol 190:293–308

122. Händel A, Siebelmann S, Hos D, Ögrünc F, Matthaei M, Cursiefen C, Bachmann B (2021) Comparison of Mini-DMEK versus predescemetal sutures as treatment of acute hydrops in keratoconus. Acta Ophthalmol 99:1326-1333

123. Hanna C, Bicknell DS, O'Brien JE (1961) Cell turnover in the adult human eye. Arch Ophthalmol 65:695–698

124. Hashemi H, Seyedian MA, Miraftab M, Fotouhi A, Asgari S (2013) Corneal collagen cross-linking with riboflavin and ultraviolet A irradiation for keratoconus: long-term results. Ophthalmology 120:1515–1520

125. Hashemi H, Miraftab M, Seyedian MA, Hafezi F, Bahrmandy H, Heidarian S, Amanzadeh K, Nikbin H, Fotouhi A, Asgari S (2015) Long-term results of an accelerated corneal cross-linking protocol (18 mW/cm^2) for the treatment of progressive keratoconus. Am J Ophthalmol 160:1164-1170

126. Hashemi H, Miraftab M, Hafezi F, Asgari S (2015) Matched comparison study of total and partial epithelium removal in corneal cross-linking. J Refract Surg 31:110–115

127. Hashemi H, Asgari S, Mehravaran S, Miraftab M, Ghaffari R, Fotouhi A (2017) Corneal biomechanics after accelerated cross-linking: Comparison between 18 and 9 mW/cm^2 protocols. J Refract Surg 33:558–562

128. Hassell JR, Birk DE (2010) The molecular basis of corneal transparency. Exp Eye Res 91:326–335

129. He J, Bazan NG, Bazan HEP (2010) Mapping the entire human corneal nerve architecture. Exp Eye Res 91:513–523

130. Henderson BW, Dougherty TJ (1992) How does photodynamic therapy work? Photochem Photobiol 55:145–157

131. Henriquez MA, Hadid M, Izquierdo L (2020) A systematic review of subclinical keratoconus and forme fruste keratoconus. J Refract Surg 36:270–279

132. Hoeltzel DA, Altman P, Buzard K, Choe K (1992) Strip extensiometry for comparison of the mechanical response of bovine, rabbit, and human corneas. J Biomech Eng 114:202–215

133. Hollingsworth JG, Efron N, Tullo AB (2005) *In vivo* corneal confocal microscopy in keratoconus. Ophthalmic Physiol Opt 25:254–260

134. Huang J, Ding X, Savini G, Pan C, Feng Y, Cheng D, Hua Y, Hu X, Wang Q (2013) A comparison between Scheimpflug imaging and optical coherence tomography in measuring corneal thickness. Ophthalmology 120:1951–1958

135. Ioannidis AS, Speedwell L, Nischal KK (2005) Unilateral keratoconus in a child with chronic and persistent eye rubbing. Am J Ophthalmol 139:356–357

136. Iqbal M, Gad A, Kotb A, Abdelhalim M (2024) Analysis of the outcomes of three different cross-linking protocols for treatment of paediatric keratoconus: A multicentre randomized controlled trial. Acta Ophthalmol 102:105-116

137. Iseli HP, Thiel MA, Hafezi F, Kampmeier J, Seiler T (2008) Ultraviolet A/riboflavin corneal cross-linking for infectious keratitis associated with corneal melts. Cornea 27:590–594

138. Jabbarvand M, Moravvej Z, Shahraki K, Hashemian H, Ghasemi H, Berijani S, Amiri Z, Jamali A (2020) Corneal biomechanical outcome of collagen cross-linking in keratoconic patients evaluated by Corvis ST. Eur J Ophthalmol 31:1577–1583

139. Jacob S, Kumar DA, Agarwal A, Basu S, Sinha P, Agarwal A (2014) Contact lens-assisted collagen cross-linking (CACXL): A new technique for cross-linking thin corneas. J Refract Surg 30:366–372

140. Jafri B, Lichter H, Stulting RD (2004) Asymmetric keratoconus attributed to eye rubbing. Cornea 23:560–564

141. Jian W, Tian M, Zhang X, Sun L, Shen Y, Li M, Zhou X (2021) One-year follow-up of corneal biomechanical changes after accelerated transepithelial corneal

cross-linking in pediatric patients with progressive keratoconus. Front Med (Lausanne) 8:663494

142. Jun AS, Cope L, Speck C, Feng X, Lee S, Meng H, Hamad A, Chakravarti S (2011) Subnormal cytokine profile in the tear fluid of keratoconus patients. PLoS One 6:e16437

143. Kanclerz P, Khoramnia R, Wang X (2021) Current developments in corneal topography and tomography. Diagnostics (Basel) 11:1466

144. Kanellopoulos AJ (2019) Management of progressive keratoconus with partial topography-guided PRK combined with refractive, customized CXL - a novel technique: The enhanced Athens protocol. Clin Ophthalmol 13:581–588

145. Kanellopoulos J (2012) Long term results of a prospective randomized bilateral eye comparison trial of higher fluence, shorter duration ultraviolet A radiation, and riboflavin collagen cross linking for progressive keratoconus. Clin Ophthalmol 6:97-101

146. Kanellopoulos J, Asimellis G (2014) OCT corneal epithelial topographic asymmetry as a sensitive diagnostic tool for early and advancing keratoconus. Clin Ophthalmol 8:2277-2287

147. Kang MJ, Hwang J, Chung SH (2021) Comparison of pulsed and continuous accelerated corneal crosslinking for keratoconus: 1-year results at a single center. J Cataract Refract Surg 47:641–648

148. Karaca EE (2021) Visual and topographical outcomes following accelerated corneal crosslinking in progressive keratoconus. Eur Eye Res 1:57-63

149. Karimian F, Aramesh S, Rabei HM, Javadi MA, Rafati N (2008) Topographic evaluation of relatives of patients with keratoconus. Cornea 27:874–878

150. Kaushik S, Pandav SS (2012) Ocular response analyzer. J Curr Glaucoma Pract 6:17–19

151. Kennedy RH, Bourne WM, Dyer JA (1986) A 48-Year clinical and epidemiologic study of keratoconus. Am J Ophthalmol 101:267–273

152. Kenney MC, Nesburn AB, Burgeson RE, Butkowski RJ, Ljubimov AV (1997) Abnormalities of the extracellular matrix in keratoconus corneas. Cornea 16:345–351

153. Kim JT, Zloty P (2012) Simplified nomenclature for describing keratoconus. Int J Kerat Ect Cor Dis 1:31–35

154. Kim WJ, Rabinowitz YS, Meisler DM, Wilson SE (1999) Keratocyte apoptosis associated with keratoconus. Exp Eye Res 69:475–481

155. Kirgiz A, Eliacik M, Yildirim Y (2019) Different accelerated corneal collagen cross-linking treatment modalities in progressive keratoconus. Eye Vis (Lond) 6:16

156. Klyce SD (1984) Computer-assisted corneal topography. High-resolution graphic presentation and analysis of keratoscopy. Invest Ophthalmol Vis Sci 25:1426–1435

157. Klyce SD, Dingeldein SA (1990) Corneal topography. In: Masters BR (ed) Noninvasive diagnostic techniques in ophthalmology. Springer New York, NY. pp 61-81

158. Knupp C, Pinali C, Lewis PN, Parfitt GJ, Young RD, Meek KM, Quantock AJ (2009) The architecture of the cornea and structural basis of its transparency. Adv Protein Chem Struct Biol 78:25-49

159. Knutsson KA, Genovese PN, Paganoni G, Ambrosio O, Ferrari G, Zennato A, Caccia M, Cataldo M, Rama P (2023) Safety and efficacy of corneal cross-linking in patients affected by keratoconus: Long-term results. Medical Sci (Basel) 11:43

160. Kodavoor S, Tiwari N, Ramamurthy D (2020) Profile of infectious and sterile keratitis after accelerated corneal collagen cross-linking for keratoconus. Oman J Ophthalmol 13:18-23

161. Koh S (2022) Topography and Tomography of Keratoconus. In: Das S (ed). Keratoconus. Springer, Singapore

162. Kohlhaas M, Spoerl E, Schilde T, Unger G, Wittig C, Pillunat LE (2006) Biomechanical evidence of the distribution of cross-links in corneas treated with riboflavin and ultraviolet A light. J Cataract Refract Surgery 32:279–283

163. Koller T, Mrochen M, Seiler T (2009) Complication and failure rates after corneal crosslinking. J Cataract Refract Surg 35:1358–1362

164. Krachmer JH, Feder RS, Belin MW (1984) Keratoconus and related noninflammatory corneal thinning disorders. Surv Ophthalmol 28:293–322

165. Krachmer JH, Rabinowich YS, Lawless M, Coster DJ, Phillips AJ, Loane M (1989) Keratoconus: Diagnosis and management. Aust N Z J Ophthalmol 17:33–60

166. Krueger RR, Kanellopoulos AJ (2010) Stability of simultaneous topography-guided photorefractive keratectomy and Riboflavin/UVA cross-linking for progressive keratoconus: Case Reports. J Refract Surg 26:827-832

167. Krumeich JH, Daniel J, Knülle A (1998) Live-epikeratophakia for keratoconus. J Cataract Refr Surg 24:456–463

168. Kumagai AK, Glasgow BJ, Pardridge WM (1994) GLUT1 glucose transporter expression in the diabetic and nondiabetic human eye. Invest Ophthalmol Vis Sci 35:2887–2894

169. Kymionis GD, Portaliou DM, Bouzoukis DI, Suh LH, Pallikaris AI, Markomanolakis M, Yoo SH (2007) Herpetic keratitis with iritis after corneal crosslinking with riboflavin and ultraviolet A for keratoconus. J Cataract Refract Surg 33:1982–1984

170. Kymionis GD, Diakonis VF, Coskunseven E, Jankov M, Yoo SH, Pallikaris IG (2009) Customized pachymetric guided epithelial debridement for corneal collagen cross linking. BMC Ophthalmol 9:10

171. Kymionis GD (2011) Editorial: Corneal collagen cross linking - PLUS. Open Ophthalmol J 5:10

172. Kymionis GD, Grentzelos MA, Kankariya VP, Pallikaris IG (2013) Combined transepithelial phototherapeutic keratectomy and corneal collagen crosslinking for ectatic disorders: Cretan protocol. J Cataract Refract Surg 39:1939

173. Kymionis GD, Tsoulnaras KI, Grentzelos MA, Plaka AD, Mikropoulos DG, Liakopoulos DA, Tsakalis NG, Pallikaris IG (2014) Corneal stroma demarcation line after standard and high-intensity collagen crosslinking determined with anterior segment optical coherence tomography. J Cataract Refract Surg 40:736–740

174. Lam FC, Geourgoudis P, Nanavaty MA, Khan S, Lake D (2014) Sterile keratitis after combined riboflavin-UVA corneal collagen cross-linking for keratoconus. Eye 28:1297–1303

175. Lema I, Duran J (2005) Inflammatory molecules in the tears of patients with keratoconus. Ophthalmology 112:654–659

176. Lema I, Sobrino T, Duran JA, Brea D, Diez-Feijoo E (2009) Subclinical keratoconus and inflammatory molecules from tears. Br J Ophthalmol 93:820–824

177. Léoni-Mesplié S, Mortemousque B, Touboul D, Malet F, Praud D, Mesplié N, Colin J (2012) Scalability and severity of keratoconus in children. Am J Ophthalmol 154:56-62

178. Levene, JR. (1965) The true inventors of the keratoscope and photo-keratoscope. Br J Hist 2:324–342

179. Lim WK, Soh ZD, Choi HKY, Theng JTS (2017) Epithelium-on photorefractive intrastromal cross-linking (PiXL) for reduction of low myopia. Clin Ophthalmol 11:1205–1211

180. Lin J (2018) Influencing factors relating the demarcation line depth and efficacy of corneal crosslinking. Invest Ophthalmol Vis Sci 59:5125-5126

181. Lin J (2018) A proposed concentration-controlled new protocol for optimal corneal crosslinking efficacy in the anterior stroma. Invest Ophthalmol Vis Sci 59:431-432

182. Lipson RL (1960) The photodynamic properties of a particular hematoporphyrin derivative. Arch Dermatol 82:508

183. Lopes BT, Roberts CJ, Elsheikh A, Vinciguerra R, Vinciguerra P, Reisdorf S, Berger S, Koprowski R, Ambrósio R (2017) Repeatability and reproducibility of intraocular pressure and dynamic corneal response parameters assessed by the Corvis ST. J Ophthalmol 2017:8515742

184. Ma J, Wang Y, Wei P, Jhanji V (2018) Biomechanics and structure of the cornea: implications and association with corneal disorders. Surv Ophthalmol 63:851–861

185. Maguire LJ, Singer DE, Klyce SD (1987) Graphic presentation of computer-analyzed keratoscope photographs. Arch Ophthalmol 105:223–230

186. Mandell RB, Chiang CS, Klein SA (1995) Location of the major corneal reference points. Optom Vis Sci 72:776–784

187. Martin JW, Chin JW, Nguyen T (2003) Reciprocity law experiments in polymeric photodegradation: a critical review. Prog Org Coat 47:292–311

188. Martínez-Abad A, Piñero DP (2017) New perspectives on the detection and progression of keratoconus. J Cataract Refract Surg 43:1213–1227

189. Matthews FJ, Cook SD, Majid MA, Dick AD, Smith VA (2007) Changes in the balance of the tissue inhibitor of matrix metalloproteinases (TIMPs)-1 and -3 may promote keratocyte apoptosis in keratoconus. Exp Eye Res 84:1125–1134

190. Maurice DM (1957) The structure and transparency of the cornea. J Physiol 136:263–286

191. Mazzotta C, Balestrazzi A, Traversi C, Baiocchi S, Caporossi T, Tommasi C, Caporossi A (2007) Treatment of progressive keratoconus by riboflavin-UVA-induced cross-linking of corneal collagen: Ultrastructural analysis by Heidelberg Retinal Tomograph II in vivo confocal microscopy in humans. Cornea 26:390–397

192. Mazzotta C, Balestrazzi A, Baiocchi S, Traversi C, Caporossi A (2007) Stromal haze after combined riboflavin-UVA corneal collagen cross-linking in keratoconus: In vivo confocal microscopic evaluation. Clin Exp Ophthalmol 35:580–58

193. Mazzotta C, Traversi C, Baiocchi S, Caporossi O, Bovone C, Sparano MC, Balestrazzi A, Caporossi A (2008) Corneal healing after riboflavin ultraviolet-A collagen cross-linking determined by confocal laser scanning microscopy in vivo: Early and late modifications. Am J Ophthalmol 146:527-533

194. Mazzotta C, Caporossi T, Denaro R, Bovone C, Sparano C, Paradiso A, Baiocchi S, Caporossi A (2012) Morphological and functional correlations in riboflavin UV A corneal collagen cross-linking for keratoconus. Acta Ophthalmol 90:259–265

195. Mazzotta C, Traversi C, Paradiso AL, Latronico ME, Rechichi M (2014) Pulsed light accelerated crosslinking versus continuous light accelerated crosslinking: One-year results. J Ophthalmol 2014:1–6

196. Mazzotta C, Romani A, Burroni A (2018) Pachymetry-based accelerated crosslinking: The “M Nomogram” for standardized treatment of all-thickness progressive ectatic corneas. Int J Kerat Ect Cor Dis 7:137–144

197. Mazzotta C, Traversi C, Baiocchi S, Bagaglia S, Caporossi O, Villano A, Caporossi A (2018) Corneal collagen cross-linking with riboflavin and ultraviolet A light for pediatric keratoconus: Ten-year results. Cornea 37:560–566

198. Mazzotta C, Wollensak G, Raiskup F, Pandolfi AM, Spoerl E (2019) The meaning of the demarcation line after riboflavin-UVA corneal collagen crosslinking. Exp Rev Ophthalmol 14:115–131

199. Mazzotta C, Bagaglia SA, Sgheri A, Di Maggio A, Fruschelli M, Romani A, Vinciguerra R, Vinciguerra P, Tosi GM (2020) Iontophoresis corneal cross-linking with enhanced fluence and pulsed UV-A light: 3-Year clinical results. J Refract Surg 36:286–292

200. Mazzotta C, Raiskup F, Hafezi F, Torres-Netto EA, Balamoun AA, Giannaccare G, Bagaglia SA (2021) Long term results of accelerated 9 mW corneal crosslinking for early progressive keratoconus: the Siena Eye-Cross Study 2. Eye Vis (Lond) 8:16

201. Mazzotta C, Ramovecchi V (2014) Customized epithelial debridement for thin ectatic corneas undergoing corneal cross-linking: epithelial island cross-linking technique. Clin Ophthalmol 8:1337-1343

202. McAlinden C, Khadka J, Pesudovs K (2011) A comprehensive evaluation of the precision (repeatability and reproducibility) of the Oculus Pentacam HR. Invest Ophthalmol Vis Sci 52:7731

203. McMahon TT, Szczotka-Flynn L, Barr JT, Anderson RJ, Slaughter ME, Lass JH, Iyengar SK (2006) A new method for grading the severity of keratoconus: The Keratoconus Severity Score (KSS). Cornea 25:794–800

204. Meek KM, Boote C (2004) The organization of collagen in the corneal stroma. Exp Eye Res 78:503–512

205. Meek KM, Tuft SJ, Huang Y, Gill PS, Hayes S, Newton RH, Bron AJ (2005) Changes in collagen orientation and distribution in keratoconus Corneas. Invest Ophthalmol Vis Sci 46:1948

206. Meek KM, Knupp C (2015) Corneal structure and transparency. Progr Retin Eye Res 49:1–16

207. Mergler S, Pleyer U (2007) The human corneal endothelium: New insights into electrophysiology and ion channels. Progr Retin Eye Res 26:359–378

208. Mitton D, Ackroyd R (2008) A brief overview of photodynamic therapy in Europe. Photodiagnosis Photodyn Ther 5:103–111

209. Mohamed-Noriega K, Butrón-Valdez K, Vazquez-Galvan J, Mohamed-Noriega J, Cavazos-Adame H, Mohamed-Hamsho J (2016) Corneal melting after collagen cross-linking for keratoconus in a thin cornea of a diabetic patient treated with topical nepafenac: A case report with a literature review. Case Rep Ophthalmol 7:119–124

210. Morishige N, Wahlert AJ, Kenney MC, Brown DJ, Kawamoto K, Chikama T, Nishida T, Jester JV (2007) Second-harmonic imaging microscopy of normal human and keratoconus cornea. Invest Ophthalmol Vis Sci 48:1087

211. Moshirfar M, Heiland MB, Rosen DB, Ronquillo YC, Hoopes PC (2019) Keratoconus screening in elementary school children. Ophthalmol Ther 8:367–371

212. Motlagh MN, Moshirfar M, Murri MS, Skanchy DF, Momeni-Moghaddam H, Ronquillo YC, Hoopes PC (2019) Pentacam® corneal tomography for screening of refractive surgery candidates: A review of the literature, Part I. Med Hypothesis Discov Innov Ophthalmol 8:177–203

213. Müller L, Thiel M, Kipfer-Kauer A, Kaufmann C (2012) Corneal cross-linking as supplementary treatment option in melting keratitis: A case series. Klin Monbl Augenheilkd 229:411–415

214. Müller LJ, Pels L, Vrensen GF (1995) Novel aspects of the ultrastructural organization of human corneal keratocytes. Invest Ophthalmol Vis Sci 36:2557–2567

215. Müller LJ, Pels L, Vrensen GF (1996) Ultrastructural organization of human corneal nerves. Invest Ophthalmol Vis Sci 37:476–488

216. Müller LJ, Pels E, Schurmans LRHM, Vrensen GFJM (2004) A new three-dimensional model of the organization of proteoglycans and collagen fibrils in the human corneal stroma. Exp Eye Res 78:493–501

217. Mustonen RK, McDonald MB, Srivannaboon S, Tan AL, Doubrava MW, Kim CK (1998) Normal human corneal cell populations evaluated by in vivo scanning slit confocal microscopy: Cornea 17:485–492

218. Naderan M, Rajabi MT, Zarrinbakhsh P, Bakhshi A (2017) Effect of allergic diseases on keratoconus severity. Ocul Immunol Inflamm 25:418–423

219. Najmi H, Mobarki Y, Mania K, Altowairqi B, Basehi M, Mahfouz MS, Elmahdy M (2019) The correlation between keratoconus and eye rubbing: a review. Int J Ophthalmol 12:1775–1781

220. Nath S, Shen C, Koziarz A, Banfield L, Nowrouzi-Kia B, Fava MA, Hodge WG (2021) Transepithelial versus epithelium-off corneal collagen cross-linking for corneal ectasia. Ophthalmology 128:1150–116

221. Newman DK (2016) Photodynamic therapy: current role in the treatment of chorioretinal conditions. Eye 30:202–210

222. Newton RH, Meek KM (1998) The integration of the corneal and limbal fibrils in the human Eye. Biophys J 75:2508–2512

223. Newton RH, Meek KM (1998) Circumcorneal annulus of collagen fibrils in the human limbus. Invest Ophthalmol Vis Sci 39:1125–1134

224. Nicula C, Nicula D, Pop RN (2017) Results at 7 years after cross-linking procedure in keratoconic patients. J Fr Ophtalmol 40:535–541

225. Nicula CA, Nicula D, Rednik AM, Bulboacă AE (2020) Comparative results of “epi-off” conventional versus “epi-off” accelerated cross-linking procedure at 5-year follow-up. J Ophthalmol 2020:1–13

226. Nowis D, Stokłosa T, Legat M, Issat T, Jakóbisiak M, Gołąb J (2005) The influence of photodynamic therapy on the immune response. Photodiagnosis and Photodyn Ther 2:283–298

227. O’Brart DPS (2014) Corneal collagen cross-linking: a review. J Optom 7:113–12

228. Olivo-Payne A, Abdala-Figuerola A, Hernandez-Bogantes E, Pedro-Aguilar L, Chan E, Godefrooij D (2019) Optimal management of pediatric keratoconus: challenges and solutions. Clin Ophthalmol 13:1183–1191

229. Özcan G, Özlenen Uçakhan Ö (2022) Surgical management of corneal hydrops: Case series. Turk J Ophthalmol 52:64–68

230. Padmanabhan P, Rachapalle Reddi S, Rajagopal R, Natarajan R, Iyer G, Srinivasan B, Narayanan N, Lakshmipathy M, Agarwal S (2017) Corneal collagen cross-linking for keratoconus in pediatric patients - Long-term results. Cornea 36:138–1433

231. Panda A, Aggarwal A, Madhavi P, Wagh VB, Dada T, Kumar A, Mohan S (2007) Management of acute corneal hydrops secondary to keratoconus with intracameral injection of sulfur hexafluoride (SF6). Cornea 26:1067–1069

232. Pearson AR, Soneji B, Sarvananthan N, Sandford-Smith JH (2000) Does ethnic origin influence the incidence or severity of keratoconus? Eye 14:625–628

233. Pedrotti E, Caldarella G, Fasolo A, Bonacci E, Gennaro N, De Gregorio A, Marchini G (2019) Topographic and biomechanical changes after application of corneal cross-linking in recurrent keratoconus. Int J Environ Res Public Health 16:3872

234. Peña-García P, Sanz-Díez P, Durán-García ML (2015) Keratoconus management guidelines. Int J Kerat Ect Cor Dis 4:1–39

235. Perry HD, Buxton JN, Fine BS (1980) Round and oval cones in keratoconus. Ophthalmology 87:905–909

236. Piñero DP, Alio JL (2010) Intracorneal ring segments in ectatic corneal disease – a review. Clin Exp Ophthalmol 38:154–167

237. Piñero DP, Alcón N (2014) In vivo characterization of corneal biomechanics. J Cataract Refract Surg 40:870–887

238. Pinnamaneni N, Funderburgh JL (2012) Concise review: Stem cells in the corneal stroma. Stem Cells 30:1059–1063

239. Prajna NV, Radhakrishnan N, Lalitha P, Austin A, Ray KJ, Keenan JD, Porco TC, Lietman TM, Rose-Nussbaumer J (2020) Cross-linking–assisted infection reduction. Ophthalmology 127:159–166

240. Rabinowitz YS (1995) Videokeratographic indices to aid in screening for keratoconus. J Refract Surg 11:371–406

241. Rabinowitz YS (1998) Keratoconus. Surv Ophthalmol 42:297–319

242. Radner W, Zehetmayer M, Aufreiter R, Mallinger R (1998) Interlacing and cross-angle distribution of collagen lamellae in the human cornea. Cornea 17:537–543

243. R Raiskup F, Hoyer A, Spoerl E (2009) Permanent corneal haze after riboflavin-UVA-induced cross-linking in keratoconus. J Refract Surg 25:824-828

244. Raiskup F, Theuring A, Pillunat LE, Spoerl E (2015) Corneal collagen crosslinking with riboflavin and ultraviolet-A light in progressive keratoconus: ten-year results. J Cataract Refract Surg 41:41–46

245. Reeves SW, Stinnett S, Adelman RA, Afshari NA (2005) Risk factors for progression to penetrating keratoplasty in patients with keratoconus. Am J Ophthalmol 140:607–611

246. Regillo CD (2000) Update on photodynamic therapy. Curr Opin Ophthalmol 11:166–170

247. Richoz O, Kling S, Hoogewoud F, Hammer A, Tabibian D, Francois P, Schrenzel J, Hafezi F (2014) Antibacterial efficacy of accelerated Photoactivated Chromophore for Keratitis–Corneal Collagen Cross-linking (PACK-CXL). J Refract Surg 30:850–854

248. Roberts CJ (2014) Concepts and misconceptions in corneal biomechanics. J Cataract Refract Surg 40:862–869

249. Roberts CJ, Mahmoud AM, Bons JP, Hossain A, Elsheikh A, Vinciguerra R, Vinciguerra P, Ambrósio R (2017) Introduction of two novel stiffness parameters and interpretation of air puff–induced biomechanical deformation parameters with a dynamic Scheimpflug analyzer. J Refract Surg 33:266–273

250. Rowsey JJ (1981) Corneal Topography: Corneascope. Arch Ophthalmol 99:1093

251. Ruan Y, Jiang S, Musayeva A, Pfeiffer N, Gericke A (2021) Corneal epithelial stem cells-physiology, pathophysiology and therapeutic options. Cells 10:2302

252. Sabti S, Tappeiner C, Frueh BE (2015) Corneal cross-linking in a 4-year-old child with keratoconus and Down syndrome. Cornea 34:1157–1160

253. Sahebjada S, Al-Mahrouqi HH, Moshegov S, Panchatcharam SM, Chan E, Daniell M, Baird PN (2021) Eye rubbing in the aetiology of keratoconus: a systematic review and meta-analysis. Graefes Arch Clin Exp Ophthalmol 259:2057–2067

254. Sakellaris D, Balidis M, Gorou O, Szentmary N, Alexoudis A, Grieshaber MC, Sagri D, Scholl H, Gatzioufas Z (2019) Intracorneal ring segment implantation in the management of keratoconus: An evidence-based approach. Ophthalmol Ther 8:5–14

255. Salomão MQ, Hofling-Lima AL, Gomes Esporcatte LP, Lopes B, Vinciguerra R, Vinciguerra P, Bühren J, Sena N, Luz Hilgert GS, Ambrósio R (2020) The role of corneal biomechanics for the evaluation of ectasia patients. Int J Environ Res Public Health 17:2113

256. Salouti R, Khalili MR, Zamani M, Ghoreyshi M, Nowroozzadeh MH (2019) Assessment of the changes in corneal biomechanical properties after collagen cross-linking in patients with keratoconus. J Curr Ophthalmol 31:262–267

257. Sandali O, El Sanharawi M, Temstet C, Hamiche T, Galan A, Ghouali W, Goemaere I, Basli E, Borderie V, Laroche L (2013) Fourier-domain optical coherence tomography imaging in keratoconus. Ophthalmology 120:2403–2412

258. Santodomingo-Rubido J, Carracedo G, Suzaki A, Villa-Collar C, Vincent SJ, Wolffsohn JS (2022) Keratoconus: An updated review. Cont Lens Anterior Eye 45:101559

259. Scheiner C (1619) Oculus hoc est: Fundamentum opticum. Freiburg im Breisgau, Germany: Danielem Agricolam Oeniponti

260. Schießl G, Suffo S, Milioti G, Seitz B (2019) Muraine-Nähte beschleunigen die Abheilung des Hydrops corneae bei akutem Keratotorus. Ophthalmologe 116:665–668

261. Schimmelpfennig B (1982) Nerve structures in human central corneal epithelium. Graefes Arch Clin Exp Ophthalmol 218:14–20

262. Schlemm TFW. (1831) Nerven der Cornea. Ammon' Z Ophthalmol 113–114

263. Schlötzer-Schrehardt U, Bachmann BO, Tourtas T, Torricelli AAM, Singh A, González S, Mei H, Deng SX, Wilson SE, Kruse FE (2015) Ultrastructure of the posterior corneal stroma. Ophthalmology 122:693–699

264. Schmidt-Erfurth U, Hasan T (2000) Mechanisms of action of photodynamic therapy with verteporfin for the treatment of age-related macular degeneration. Surv Ophthalmol 45:195–214

265. Schumacher S, Oeftiger L, Mrochen M (2011) Equivalence of biomechanical changes induced by rapid and standard corneal cross-linking, using riboflavin and ultraviolet radiation. Invest Ophthalmol Vis Sci 52:9048-9052

266. Schumacher S, Mrochen M, Wernli J, Bueeler M, Seiler T (2012) Optimization model for UV-riboflavin corneal cross-linking. Invest Ophthalmol Vis Sci 53:762

267. Scott JE, Bosworth TR (1990) A comparative biochemical and ultrastructural study of proteoglycan–collagen interactions in corneal stroma. Functional and metabolic implications. Biochem J 270:491–497

268. Scott JE (1992) Morphometry of cupromeronic blue-stained proteoglycan molecules in animal corneas, versus that of purified proteoglycans stained in vitro, implies that tertiary structures contribute to corneal ultrastructure. J Anat 180:155-164

269. Sedaghat MR, Momeni-Moghaddam H, Ambrósio R, Roberts CJ, Yekta AA, Danesh Z, Reisdorf S, Khabazkhoob M, Heidari HR, Sadeghi J (2018) Long-term evaluation of corneal biomechanical properties after corneal cross-linking for keratoconus: A 4-year longitudinal study. J Refract Surg 34:849–856

270. Seifert FK, Theuersbacher J, Schwabe D, Lamm OS, Hillenkamp J, Kampik D (2022) Long-term outcome of corneal collagen crosslinking with riboflavin and UV-A irradiation for keratoconus. Curr Eye Res 47: 1472-1478

271. Seiler T, Matallana M, Sendler S, Bende T (1992) Does Bowman's layer determine the biomechanical properties of the cornea? Refract Corneal Surg 8:139–142

272. Seiler T, Hafezi F (2006) Corneal cross-linking-induced stromal demarcation line. Cornea 25:1057–1059

273. Seitz B, Daas L, Hamon L, Xanthopoulou K, Goebels S, Spira-Eppig C, Razafimino S, Szentmáry N, Langenbucher A, Flockerzi E (2021) Stadiengerechte Therapie des Keratokonus. Ophthalmologe 118:1069–1088

274. Shajari M, Kolb CM, Agha B, Steinwender G, Müller M, Herrmann E, Schmack I, Mayer WJ, Kohnen T (2019) Comparison of standard and accelerated corneal cross-linking for the treatment of keratoconus: a meta-analysis. Acta Ophthalmol 97:22-35

275. Sharma A, Nottage JM, Mirchia K, Sharma R, Mohan K, Nirankari VS (2012) Persistent corneal edema after collagen cross-linking for keratoconus. Am J Ophthalmol 154:922-926

276. Sharma N, Maharana PK, Jhanji V, Vajpayee RB (2012) Management of acute corneal hydrops in ectatic corneal disorders. Curr Opin Ophthalmol 23:317–323

277. Shaw EL (1976) Pathophysiology and treatment of corneal hydrops. Ophthalmic Surg 7:33–37

278. Shetty R, Arora V, Jayadev C, Nuijts RMMA, Kumar M, Puttaiah NK, Kummelil MK (2014) Repeatability and agreement of three Scheimpflug-based

imaging systems for measuring anterior segment parameters in keratoconus. Invest Ophthalmol Vis Sci 55:5263-5268

279. Shetty R, Nagaraja H, Jayadev C, Pahuja NK, Kurian Kummelil M, Nuijts RMMA (2014) Accelerated corneal collagen cross-linking in pediatric patients: two-year follow-up results. Biomed Res Int 2014:894095

280. Shetty R, Kaweri L, Nuijts RMMA, Nagaraja H, Arora V, Kumar RS (2014) Profile of microbial keratitis after corneal collagen cross-linking. BioMed Res Int 2014:1–7

281. Shetty R, Pahuja NK, Nuijts RMMA, Ajani A, Jayadev C, Sharma C, Nagaraja H (2015) Current protocols of corneal collagen cross-linking: Visual, refractive, and tomographic outcomes. Am J Ophthalmol 160:243–249

282. Shetty R, Rao H, Khamar P, Sainani K, Vunnava K, Jayadev C, Kaweri L (2017) Keratoconus screening indices and their diagnostic ability to distinguish normal from ectatic corneas. Am J Ophthalmol 181:140–148

283. Singer SJ, Nicolson GL (1972) The fluid mosaic model of the structure of cell membranes: Cell membranes are viewed as two-dimensional solutions of oriented globular proteins and lipids. Science 175:720–731

284. Smolin G, Foster CS, Azar DT, Dohlman CH (eds) (2005) Smolin and Thoft's The cornea: scientific foundations and clinical practice. 4th ed edition. Lippincott Williams & Wilkins, Philadelphia

285. Soeters N, Van Der Valk R, Tahzib NG (2014) Corneal cross-linking for treatment of progressive keratoconus in various age groups. J Refract Surg 30:454–460

286. Spadea L, Tonti E, Vingolo EM (2016) Corneal stromal demarcation line after collagen cross-linking in corneal ectatic diseases: A review of the literature. Clin Ophthalmol 10:1803–1810

287. Spadea L, Di Genova L, Tonti E (2018) Corneal stromal demarcation line after 4 protocols of corneal crosslinking in keratoconus determined with anterior segment optical coherence tomography. J Cataract Refract Surg 44:596–602

288. Spoerl E, Huhle M, Seiler T (1998) Induction of cross-links in corneal tissue. Exp Eye Res 66:97–103

289. Spoerl E, Wollensak G, Seiler T (2004) Increased resistance of crosslinked cornea against enzymatic digestion. Curr Eye Res 29:35–40

290. Sridhar U, Tripathy K (2023) Corneal Topography. StatPearls Publishing, Treasure Island (FL)

291. Steinberg J, Katz T, Mousli A, Frings A, Casagrande MK, Druchkiv V, Richard G, Linke SJ (2014) Corneal biomechanical changes after crosslinking for progressive keratoconus with the Corneal Visualization Scheimpflug Technology. J Ophthalmol 2014:1–8

292. Tăbăcaru B, Stanca TH (2020) Corneal topography in preoperative evaluation for laser keratorefractive surgery – a review. Rom J Ophthalmol 64:333-341

293. Tabibian D, De Tejada BM, Gatzioufas Z, Kling S, Meiss VS, Boldi M-O, Othenin-Girard V, Chilin A, Lambiel J, Hoogewoud F, Hafezi F (2017) Pregnancy-induced changes in corneal biomechanics and topography are thyroid hormone related. Am J Ophthalmol 184:129–136

294. Tan L, Shen X, He Z, Lu Y (2022) The Role of photodynamic therapy in triggering cell death and facilitating antitumor immunology. Front Oncol 12:863107

295. Tervo T, Palkama A (1975) Electron microscopic localization of adenosine triphosphatase (NaK-ATPase) activity in the rat cornea. Exp Eye Res 21:269–279

296. Theuring A, Spoerl E, Pillunat LE, Raiskup F (2015) Hornhautkollagenvernetzung mit Riboflavin und UVA-Licht bei Patienten mit progressivem Keratokonus: 10-Jahres-Ergebnisse. Ophthalmologe 112:140–147

297. Thiel HJ (1974) Das Epithel der Hornhaut und seine Bedeutung für die Transparenz. Dtsch med Wochenschr 99:1630–1635

298. Tillmann A, Kampik D, Borrelli M, Seidl M, Menzel-Severing J, Seiler TG, Geerling G (2022) Acute corneal melt and perforation – A possible complication after riboflavin/UV-A crosslinking (CXL) in keratoconus. Am J Ophthalmol Case Rep 28:101705

299. Ting DSJ, Rana-Rahman R, Chen Y, Bell D, Danjoux J-P, Morgan SJ, Ghosh S, Baylis O (2019) Effectiveness and safety of accelerated (9 mW/cm^2) corneal collagen cross-linking for progressive keratoconus: a 24-month follow-up. Eye 33:812–818

300. Toker E, Çerman E, Özcan DÖ, Seferoğlu ÖB (2017) Efficacy of different accelerated corneal crosslinking protocols for progressive keratoconus. J Cataract Refract Surg 43:1089–1099

301. Tomita M, Mita M, Huseynova T (2014) Accelerated versus conventional corneal collagen crosslinking. J Cataract Refract Surg 40:1013–1020

302. Torres Netto EA, Al-Otaibi WM, Hafezi NL, Kling S, Al-Farhan HM, Randleman JB, Hafezi F (2018) Prevalence of keratoconus in paediatric patients in Riyadh, Saudi Arabia. Br J Ophthalmol 102:1436–1441

303. Tuft SJ, Coster DJ (1990) The corneal endothelium. Eye 4:389–424

304. Tuft SJ, Moodaley LC, Gregory WM, Davison CR, Buckley RJ (1994) Prognostic factors for the progression of keratoconus. Ophthalmology 101:439–447

305. Turhan SA, Yargi B, Toker E (2020) Efficacy of conventional versus accelerated corneal cross-linking in pediatric keratoconus: Two-year outcomes. J Refract Surg 36:265–269

306. Tzamalis A, Romano V, Cheeseman R, Vinciguerra R, Batterbury M, Willoughby C, Neal T, Ahmad S, Kaye S (2019) Bandage contact lens and topical steroids are risk factors for the development of microbial keratitis after epithelium-off CXL. BMJ Open Ophth 4:e000231

307. Vega Estrada A, Sanz Díez P, Alió JL (2017) Keratoconus grading and its therapeutic implications. In: Alió JL (ed) Keratoconus: Springer Cham pp 177-184

308. Vinciguerra P, Albè E, Trazza S, Rosetta P, Vinciguerra R, Seiler T, Epstein D (2009) Refractive, topographic, tomographic, and aberrometric analysis of keratoconic eyes undergoing corneal cross-linking. Ophthalmology 116:369–378

309. Vinciguerra P, Albé E, Frueh BE, Trazza S, Epstein D (2012) Two-year corneal cross-linking results in patients younger than 18 years with documented progressive keratoconus. Am J Ophthalmol 154:520–526

310. Vinciguerra P, Rosetta P, Legrottaglie EF, Morenghi E, Mazzotta C, Kaye SB, Vinciguerra R (2019) Iontophoresis CXL with and without epithelial debridement versus standard CXL: 2-year clinical results of a prospective clinical study. J Refract Surg 35:184–190

311. Vinciguerra R, Ambrósio R, Elsheikh A, Roberts CJ, Lopes B, Morenghi E, Azzolini C, Vinciguerra P (2016) Detection of keratoconus with a new biomechanical index. J Refract Surg 32:803–810

312. Vinciguerra R, Romano V, Arbabi EM, Brunner M, Willoughby CE, Batterbury M, Kaye SB (2017) In vivo early corneal biomechanical changes after corneal cross-linking in patients with progressive keratoconus. J Refract Surg 33:840–846

313. Vinciguerra R, Pagano L, Borgia A, Montericcio A, Legrottaglie EF, Piscopo R, Rosetta P, Vinciguerra P (2020) Corneal cross-linking for progressive keratoconus: Up to 13 years of follow-up. J Refract Surg 36:838–843

314. Vinciguerra R, Ambrosio R, Wang Y, Zhang F, Zhou X, Bai J, Yu K, Chen S, Fang X, Vinciguerra P (2023) Detection of keratoconus with a new Corvis biomechanical index optimized for chinese populations. Am J Ophthalmol 252:182–187

315. Vounotrypidis E, Athanasiou A, Kortüm K, Kook D, Shajari M, Priglinger S, Mayer WJ (2018) Long-term database analysis of conventional and accelerated crosslinked keratoconic mid-European eyes. Graefes Arch Clin Exp Ophthalmol 256:1165–1172

316. Wachowska M, Muchowicz A, Demkow U (2015) Immunological aspects of antitumor photodynamic therapy outcome. Cent Eur J Immunol 4:481–485

317. Wagner H, Barr JT, Zadnik K (2007) Collaborative Longitudinal Evaluation of Keratoconus (CLEK) Study: Methods and findings to date. Cont Lens Anterior Eye 30:223–232

318. Wang Q, Savini G, Hoffer KJ, Xu Z, Feng Y, Wen D, Hua Y, Yang F, Pan C, Huang J (2012) A comprehensive assessment of the precision and agreement of anterior corneal power measurements obtained using 8 different devices. PLoS One 7:e45607

319. Wernli J, Schumacher S, Spoerl E, Mrochen M (2013) The efficacy of corneal cross-linking shows a sudden decrease with very high intensity UV light and short treatment time. Invest Ophthalmol Vis Sci 54:1176

320. Wilson A, Marshall J (2020) A review of corneal biomechanics: Mechanisms for measurement and the implications for refractive surgery. Indian J Ophthalmol 68:2679

321. Wilson A, Jones J, Tyrer JR, Marshall J (2020) An interferometric ex vivo study of corneal biomechanics under physiologically representative loading, highlighting the role of the limbus in pressure compensation. Eye Vis (Lond) 7:43

322. Wilson SE, Klyce SD (1991) Advances in the analysis of corneal topography. Surv Ophthalmol 35:269–277

323. Wollensak G, Spoerl E, Seiler T (2003) Riboflavin/ultraviolet-a–induced collagen crosslinking for the treatment of keratoconus. Am J Ophthalmol 135:620–627

324. Wollensak G, Spörl E, Reber F, Pillunat L, Funk R (2003) Corneal endothelial cytotoxicity of riboflavin/UVA treatment in vitro. Ophthalmic Res 35:324–328

325. Wollensak G, Spoerl E, Reber F, Seiler T (2004) Keratocyte cytotoxicity of riboflavin/UVA-treatment in vitro. Eye 18:718–722

326. Wollensak G, Wilsch M, Spoerl E, Seiler T (2004) Collagen fiber diameter in the rabbit cornea after collagen crosslinking by riboflavin/UVA. Cornea 23:503–507

327. Wollensak G, Aurich H, Pham DT, Wirbelauer C (2007) Hydration behavior of porcine cornea crosslinked with riboflavin and ultraviolet A. J Cataract Refract Surg 33:516–521

328. Wollensak G, Aurich H, Wirbelauer C, Pham DT (2009) Potential use of riboflavin/UVA cross-linking in bullous keratopathy. Ophthalmic Res 41:114–117

329. Woo JH, Iyer JV, Lim L, Hla MH, Mehta JS, Chan CM, Tan DT (2017) Conventional versus accelerated collagen cross-linking for keratoconus: A comparison of visual, refractive, topographic and biomechanical outcomes. Open Opthalmol J 11:262–272

330. Wu D, Lim DK-A, Lim BXH, Wong N, Hafezi F, Manotosh R, Lim CHL (2021) Corneal cross-linking: The evolution of treatment for corneal diseases. Front Pharmacol 12:686630

331. Wulle KG, Richter J (1978) Electron microscopy of the early embryonic development of the human corneal epithelium. Graefes Arch Clin Ophthalmol 209:39–49

332. Xanthopoulou K, Milioti G, Daas L, Munteanu C, Seitz B, Flockerzi E (2022) Accelerated corneal crosslinking causes pseudoprogression in keratoconus within the

first 6 weeks without affecting posterior corneal curvature. Eur J Ophthalmol 32:2565–2576

333. Xanthopoulou K, Seitz B, Belin MW, Flockerzi E (2023) Reliability analysis of successive Corvis ST® measurements in keratoconus 2 years after accelerated corneal crosslinking compared to untreated keratoconus corneas. Graefes Arch Clin Exp Ophthalmol 261:1055–1061

334. Xanthopoulou K, Milioti G, Daas L, Munteanu C, Seitz B, Flockerzi E (2022) Accelerated corneal crosslinking for treatment of keratoconus in children and adolescents under 18 years of age. Klin Monbl Augenheilkd 240:1131-1142

335. Yahia Chérif H, Gueudry J, Afriat M, Delcampe A, Attal P, Gross H, Muraine M (2015) Efficacy and safety of pre-Descemet's membrane sutures for the management of acute corneal hydrops in keratoconus. Br J Ophthalmol 99:773–777

336. Yang K, Xu L, Fan Q, Zhao D, Ren S (2019) Repeatability and comparison of new Corvis ST parameters in normal and keratoconus eyes. Sci Rep 9:15379

337. Zhang Y, Mao X, Schwend T, Littlechild S, Conrad GW (2013) Resistance of corneal RF UVA–cross-linked collagens and small leucine-rich proteoglycans to degradation by matrix metalloproteinases. Invest Ophthalmol Vis Sci 54:1014-1025

338. Zhao Y, Shen Y, Yan Z, Tian M, Zhao J, Zhou X (2019) Relationship among corneal stiffness, thickness, and biomechanical parameters measured by Corvis ST, Pentacam and ORA in keratoconus. Front Physiol 10:740

339. Zhao Z, Wu S, Ren W, Zheng Q, Ye C, Kim AD, Jhanji V, Wang MTM, Chen W (2021) Compression sutures combined with intracameral air injection versus thermokeratoplasty for acute corneal hydrops: a prospective-randomised trial. Br J Ophthalmol 105:1645–1650

340. Ziaei M, Meyer J, Gokul A, Vellara H, McGhee CNJ (2018) Direct measurement of anterior corneal curvature changes attributable to epithelial removal in keratoconus. J Cataract Refract Surg 44:71–77

341. Ziaei M, Yoon JJ, Vellara HR, Gokul A, Meyer JJ, Thakur SS, McGhee CN, Patel DV (2022) Prospective one year study of corneal biomechanical changes following high intensity, accelerated cornea cross-linking in patients with keratoconus using a non-contact tonometer. Eur J Ophthalmol 32:806–814

342. Oculus Pentacam, Pentacam HR. Interpretation guide, 3rd edition. Oculus Optikgeraete GmbH, Wetzlar, Germany

10. List of publications

- 1. Xanthopoulou K, Milioti G, Daas L, Munteanu C, Seitz B, Flockerzi E (2022). Accelerated corneal crosslinking causes pseudoprogression in keratoconus within the first 6 weeks without affecting posterior corneal curvature. Eur J Ophthalmol 32:2565-2576. doi: 10-1177/11206721221099257 [332]

- 2. Xanthopoulou K, Seitz B, Belin MW, Flockerzi E (2023). Reliability analysis of successive Corvis ST measurements in keratoconus 2 years after accelerated corneal crosslinking compared to untreated keratoconus corneas. Graefes Arch Clin Exp Ophthalmol 261:1055-1061. doi: 10.1007/s00417-022-05881-6 [333]

- 3. Xanthopoulou K, Milioti G, Daas L, Munteanu C, Seitz B, Flockerzi E (2023). Accelerated corneal crosslinking for the treatment of keratoconus in children and adolescents under 18 years of age. Klin Monbl Augenheilkd 240:1131-1142. doi: 10.1055/a-1933-3084 [334]

11. Acknowledgements

I would sincerely like to thank my “Doktorvater” – Supervisor, Prof. Dr. med. Berthold Seitz ML, FEBO, Director of the Department of Ophthalmology at Saarland University Medical Center (UKS) not only for entrusting me with this subject for my Dr. thesis but also for encouraging me, pushing my best self and believing in my abilities from the first day of my path in the Department of Ophthalmology of UKS until today, as a mentor. I am always thankful for the time investment, for the advices, education, invaluable knowledge, opportunities and life lessons that I had the privilege to acquire standing next to him.

I am also incredibly thankful to PD Dr. med. Elias Flockerzi who guided me through my journey as well and was always patient and by my side to help me with the setup, organization, promotion and publication of our research. Thank you for the time and knowledge I had the privilege to acquire next to you.

A sincere gratefulness for my former supervisor Dr. med. Georgia Milioti, FEBO, FICO, who was and is always by my side and awakens me since my first steps in Ophthalmology as well as at my Dr. thesis, and consists a special figure in my life.

Moreover, I would like to thank Prof. Michael Belin who supported us in our study with his innovative ideas and vision, it was a great privilege of having the opportunity to meet him and cooperate with him in our studies.

I am very thankful for the scientific contribution of Dr. med. Loay Daas for this Dr. thesis as well as for the enlightening and support through my path in Ophthalmology.

I am also very thankful for the help and patience of Mr. Cristian Munteanu who contributed to the statistical analysis of the results of the study and was always ready to support and solve every problem, as well as for the invaluable contribution of Dr. med. Tim Berger and Ms. Christina Turner.

I am always grateful to all the staff of the Ophthalmology Department of Saarland University Medical Center, which has been for long like a second home for me, for all the help from the start until the last steps of my journey with this dissertation.

Last but not least, I would like to thank my family, my husband, my two sons, my parents and sister, who are always a source of strength, wisdom, encouragement and love, which are always the basic ingredients in my path and especially for the completion of this dissertation. Thank you for always being by my side.

12. Curriculum vitae

The curriculum vitae was removed from the electronic version of the doctoral thesis for reasons of data protection.